2020

In Partial Fulfillment of the Requirement for the Degree of Master of Science In Geo-Technical Engineering

Yohannes, Kidusu

Bahir Dar University

Bahir Dar Institute of Technology

School of Research and Graduate Studies

Two Dimensional Numerical Analysis of the Behavior of Reinforced Earth Walls

Faculty of Civil and Water Resource Engineering

Thesis Submitted to the School of Graduate Studies of Bahir Dar University

In Partial Fulfillment of the Requirement for the Degree of Master of Science

In Geo-Technical Engineering

By

Kidusu Yohannes

June, 2020

Bahir Dar, Ethiopia

Bahir Dar University

Bahir Dar Institute of Technology

School of Research and Graduate Studies

FACULTY OF CIVIL AND WATER RESOURCE ENGINEERING

Two Dimensional Numerical Analysis of the Behavior of Reinforced Earth Walls

By

Kidusu Yohannes

A Thesis Submitted to School of Graduate Studies In

Partial Fulfillment of the Requirement for Degree of

Master of Science

In

Geotechnical Engineering

Advisor

Dr. Siraj M.

Bahir Dar

2020

DECLARATION

I hereby declare that all information in this document has been obtained and presented in accordance with academic rules and ethical conduct. I also declare that, as required by these rules and conduct, I have fully cited and referenced all material and results that are not original to this work.

Name: Kidusu Yohannes

Signature: ______________ Date: - 11/01/2020

Advisor: Dr. Siraj

Signature: ______________ Date: - 11/01/2020

iii

BAHIR DAR UNIVERSITY

Bahir Dar Institute of Technology

School of Research and Graduate Studies

THESIS APPROVAL SHEET

Kidusu Yohannes Tegegne		25/05/2020
Student Name	Signature	Date

The final thesis entitled "TWO DIMENSIONAL NUMERICAL ANALYSIS OF THE BEHAVIOUR OF REINFORCED EARTH WALLS" has been approved by the following examiners in partial fulfillment of the requirement for the degree of Master of Science in Geotechnical Engineering

APPROVED BY BOARD OF EXAMINERS:

Dr. Siraj Mulugeta		25/05/2020
Advisor	Signature	Date
Dr. Addiszemen Teklay		July 20, 2020
Internal Examiner	Signature	Date
Dr. Aserat Worku	for	July 20, 2020
External Examiner	Signature	Date
Mr. Wubete Mengiste		20/7/2020
Chair Holder	Signature	Date
Temesgen Enku Nigussie (PhD) Faculty Dean		July 20, 2020
Faculty dean	Signature	Date

Bahir Dar Institute of Technology Faculty of Civil and Water Resources Engineering

ACKNOWLEDGEMENTS

I am deeply grateful to my Father God for helping me all the way throughout this thesis. Nothing would have been possible without him. I thank my advisor, Dr. Siraj (Civil Engineering Geotechnical Department, Kombolcha Institute of Technology) for his availability for supervision and for his advices during my research work. I will also have to thank my family and other colleagues for their supports and encouragements throughout my study at the Bahir Dar University, Institute of Technology, Bahir Dar, Ethiopia.

ABSTRACT

In recent years reinforced soil retaining structures are both technically and economically various advantages over other retaining structures; especially when their will be property limitation and under poor soil conditions. This thesis presented about the two dimensional numerical analysis of reinforced earth retaining wall models using finite element method analysis program PLAXIS 2D version 8.5.

The walls were constructed with modular block facing unit, reinforcing material /geogrid and different backfill materials on rigid rock foundation. The soil reinforcement comprises different strength and arrangement geogrid reinforcement material. Methods of construction, the wall geometry and boundary conditions were otherwise nominally the same for each of retaining walls. The behavior of the geosynthetically reinforced earth wall at the end of construction and after surcharge load application for different backfill material properties, geogrid lengths, stiffness and spacing’s were analyzed.

TABLE OF CONTENTS

LIST OF ABBREVIATIONS

Abbreviation

AASHTO	American Association of State Highway and Transportation Office
ASTM	American Society for Testing and Materials
FE	Finite Element
FEM	Finite Element Modeling
FHWA	Federal Highway Administration
GRS	Geosynthetics Reinforce Soil
MSE	Mechanically Stabilized Earth
GRS	Geosynthetically Reinforced Soil
SRW	Segmental Retaining Wall
LTRC	Louisiana Transportation Research Center
UU	Unconsolidated Undrained

LIST OF SYMBOLS

EA	Axial Stiffness of Soil Reinforcement
γunsat	Unsaturated Unit Weight of Soil
γsat	Saturated Unit Weight of Soil
Kx	Horizontal Permeability
Ky	Vertical Permeability
Eref	Reference Young's Modulus
ν	Poisson's Ratio
Cref	Reference Cohesion
φ	Angle of Internal Friction
ψ	Dilatancy
Rinter.	Angle Interface Strength Reduction Factor
T	Tensile Force of the Soil Reinforcement
Ho	Height of Wall from the Toe to the Top of Wall Facing
Sz	Vertical Reinforcement Spacing
L	Length of Reinforcement

LIST OF FIGURES

LIST OF TABLES

CHAPTER 1
INTRODUCTION

1.1. Background

Soil is one of the most abundant materials on earth but it is far from being an ideal construction material. This is because, in general, soil is inherently weak in tension and shear, although it is comparatively stronger in compression. Tension failure can manifest itself in the form of tension cracks in certain situations, but for the vast majority of engineering structures, such as slopes and embankments, the predominant mode of failure is in shear. Traditionally, the inherent weakness of the most soils has placed serious limitations on what can be accomplished in engineering construction using soils. However, nowadays it is feasible to reinforce soils with different forms of reinforcements. Throughout the world there is an increasing demand for geotechnical structures which are more economical and environmentally acceptable. To reduce the negative environmental effects caused by aggregate extraction and to save costs, there is a tendency to use local cohesive soils as construction materials. If the properties of these materials do not fulfill the geotechnical requirements, their engineering behavior can be modified using chemical additives (i.e. lime or cement) or they can be reinforced by inclusions (Guru Nanak 2012).

Geosynthetics have been used in geotechnical engineering for the past three decades because of speed of construction, flexibility, durability, use of local soils rather than imported material, and cost effectiveness. Their use is well established for the purpose of material separation, filters and as reinforcement for improving the stability of embankments and walls.

Geosynthetics have been more and more frequently included as reinforcement in the four major types of earth works, i.e., retaining walls, embankments, soil slopes, and paved/unpaved roads. Nowadays, mechanically stabilized earth (MSE) walls, reinforced embankments, slopes, and paved/unpaved roads constitute the majority of the newly constructed earth works compared with their unreinforced counterparts. Extensive researches have been conducted to either investigate the reinforcement mechanisms or quantify a certain aspect of the reinforcement effects such as stress reduction for reinforced embankments which includes field and full-scale tests and as well as numerical modeling (J.Huang 2011).

Numerical modeling has been increasingly adopted in researches since in addition to their outstanding cost and time effectiveness, they possess the following preferable advantages as compared with the field and full-scale tests: Flexibility: Variables can be easily fixed or varied to assess their effects. Parametric studies can be easily performed. Comprehensive data: The numerical modeling can provide a complete set of data, some of which are difficult or not able to be obtained from instrumentations such as shear stress/strain. Efficiency for long-term behavior performance study: The long-term performance is one of the interests for research and practice, e.g., consolidation of reinforced embankments and creep behavior of MSE walls. Numerical modeling can extend the time domain to the point of interest. Exclusion of scale effect and external disturbance: Full-scale laboratory tests tend to be influenced by scale, more or less. And field tests are inevitably disturbed by external impacts. These scale effect and external disturbance can be easily excluded from or minimized in the numerical modeling. Minimum measurement errors: The experimental data intrinsically possess measurement errors, which is not a problem in numerical modeling. Considering the above merits of the numerical modeling, numerical modeling plays an important, sometime irreplaceable, role in promoting the research and practice (J.Huang 2011).

So far, two analysis approaches have been employed, that is, continuum modeling based on constitutive theories and micro-mechanical modeling based on assembly of soil mass from a collection of individual particles (J.Huang 2011). The numerical modeling based on the continuum approach has been successfully used to simulate all of the above-discussed Geosynthetics reinforced earth works. Such an approach is conceptually more appealing than micro-mechanical modeling approach because the interaction of the reinforcing material and the soil is indeed three-dimensional in nature. The most versatile continuum-based method of analysis available is the finite element/finite difference method.

1.2. Statement of the Problem

In tropical regions like Ethiopia good quality granular backfill was mostly used for earth structures/works. But the use of fine grained soils/cohesive soils as an alternative is necessary for different constructions; since the use of solely granular soils is an ever-increasing cost owing to transporting the backfill material. But for using cohesive soils it is mandatory to investigate their behavior with interaction of reinforcements. Many investigations of cohesive soils-Geosynthetics interactions using experimental and full scale tests has been done in the previous researchers. But there work was limited in different assumptions, formulations and solutions are tedious and complex, thus the need to use cost and time effective, relatively non conservative and flexible analysis technique that is numerical modeling using finite element method is crucial to investigate the behavior of clay-geogrid reinforcement earth structures under static loading conditions. Many developed countries adopted the use of Geosynthetics earth retaining structures. For instance, FHWA 2001 statistic data indicated that over 700,000 m2 of MSE walls were constructed in the United States every year, which counted for more than 50% of all types of retaining walls in the US transportation system. But, in case of our country the application of such structures is not well adopted yet, this is due to lack of detail study in this area so as it is very crucial to understand and analyze the behavior of geosynthetically reinforced earth retaining walls.

1.3. Objective of the Study

1.3.1 General objective

To numerically investigate the two dimensional behavior of reinforced earth retaining walls by performing parametric study using finite element software PLAXIS 2D.

1.3.2 Specific objective

- To investigate the backfill material property effect on the performance of geogrid reinforced earth retaining structures at different surcharge load, geogrid stiffness, vertical spacing and length.
- To numerically study the effect of geogrid strength in earth retaining structures at different backfill material properties, loadings, geogrid spacing and length.
- To investigate the influence of geogrid vertical spacing on the performance of GRS walls at different backfill material properties, loadings, geogrid stiffness and length.
- To determine the influence of changes in uniformly distribute surcharge loads on the performance of reinforced soil retaining walls at different backfill material properties, geogrid spacing and length.
- To determine the influence of changes in stiffness of geogrid on the performance of reinforced soil retaining walls at different backfill material properties, surcharges, geogrid spacing and length.

.

1.4. Scope of the Study

An investigation of reinforced earth retaining structures behavior by numerical modeling using finite element method considering only monotonic loading is presented. Different backfill materials, geogrid stiffness, geogrid spacing and geogrid length of retaining walls after the end of construction (i.e. at serviceability condition) were analyzed. Numerical model and Analysis results are validated using previous research findings. Numerical modeling of reinforced earth structure under dynamic loading condition is beyond the scope of this paper. This thesis presents a literature review on the considerations involved in using reinforced soil walls (Chapter 2); a complete description of the numerical modeling method and material (Chapter 3); a description of the different parameter effects and a detailed report of the results and discussion of the overall findings from the study (Chapter 4). The thesis conclusion (Chapter 5) provides a summary of completed research, major findings, and suggestions for future work.

1.5 Significance of the Study

Geosynthetics are used as reinforcement in a soil mass, they improve the strength and settlement characteristic of the soil mass by showing the following effects: shear stress reduction effect, confinement effect, membrane effect, and interlocking effect. Comparing with other type of retaining structure geosynthetically reinforced earth structures has reduced cost and environmentally friendly.

This investigation of reinforced earth walls using numerical methods was mainly used for approving the use of reinforced retaining walls constructed from poor quality materials in the constructions especially in tropical regions like Ethiopia where good-quality granular backfill is mostly used.

Even though many researchers were studied reinforced earth retaining structures behaviors through experimental, full scale and numerical methods. But the structures applicabilityis not well spread in countries like Ethiopia widely due to lack of detail studies. So this research may increase the construction applicability of reinforced earth retaining structures and can attract local researchers for further study in the issue.

CHAPTER 2
LITERATURE REVIEW

2.1 Retaining Walls

Retaining walls are used to prevent retained material from assuming its natural slope. Wall structures are commonly used to support earth, coal, ore piles, and water. Retaining walls may be classified according to how they produce stability: (Bowles 1997).

a. Mechanically reinforced earth

b. Gravity— masonry, or concrete

c. Cantilever—concrete or sheet-pile

d. Anchored—sheet-pile and certain configurations of reinforced earth

2.1.1 Mechanically Stabilized Earth Walls

2.1.1.1 Segmental Retaining Walls

Dry cast modular block units are commonly used with Geogrid and geotextile reinforcements to construct what is referred to as reinforced segmental retaining walls (SRW). This method of retaining earth has seen tremendous growth in recent years because of several factors shown below. SRWs are advantageous because they are: (Ambauen 2014).

- Easy and fast to construct; requiring less experience/specialization from the craftsmen
- Cost-effective; potentially the lowest cost retaining wall option when applicable
- Seismically resistant; especially when reinforcement creates a composite mass
- Flexible; able to withstand large deformation and differential settlement

The flexibility of the modular block facing allows for more deformation than many other facing types, which in turn decreases the lateral earth pressures built up in the wall. SRWs are a competitive and efficient option among the existing options for earth retention.

2.1.1.2 Geosynthetics Reinforced Soil Walls

Segmental retaining walls (SRWs) with concrete block facing units and reinforced by geogrid or geotextiles are the least expensive of all wall categories at a large range of wall heights and involve some of the simplest construction methods available. The primary causes of poor performance or collapse of SRWs are improper backfill soil selection, inadequate drainage, and insufficient quality control and inspection. However, with appropriate design and construction methods, mechanically stabilized earth (MSE) walls are clearly recognized as being advantageous over other wall types in most situations. Geosynthetics reinforced soil (GRS) walls in particular are cost-effective and time-efficient retaining walls. GRS walls may be constructed using a variety of facing types including Geosynthetics wrap facing, timber, welded wire mesh, gabions, precast/cast-in-place full-height concrete, precast panel units, and modular concrete blocks (Ambauen 2014). The last facing type is especially versatile and practical for numerous reasons. The use of Geosynthetics reinforced soil structures have rapidly increased over recent years for the following reasons (Ambauen 2014):

a. Because of their flexibility, GRS retaining structures are more tolerant to differential movements than conventional retaining structures or concrete faced reinforced walls.

b. Geosynthetics are more resistant to corrosion and other chemical reactions than other reinforcement materials such as steel.

c. GRS retaining structures are cost effective because the reinforcement is cheaper than steel and construction is more rapid in comparison to conventional retaining walls.

2.1.1.3 Geosynthetics Reinforced Soil Bridge Abutments

Geosynthetics reinforced Soil Bridge abutments are an increasingly common means of earth retention for a variety of applications. Their function is simple and efficient; using tensile reinforcements and a stiff facing to allow for soil to retain itself as well as surcharge loads. This coupled stability problem can be difficult to fully evaluate using current design methodology. The lateral earth pressure approach has been refined to include a variety of geometries, but little insight exists into the stability and design requirements for GRS structures supporting a footing – an increasingly important function, especially in context of these true reinforced soil bridge abutments. A true reinforced soil bridge abutment supports the deck via spread footings instead of the conventional method of using of piles or shafts, which carry the bridge load and essentially bypass the reinforced structure (Ambauen 2014). Along with simplifying construction, the use of directly loaded reinforced soil abutments reduces differential settlement and minimizes the "bump" at transition from bridge to embankment (Admas 1999).When a reinforced soil true bridge abutment is designed to support the bridge superstructure, as well as retain the approach embankment, the service-state deformations and reinforcement working stresses become critical to the overall performance of the system (Helwany 2003). Additionally, GRS bridge abutments have been shown to exhibit high static and dynamic performance under static cyclic load tests and shake-table tests (Tatsuoka 2009). Hence, Geosynthetics reinforced integrated bridge systems offer substantial advantages over other bridge abutment methodologies (Ambauen 2014).

Reinforced soil is a composite construction material formed by combining soil and reinforcement.

This material possesses high compressive and tensile strength similar, in principle, to the reinforced cement concrete. One of the common applications of soil reinforcement is a reinforced soil retaining wall which is an alternative to a conventional heavy concrete/brick masonry/stone masonry retaining wall Reinforcement improves the mechanical properties of a soil mass as a result of its inclusion.

Figure 2.1 shows typical application of Geosynthetics materials in retaining walls and slopes (Guru Nanak 2012).

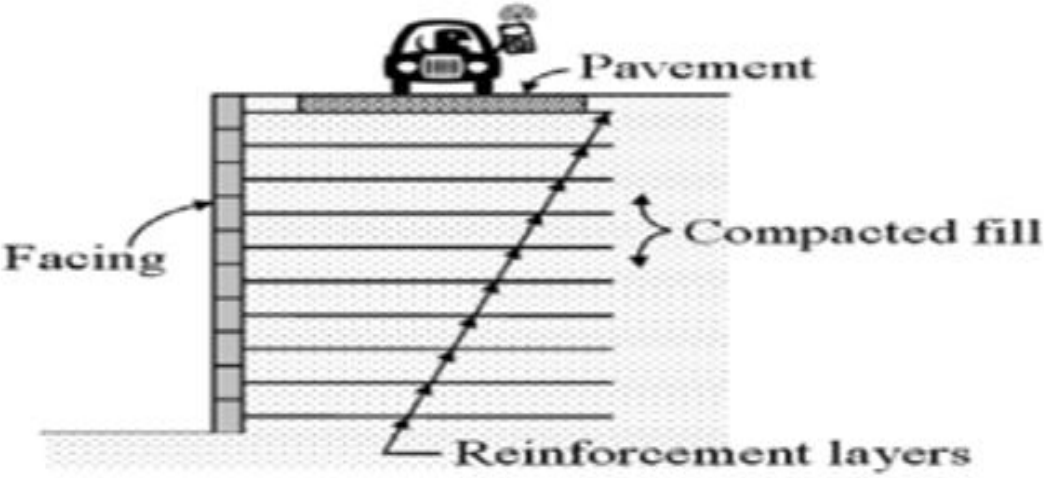

Figure 2. 1 Soil Reinforcement Application on Retaining Walls (Guru Nanak 2012)

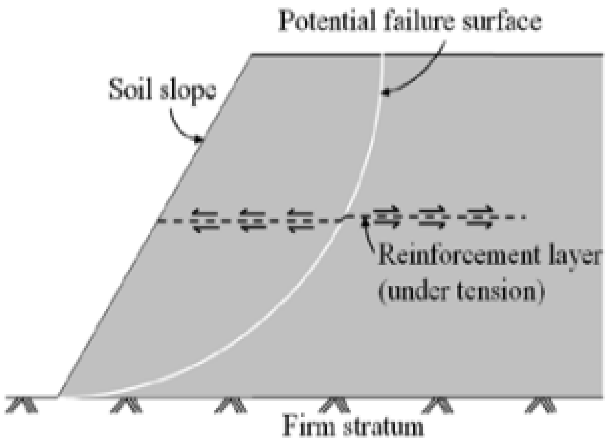

Figure 2. 2 Effect of Reinforcement on Stability of Slope (Guru Nanak 2012)

2.1.2 Applications of Reinforcements in Retaining Walls

Reinforced soil material has the characteristics of load transfer between soil and inclusion take place continuously along the inclusion, that is the load transfer mechanism should be by ‘reinforcement’ and this reinforcement be distributed throughout the soil mass with a certain regular interval.

2.1.2.1 Stress transfer mechanisms

Stresses are transferred between soil and reinforcement by two mechanisms: friction and passive resistance (FHWA 1990).

Passive resistance: this resistance occurs through the development of bearing type stresses on transverse reinforcement surfaces normal to the direction of soil reinforcement relative movement. Passive resistance is generally considered to be the primary interaction for geogrid, bar mat and wire mesh type reinforcement.

Friction: friction develops at the locations where is a relative shear displacement and corresponding shear stress between the soil and reinforcement surface. Reinforcing elements where friction is important should be aligned with the direction of the soil reinforcement relative movement. Example of such reinforcing element is geogrid.

2.1.2.2 Reinforcing materials

The reinforcing materials in reinforced earth retaining walls have mechanical property, i.e. load-strain-time (stiffness) and geometry properties. The deformation of reinforcement at failure is much less than deformation of the soil the reinforcement is said to be inextensible. But when we see extensible reinforcements the deformation of reinforcement at failure is comparable to or even greater than the deformation of soil. If the reinforcement is highly extension under stress but adequate tensile strength the soil may show large movement. Under the load application the horizontal force that is tension was developed in the reinforcement and the most critical slip surface in the reinforced soil wall is assumed to concede with the maximum tension forces line for each layer. For inextensible reinforcements the failure surface is bilinear and for extensible reinforcements linear failure surface were observed as Shown in figure 2.3 (FHWA 1990)

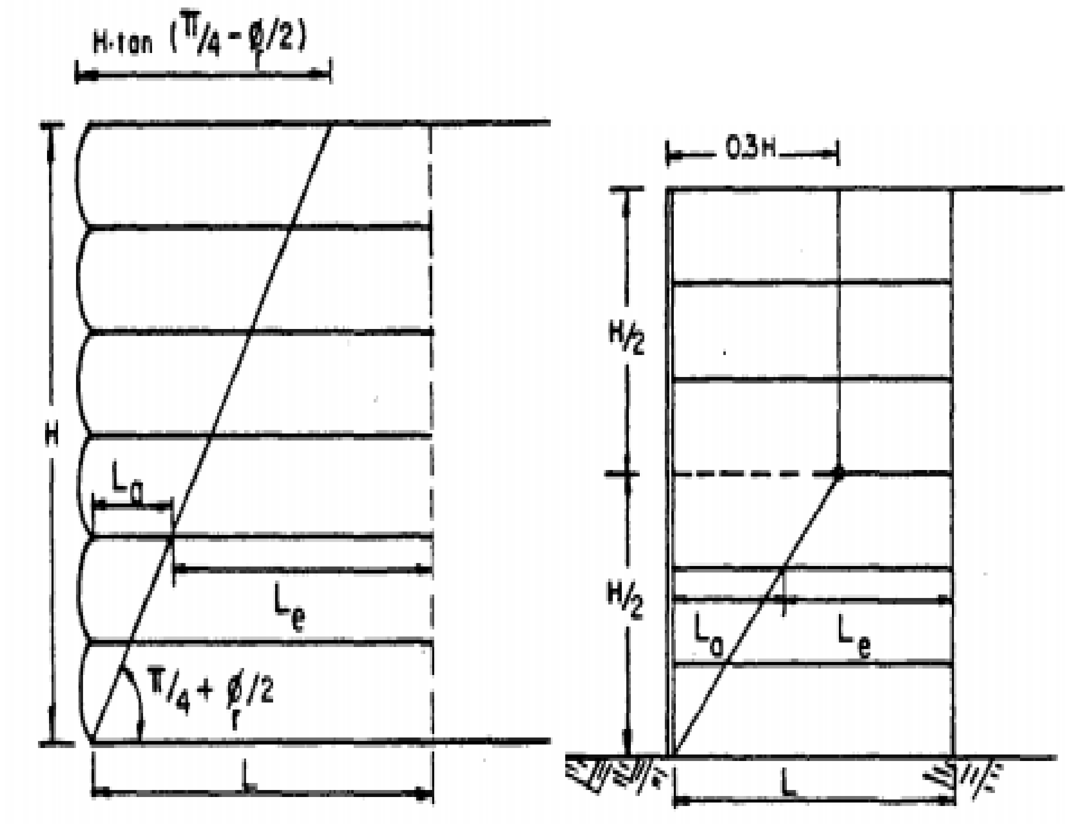

a) b)

Figure 2. 3 Failure Surface of GRS Wall a) Inextensible Reinforcement, b) Extensible Reinforcements

2.1.2.3 Geogrid

The use of geogrid has another benefit owing to the interlocking of the soil through the openings which is known as interlocking effect. But for soils of significant fine contents the transfer of stress from the soil and geogrid reinforcement is made through bearing at the interface and also when soil particles are small interlocking effect is negligible (Guru Nanak 2012).The transfer of stress from the soil to the geogrid reinforcement is made through bearing (passive resistance) at the soil to the grid cross-bar interface. It is important to underline that because of the small surface area and large apertures of geogrid, the interaction are due mainly to interlocking rather than to friction. However, an exception occurs when the soil particles are small. In this situation the interlocking effect is negligible because no passive strength is developed against the Geogrid.

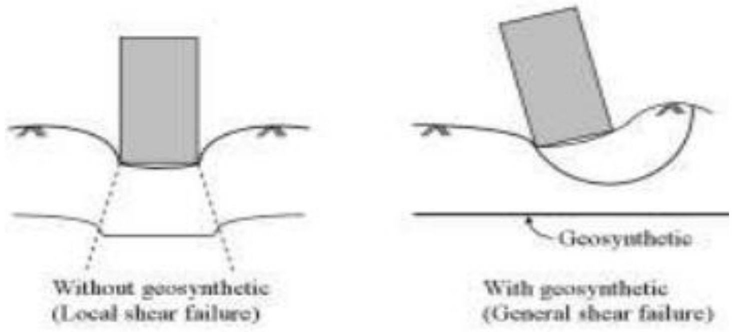

a)

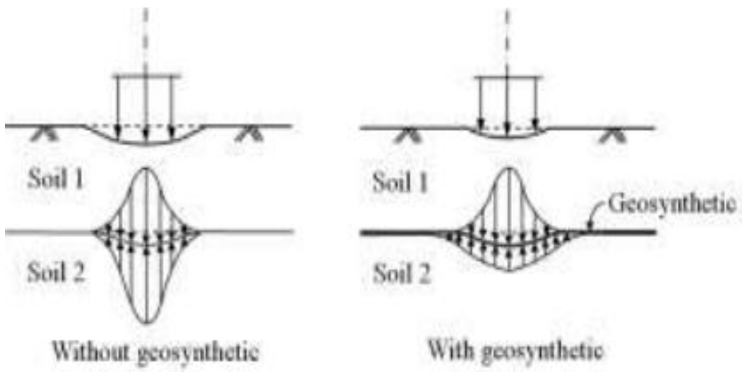

b)

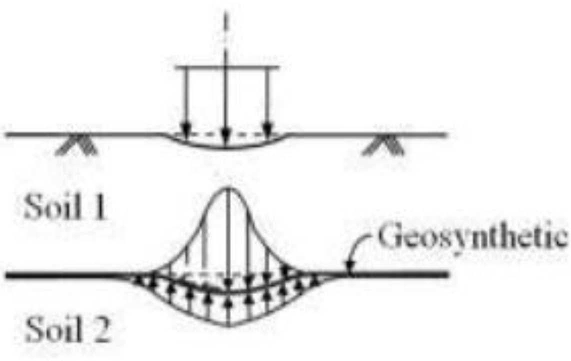

c)

Figure 2. 4 a) Failure Mode (shear stress reduction effect), b) Redistribution of Applied Surface Load (confinement effect), c) Providing Vertical Support, (membrane effect) (Guru Nanak 2012)

2.2 Stability of Reinforced Earth Retaining Walls

Earth retaining structures has two sets of failure criteria's to be satisfied, one is the internal stability and the other one is external stability. External stability was determined like that of gravity retaining walls. The internal stability depends on the tensile strength of the reinforcing material and the interface friction between reinforcing material and the soil. The tensile failure of reinforcing material at any depth leads to progressive collapse of the wall.

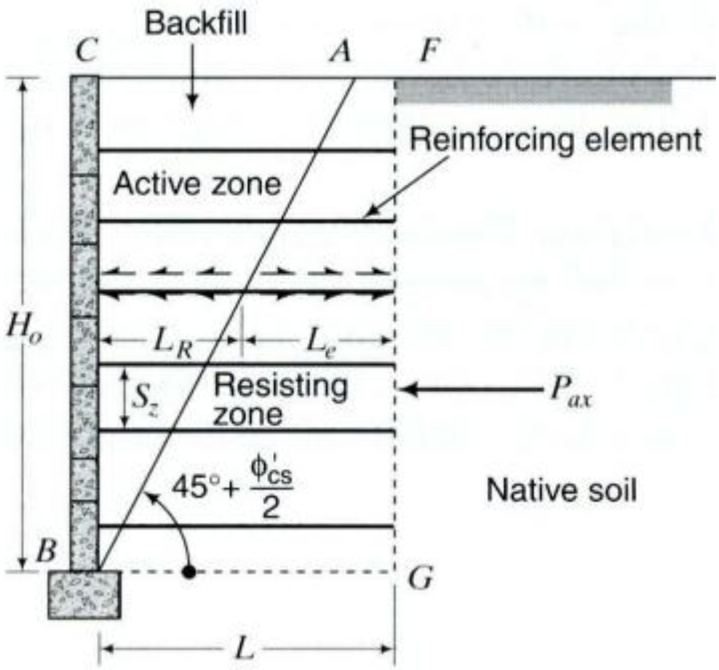

Figure 2. 5 Forces on Earth Retaining Structure (Budha 2008)

2.2.1 Mode of failure of reinforced soil walls

Reinforced soil wall design consists of determining the geometric and reinforcement requirements to prevent internal and external failure (FHWA 1990).

Internal failure: there are two modes of internal failures:

- By breakage or excessive elongation of reinforcements
- By reinforcement pullout

Each mode of failure can be analyzed using the maximum tensile force line. This line is assumed to be the most critical potential slip surface. The length of reinforcement extending beyond this line will thus be the available pullout length.

External failure: as with conventional unreinforced retaining structures, four potential external failure mechanisms are usually considered for reinforced soil structures as shown in figure 2.6. They include:

- Sliding on the base
- Overturning
- Bearing capacity failure
- Deep seated stability failure (rotational slip surface or slip along a plane of weakness).

2.2.1.1 Sliding stability

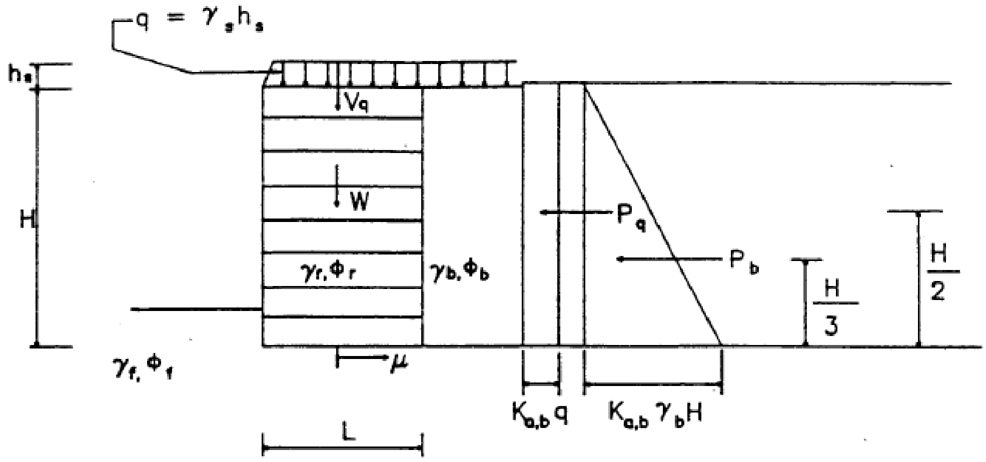

To Calculate FS $_{SLIDING}$:

$V_q = \gamma_s h_s L$

$W = \gamma_r HL$

$P_b = 0.5 K_{a,b} \gamma_b H^2$

μ = Minimum of $\tan\phi_r$ or $\tan\phi_f$ or $\tan\rho$

$K_{a,b} = \tan^2(\pi/4 - \phi_b/2)$

$P_q = K_{a,b} \gamma_s h_s H$

$$FS_{SLIDING} = \frac{\Sigma \text{ Horizontal Resisting Forces}}{\Sigma \text{ Horizontal Sliding Forces}} = \frac{(V_q + W)\mu}{P_b + P_q}$$

$$= \frac{[(\gamma_s h_s + \gamma_r H)\mu] L}{K_{a,b} H (0.5\gamma_b H + \gamma_s h_s)} \geq 1.5$$

Figure 2. 6 External Sliding Stability of A Reinforced Soil Wall with Extensible Reinforcement

2.2.1.2 Overturning

Owing to the flexibility of reinforced soil structures,' it is unlikely that a block overturning failure could occur.

Nonetheless, an adequate factor of safety against this classical failure mode will limit excessive outward tilting and distortion of a suitably designed wall. Overturning stability is analyzed by considering rotation of the wall about its toe. It is required that:

$$[FS]_o = \text{resisting moments/driving moments} \geq 2.$$

The resisting moments result from the weight of the reinforced fill, the vertical component of the thrust, and the surcharge applied on the reinforced fill (dead load only). The driving moments result from the horizontal component of the thrust exerted by the retained fill on the reinforced fill and the surcharge applied on the retained fill (dead load and live load).

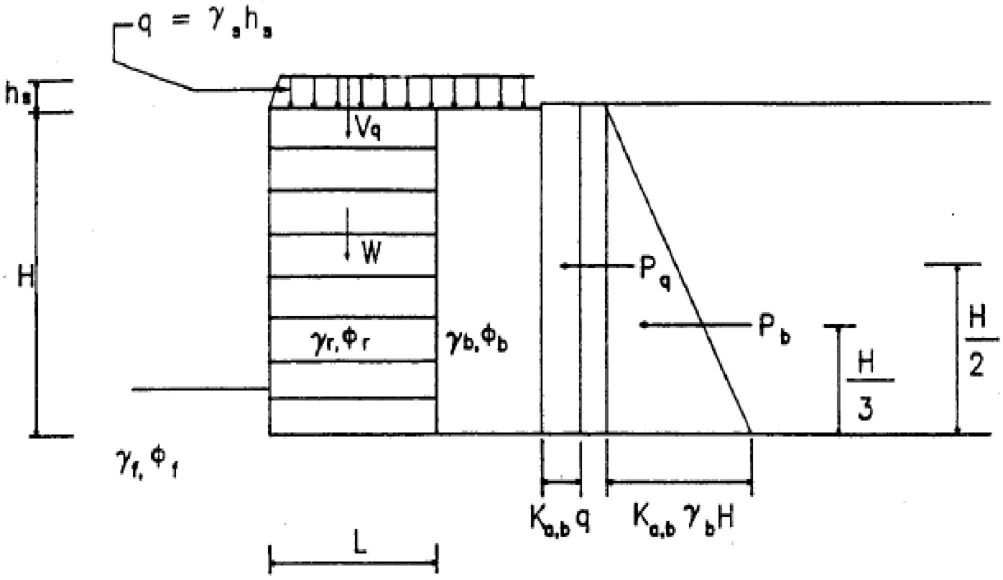

To Calculate FS OVERTURNING :

$V_q = \gamma_s h_s L$

$W = \gamma_r HL$

$K_{a,b} = Tan^2(45-\phi_b/2)$

$P_b = 0.5K_{a,b}\gamma_b H^2$

$P_q = K_{a,b}\gamma_s h_s H$

$$FS_{OVERTURNING} = \frac{\Sigma \text{ Moments Resisting}}{\Sigma \text{ Moments Overturning}} = \frac{(V_q + W)(L/2)}{P_b(H/3) + P_q(H/2)}$$

$$= \frac{3L^2(\gamma_s h_s + \gamma_r H)}{H^2 K_{a,b}(\gamma_b H + 3\gamma_s h_s)} \geq 2.0$$

Figure 2. 7 Extensible Overturning Stability of A Reinforced Soil Wall with Extensible Reinforcements

2.2.1.3 Bearing capacity

To prevent bearing capacity failure, it is required that the vertical stress at the base calculated with the Meyerhof distribution does not exceed the allowable bearing capacity of the foundation soil, determined considering a safety factor of 2 with respect to the ultimate bearing capacity:

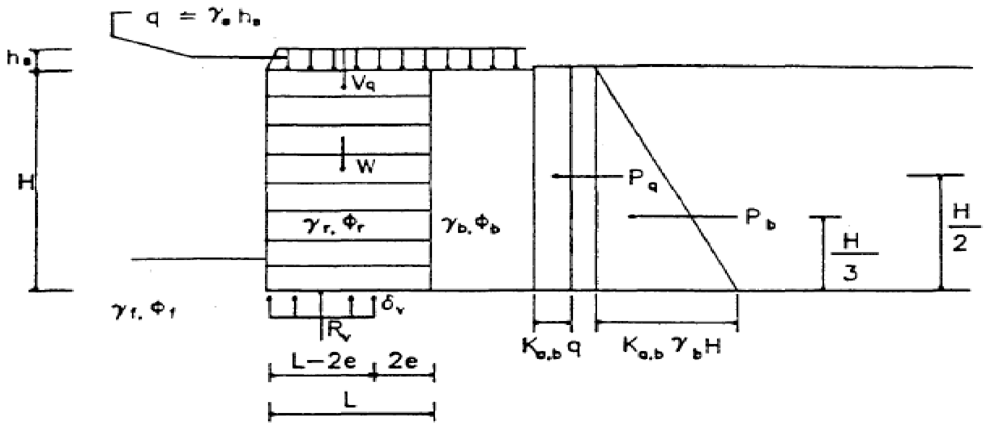

To calculate the bearing capacity :

$V_q = \gamma_s h_s L$

$W = \gamma_r H L$

$P_b = 0.5 K_{a,b} \gamma_b H^2$

$P_q = K_{a,b} \gamma_s h_s H$

$K_{a,b} = Tan^2(45 - \phi_b/2)$

q_a = allowable bearing capacity of the soil.

1) The eccentricity, e, of the resultant loads:

$$e = \frac{\Sigma \text{ Driving Moments}}{\Sigma \text{ Resisting Forces}} = \frac{P_b (H/3) + P_q (H/2)}{W + V_q}$$

$$= \frac{K_{a,b} H^2 (\gamma_b H + 3 \gamma_s h_s)}{6L (\gamma_r H + \gamma_s h_s)} \leq L/6$$

2) The magnitude of the vertical stress, $\sigma_{v\ max}$:

$$\sigma_{v\ max} = \frac{V_q + W}{L - 2e} = \frac{\gamma_r H + \gamma_s h_s}{1 - 2e/L} \leq q_a$$

where: $q_a = q_{ult}/2$

Figure 2. 8 Bearing Capacity for External Stability of A Reinforced Soil Wall with Extensible Reinforcement

Due to the flexibility and satisfactory field performance of reinforced soil walls, the adopted values for the factor of safety for external failure are lower than those used for reinforced concrete cantilever or gravity walls.

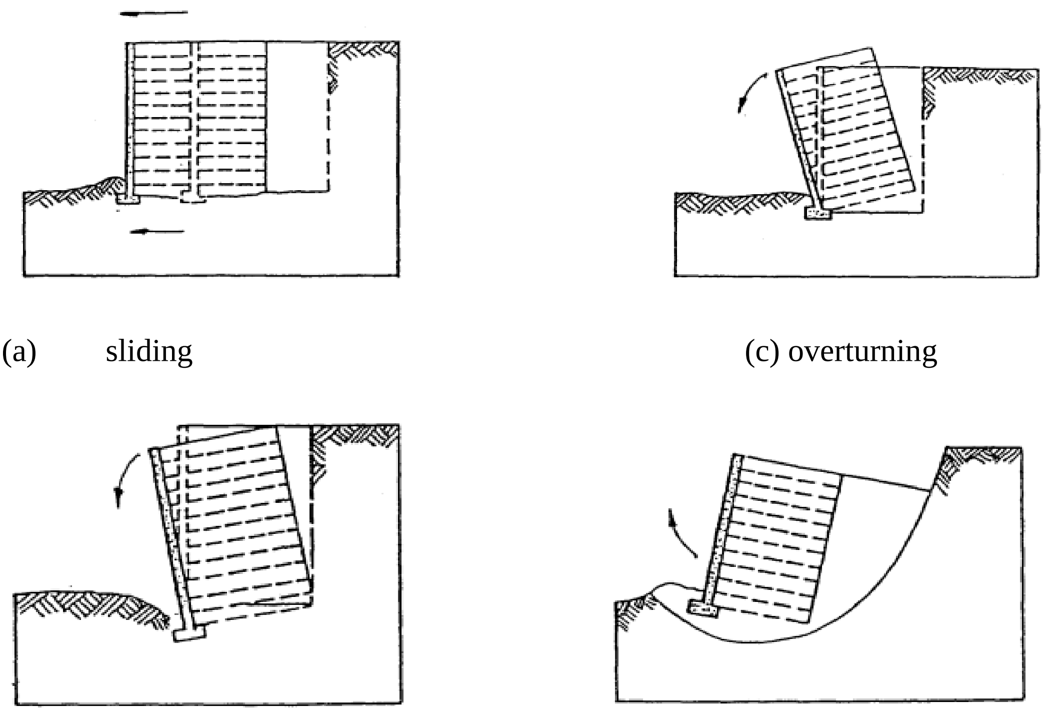

(a) sliding (c) overturning

(b) Bearing capacity (d) deep seated/ rotational slip surface

Figure 2. 9 External Failures of GRS Walls (FHWA 1990)

2.3 Finite Element Method

Finite element method (FEM) is a vigorous well-known method of numerically solving boundary value problems, which can accommodate highly non- linear stress-strain relations of materials including even creep, any geometrical configuration with complex boundaries, construction sequence, etc. FEM has been used as the standard tool for the design and analysis (e.g. prediction of safety factor and settlement analysis) of many geotechnical structures. Similarly, it is becoming a design and analysis tool for the reinforced soil structures. These features of FEM can be achieved only when material parameters, constitutive equations and boundaries are appropriately defined or modeled. Finite element method is the representation of a body or a structure by an assemblage of subdivisions called finite elements, these elements are considered to be interconnected at points, which are called nodes. This method is a numerical procedure for analyzing structures and continua. FEM is a powerful tool in structural analysis of simple to complicated geometries. (Oyegible 2011).

2.3.1 Modeling of Components: Soil, Reinforcement and Facing

The incorporation of mechanism of soil-reinforcement- facing interaction in the FEM are greatly influenced by the construction method, compaction, propping of facing during construction and its release later including the boundary conditions (loading on top, etc.), thus, making it difficult to model the problem.

Soil: most researchers as pointed out by (Gourc 1993), have adopted nonlinear elastic or elasto- plastic models. The initial deformation is sometimes calculated using linear elastic constitutive models and failure load is calculated using limiting equilibrium methods employing appropriate constitutive models e.g. van Mises or Mohr- Coulomb, Drucker- Prager etc.

Reinforcement: Geosynthetics are more favorable in most of the MSE wall applications, since they possess excellent resistance to corrosion. However, Geosynthetics are non-linear, elasto-plastic, or visco-plastic materials, which demand more sophisticated models to depict their behavior.

2.3.2 Modeling of MSE Wall Based On Continuum Approach

Numerical modeling of MSE walls comprises of, how the MSE wall system was simulated, which is itemized into the following six aspects (Bathrust 2001).

- ✓ How the backfill soil was modeled, i.e., constitutive models being used;
- ✓ How the MSE wall facing was modeled, i.e., constitutive model(s) for modular-blocks;
- ✓ How the Geosynthetics reinforcement was modeled; reinforcement strength
- ✓ How the interfaces were modeled, i.e., the interface between soil and modular-block, the interface between soil and Geosynthetics, and the interface between modular blocks;
- ✓ How the construction was modeled, i.e., compaction

2.4 Applicability of Cohesive Soils In MSE Walls

Using available low quality cohesive soil as a backfill material presents an economical and practical solution for the construction of reinforced-soil walls. Design specifications of reinforced-soil walls to date have focused on the use of high quality granular soil as a backfill material (Khalid Farrag 2004). For this purpose, the Louisiana Transportation Research Center (LTRC) has constructed a full-scale reinforced test wall with low quality backfill. The two major objectives of the test wall's construction were to investigate the interaction mechanism between various Geosynthetics materials and the Silty-clay and to monitor the state of stresses and deformations of the wall.

2.5 Summary of Previous Researchers

Behavior of Reinforced Soil Retaining Walls under Static Loads by Using Plaxis (Ramulu 2017)**.**

Case studies and analyses of reinforced soil retaining walls were carried out. The behavior of the walls under static loadings was investigated numerically with the aid of finite element program-Plaxis. The finite element analyses provide relevant information on the mechanical behavior of the wall that was otherwise difficult to obtain from the limit equilibrium based current design approaches. Practical implications of the findings of this study are highlighted along with the role of numerical modeling in the analysis and design of Geosynthetics - reinforced retaining walls. Using loose and dense sand backfill materials the general performance in reinforced retaining structure was observed.

Numerical Evaluation of the Behavior of Reinforced Soil Retaining Walls (Mirmoradi 2013)**.**

The numerical approach was validated with the results of a wrapped-faced full-scale reinforced soil wall. In addition, parametric studies were carried out with different combinations of: facing type, reinforcement stiffness, compaction efforts, and shear resistance parameters of the backfill soil. An increase of reinforcement stiffness led to greater values of tension in the reinforcement for both wrapped and block faced walls. Moreover, an increase of backfill soil shear resistance led to lower values of tension in the reinforcements. In addition block facing wall, the maximum tension in the reinforcement occurred near the mid-height of the wall.

Clay Reinforcement Using Geogrid Embedded In Thin Layers of Sand (M.R. Abdil september 2009)

Large size direct shear tests (i.e.300 x 300mm) were conducted to investigate the interaction between clay reinforced with Geogrid embedded in thin layers of sand. Test results for the clay, sand, clay-sand, clay-Geogrid, sand-Geogrid and clay-sand-Geogrid are discussed. Thin layers of sand including 4, 6, 8, 10, 12 and 14mm were used to increase the interaction between the clay and the Geogrid. Effects of sand layer thickness, normal pressure and transverse Geogrid members were studied. All tests were conducted on saturated clay under unconsolidated- undrained (UU) conditions. Test results indicate that provision of thin layers of high strength sand on both sides of the Geogrid is very effective in improving the strength and deformation behavior of reinforced clay under UU loading conditions. Using Geogrid embedded in thin layers of sand not only can improve performance of clay backfills but also it can provide drainage paths preventing pore water pressure generations. For the soil, Geogrid and the normal pressures used, an optimum sand layer thickness of 10mm was determined which proved to be independent of the magnitude of the normal pressure used. Effect of sand layers combined with the

Geogrid reinforcement increased with increase in normal pressures. The improvement was more pronounced at higher normal pressures.

Evaluation of mechanical behavior of a Brazilian marginal soil for reinforced soil structures (Patias 2006)

Marginal soils are characterized by a large percentage of fine particles and, in general, are not recommended by current standard codes as backfill material for reinforced soil structures because of their poor draining capacity and low shear strength. Notwithstanding, in Brazil, reinforced soil structures are often built using fine soils due to their large availability. Case studies of historical importance in Brazil show a very good long-term performance. This behavior occurred probably due to the significantly different characteristics of tropical soil compared to similar soils from the northern hemisphere, since tropical soils show excellent shear strength parameters and relatively low compressibility's. To carefully verify the changes in mechanical behavior caused by reinforcing inclusions, an experimental program based on Triaxial compression tests was carried out. The tested soils were classified as sandy Silty clay (according to the Brazilian Standard Code for grain size analysis-ABNT-NBR 7181) and lateritic soil according to the MCT classification system. Unconsolidated-undrained and consolidated-undrained Triaxial tests were carried out on unreinforced and reinforced specimens. The specimens were reinforced with inextensible and impermeable aluminum foil and extensible and permeable nonwoven geotextiles as inclusions. A comparison of the results obtained for the unreinforced and reinforced cases confirmed an increase in stiffness for geotextiles inclusion reinforced specimens under short and long terms analyses. For the geotextiles reinforced soil, the mobilized cohesion parameter was found to increase even for higher values of strain in the two situations analyzed.

Numerical Modeling of Geosynthetics-Reinforced Earth Structures and Geosynthetics Soil Interactions (J.Huang 2011)

Geosynthetics have been used as a routine reinforcement in earth structures such as mechanically stabilized earth (MSE) walls, column-supported embankments, soil slopes, and paved/unpaved roads. In those applications, reinforcement mechanisms of the Geosynthetics are vaguely described as confinement, interlocking, and load shedding respectively but not fully understood. The uncertainties of the mechanisms have been reflected as over conservativeness, inconsistence and empiricism in current design methods of those applications. Numerical modeling characterized as cost- and time- saving, is preferred in many circumstances. An appropriate modeling strategy is vital to yield reliable results. His paper reviewed and summarized the modeling techniques used to model modular-block MSE walls, reinforced embankments/slopes, and reinforced paved/unpaved roads, which include conventional continuum modeling based on constitutive relationships as well as micro-mechanical modeling based on Newton's law of motion. The objective of his paper is to provide a state-of-art review of the various numerical modeling techniques and consequently promote the usage of numerical modeling in research and practice of Geosynthetics-reinforced earth structures.

Numerous case studies of field, laboratory and numerical GRS walls were also mentioned to establish the need for more extensive research into the complex behavior of these composite structural systems; both to ensure adequate performance and to reduce conservatism through greater understanding and refinement of design approaches. The application of poor quality backfill material were uncertain till now for researchers and design specifications thus investigate the behavior of reinforced earth retaining walls in numerical modeling using finite element method PLAXIS software is vital.

CHAPTER 3
MATERIALS AND METHODS

3.1 Analysis Using Modeling Software

Different analysis methods have been used for many structures including earth retaining walls. But analysis of those structures using modeling software's was preferable due to variety of reasons. Despite of difficulties to obtain accurate model of the case and approximate result finding; modeling software's increase our computational speed, scale effects, minimum measurement errors are not the problem of analyzing using modeling software's among many others.

3.1.1 Continuum model analysis approach

The use of full-scale tests to establish design parameters is desired choice in soil-Geosynthetics interaction simulations. However, the significant scattered and insufficient data from experiments indicates obvious difficulties in being able to clearly assess soil–Geosynthetics interaction in the complex environment that nature presents. The finite element method (FEM) is based on the concept that one can replace any continuum by an assemblage of simply shaped elements with well-defined force–displacement and material relationships (J.Huang 2011). While one may not be able to derive a closed-form solution for the continuum, one can derive an approximate solution for the element assemblage that replaced it.

3.1.2 Plaxis 2D software

In this project the finite element software, PLAXIS (Vermeer and Brinkgreve, 1998), was employed to model reinforced soil retaining structures. In this finite element program a two-dimensional plane-strain model is used. A geometrical model in this program is a representation consisting of points, lines and clusters. The program automatically recognizes clusters based on the input geometry lines. Within the cluster the soil properties are homogeneous (Brinkgreve and Vermeer 1998). In the 2D analyses, I used the triangular elements which are 15 node elements this is due to obtaining highly accurate element that can produce quality results of stress and displacements. While 15 node element consumes more memory and relatively slow calculation time. Displacements are calculated at the nodes, whereas the stresses in each element are calculated at the stress points. The element stiffness matrix is evaluated by numerical (Gaussian) integration using the three stress points. The reinforced structure was modeled with the same properties as the unreinforced model, the only difference being a Geogrid-reinforcement placed at the interface between soil layers. (Brinkgreve 2002).

3.1.2.1 Input

The software requires the following parameters to model the problem; which are retaining wall width & height, soil and interface properties such as material model type, unit weight, permeability, Young's modulus, Poisson's ratio, cohesion, friction angle, Dilatancy angle, interface reduction factor, Geogrid properties such as Geogrid axial stiffness, length, installation, spacing, modulus of elasticity and facing material properties. For the generation of mesh it is advisable to set the Global coarseness to medium. In addition the stress concentration is expected around the reinforcement materials so a local refinement is proposed here. Then finally the initial conditions are generated (Brinkgreve 2002).

3.1.2.2 Conditions and process

The structure construction follows a staged construction process which consists of different phases. All calculation phases are defined as plastic calculation using staged construction as loading input and standard settings for all other parameters. The activities involved in each phase of the staged construction that are used for this research model can be stated as follows:

Phase 1: Activate the first layer of construction including facing walls, backfill material, Geogrid and interfaces

Phase 2: Activate the next cluster of the construction like phase 1 and all the construction will continue like this.

3.1.2.3 Output

The outputs of the PLAXIS analysis are presented numerically incorporated with pictorial representation. The results of the analysis include wall, facing and Geogrid deformations, Geogrid loads and maximum load locations. The lateral deformation and reinforcement loads of the retaining wall for the different case studies are presented on the next chapter. The different outputs of the analysis for each phase and each case can found on the annex portion of the paper and it demonstrated some of the outputs found from the software pictorially.

3.1.3 Soil model

Soil behavior has lots of complexities and using a comprehensive soil model which can capture these complexities is the ideal solution for research and study. For each problem some simplifications are needed to find the proper model depending on the nature and aspects of the problem. The Mohr-Coulomb model is a classic model used to represent shear failure in soils and rocks. The Mohr-Coulomb model simulates elastic-perfectly plastic behavior. The elastic behavior is linear.

3.1.4 Constitutive Models for Soil Reinforcement Interface:

There are several constitutive models for normal stress and relative displacement relations that has been developed which can be divided as: linear elastic-perfectly plastic, hyperbolic, and Elastic-plastic model, the shear strength of the interface is governed by Mohr-coulomb failure criteria.

3.1.5 Continuum Model Validation

The study is based on numerical analyses; therefore, the validity of the numerical model should be evaluated thoroughly. Validation is the procedure of determining the degree to which a model is an accurate representation of the real world from the perspective of the intended uses of the model. Previous research data's and studies of full scale tests and analytical solutions on reinforced earths are used as a primary validation. Some studies report direct comparison of numerical results and experimentally measured results from full scale instrumented walls. According to survey by Bathurst and Hatami (2001) classified the numerical modeling attempts into two major groups on the basis of whether or not numerical results were compared with measurements from physical models, including field-instrumented walls. Many of the studies reviewed by the authors investigated the response of idealized reinforced soil wall models. In this thesis models were idealized model walls that quantitatively and qualitatively report results and comparison of different case studies.

3.2 Numerical Modeling

3.2.1 General Information about the Model

Model inputs and outputs of the study reinforced retaining wall were reported with the units shown in table 3.1.

Table 3. 1 Units

Type	**Unit**
Force	kN
Length	M
Time	Day

Table 3. 2Model and Element

Model	Plane strain
Element	15-Noded

Table 3.3 Wall Model Dimension

Axis	Minimum(m)	Maximum(m)
X	0	14.5
Y	0	7

3.2.2 Soil Models and Input Parameters

The backfill used in the wall was soft clay, medium sand and stiff clay soils in which the material model is based on Mohr coulomb model. Elastic modulus, Friction angle, Cohesion, Poisson’s ratio, Dilation angle and Unit weight are Mohr coulomb material models.

3.2.3 Reinforcement Model and Material Properties

Geosynthetics have been modeled as simple linear elastic, non-linear elastic, elastic-plastic, and viscos-plastic materials, depending on chemical compositions, loading conditions, and exposure to temperature fluctuations. Commonly, Geosynthetics are deemed of zero compressive strength. The load-strain response relationship is in reality a tension-strain response. Some of properties of Geosynthetics materials include Tensile strength and Stiffness. Reinforcement layers were modeled as tension-only elastic elements, which simulates a geogrid.

3.2.3.1 Modular Blocks

To simulate the modular blocks as a concrete material a high value of cohesion of 200 kN/m^2 and an internal friction angle of 35^0 and a higher elasticity modulus of 300 000 kN/m^2 was assigned to the modular facing elements. Precast concrete blocks of size 400mm width and 200mm height were used.

3.2.3.2 Interfaces

The complexity of the MSE wall system is largely attributed to the materials of dissimilar properties, including backfill soil, Geosynthetics reinforcement, and modular blocks. The interactions between these materials have to be appropriately represented in order to explore the reinforcing mechanisms. Various approaches have been used to simulate the interfaces between backfill soil and Geosynthetics, between modular blocks and backfill soil, and between modular blocks.

Interface between backfill soil and Geosynthetics has negligible bending stiffness, thus, the interaction between Geosynthetics and backfill soil occurs mainly through surface friction and particle interlocking. Mohr-Coulomb slip interface, characterized as a linear spring slider assembly with slippage governed by the Mohr-Coulomb criterion, is the most commonly used one to represent the interface between Geosynthetics and backfill soil. The key of using this interface is to select suitable parameters for interface. The frictional parameters of the interface can be easily derived from friction angle and cohesion of the backfill soil by applying reduction factors (J.Huang 2011).

Table 3. 4 Interface Friction Reduction Factor

Interface reduction factor	R_{inter}
For stiff clay soil	0.5
For medium sand soil	0.67
For soft clay soil	0.5
Block to block	0.7

3.2.4 Construction Simulation

The MSE walls are constructed by sequential placement of modular blocks, Geosynthetics layers, and backfill soil from the bottom to the top. During the process, compaction is exercised to meet the relative density requirement. The backfill soil compaction has two effects: (1) increasing the lateral earth pressure; and (2) reducing Poisson's ratio. Neglecting compaction leads to significant underestimation of lateral deformation at the end of construction; in some cases as much as 6mm. Additionally, induced compaction stresses increase tension in the reinforcements through the construction process; leading to a different distribution of reinforcement strains than if compaction was not simulated (Ambauen 2014).

The compaction effect included in the modeling was equivalent static uniform vertical stress of 8 kPa (vibrating plate compactor) that represented the compaction effect regardless the compaction methods for each layer (Bathurst 2005).

3.3 Checking The External Stability Of The Proposed Models

External failure of the reinforced soil mass is generally assumed to be possible by:

- ✓ Sliding of the stabilized soil mass over the foundation soil.
- ✓ Bearing capacity failure of the foundation soil.
- ✓ Overturning of the stabilized soil mass.
- ✓ Slip surfaces failure entirely outside the stabilized soil mass.

Factors of safety for external stability are based on classical analysis of reinforced concrete and gravity wall type systems.

3.3.1 Checking sliding stability

Table 3. 5 checking sliding stability of the model walls

Models	γ_r (kN/m^3)	H (m)	L (m)	$Ø_f$	$Ø_b$	$K_{a,b}$	Resisting forces	Sliding forces	FOS
Model 1	18	4	3	35	20	0.2245	102.34	32.33	3.16>1.5 safe!
Model 2	20	4	3	35	34	0.0792	113.71	12.67	8.97>1.5 safe!
Model 3	19	4	3	35	28	0.1951	108.03	29.65	3.64>1.5 safe!

3.3.2 Checking overturning

Table 3. 6 checking overturning stability of model walls

Models	γ_r (kN/m^3)	H (m)	L (m)	Ka	Pa (kN/m)	Resisting moment (Mwr)	Driving moment (Md)	FOS_o
Model 1	18	4	3	0.2245	32.33	324	43.104	7.51>2 Safe!
Model 2	20	4	3	0.0792	12.67	360	16.89	21.3>2 Safe!
Model 3	19	4	3	0.195	29.65	342	39.54	8.65>2 Safe!

3.3.3 bearing capacity

Determining the ultimate bearing capacity q_{ult} using Meyerhof's recommendation (KANIRAJ 2008)

Table 3. 7 ultimate bearing capacity calculation

Item	$Ø_f$	Nc	Nq	$N\gamma$	$q_{ult}/2$
foundation	35	46.4	33.6	37.8	5082.43

Table 3. 8 checking bearing capacity of model walls

Models	$\gamma_{r,f}$ (kN/m^3)	H (m)	L (m)	Ka	Pa (kN/m)	e<=L/6	δv	$q_{ult}/2$	$\delta v <= q_{ult}/2$
Model 1	18	4	3	0.2245	32.33	0.1995	83.05	5082.43	Safe!
Model 2	20	4	3	0.0792	12.67	0.0704	83.93	5180.34	Safe!
Model 3	19	4	3	0.195	29.65	0.1734	85.93	5116.38	Safe!

Since our assumption at the beginning doesn't allow any failure at the foundation soil; bearing capacity was safe. So in general our models was safe in external stability analysis; those models then be analyze with Plaxis 2D program.

3.4 PLAXIS 2D Analysis

PLAXIS has both the options undrained and drained in its material property input. If reinforced retaining soil wall were only used as temporary support structures, Then the soil retained could be modeled as undrained material since the time of construction is relatively short as compared to other constructions. For undrained case, the effective soil parameters or the drained soil parameters are entered because the PLAXIS automatically adds bulk stiffness for the water and distinguishes between effective stresses and excess pore pressures.

3.4.1 Geometric Model

The PLAXIS model used in this study is geosynthetically reinforced earth retaining wall type. This model type has reinforced backfill of 4m height and the width of 11.4m including 40cm width and 20cm height facing block units. All the reinforcements has a length of 3m, varied stiffness and varied vertical spacing, the soil layers constructing with 20cm thickness with the compaction effort of 8 kN/m^2uniform vertical pressure for each layer.

3.4.2 Boundary Condition

A fixed boundary condition in the horizontal direction was assumed at the numerical grid points on the backfill far-end boundary allowing for free settlement of soil along that boundary. A fixed boundary condition in both horizontal and vertical directions was used at the bottom boundary.

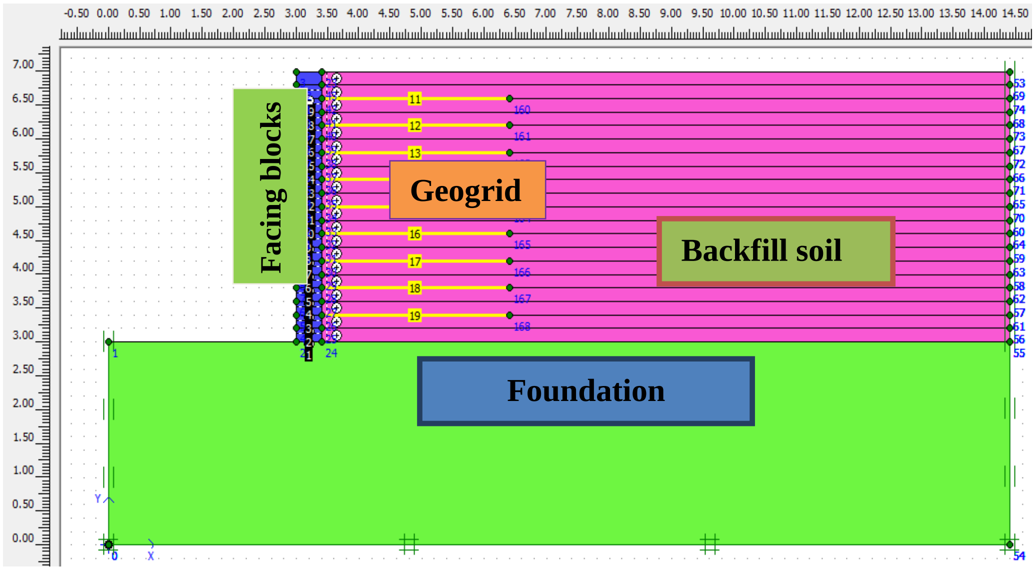

Figure 3. 1 Reinforced Soil Wall Model

This PLAXIS model is used for analyzing the performance of reinforced earth retaining walls by using different geogrid strength, geogrid spacing, geogrid length, surcharge pressure applied and backfill soils properties.

Table 3. 9 Soil data parameters

Mohr Coulomb	Model 1	Model 2	Model 3
	Soft Clay	Medium Sand	Stiff Clay
Type	Drained	Drained	Drained
γunsat [κN/m3]	16	18	17
γsat [κN/m3]	18	20	19
kx [m/day]	0.001	0.001	0.001
ky [m/day]	0.001	0.001	0.001
Eref [kN/m²]	25000	50000	30000
ν [–]	0.25	0.3	0.2
Cref [kN/m²]	10	2	20
φ [°]	20	34	28
ψ [°]	0	2	0
Rinter. [-]	0.5	0.67	0.5

Table 3. 10 Reinforcement data parameters

Reinforcement	EA [kN/m]	Sz [m]
Geogrid	1500	0.4

3.4.3 Foundation

In order not to allow any failure inside the foundation soil, a high cohesion (c = 200 kN/m2) and internal friction angle (phi = 35) were assigned to the foundation soil. The elastic moduli of the foundation soil were taken as 50000 kN/m^2.

3.4.4 GRS wall Displacements

The analysis results compared and reported here shown in the Figure 3.2was the maximum horizontal displacement and Figure 3.3 shows maximum vertical deformations.

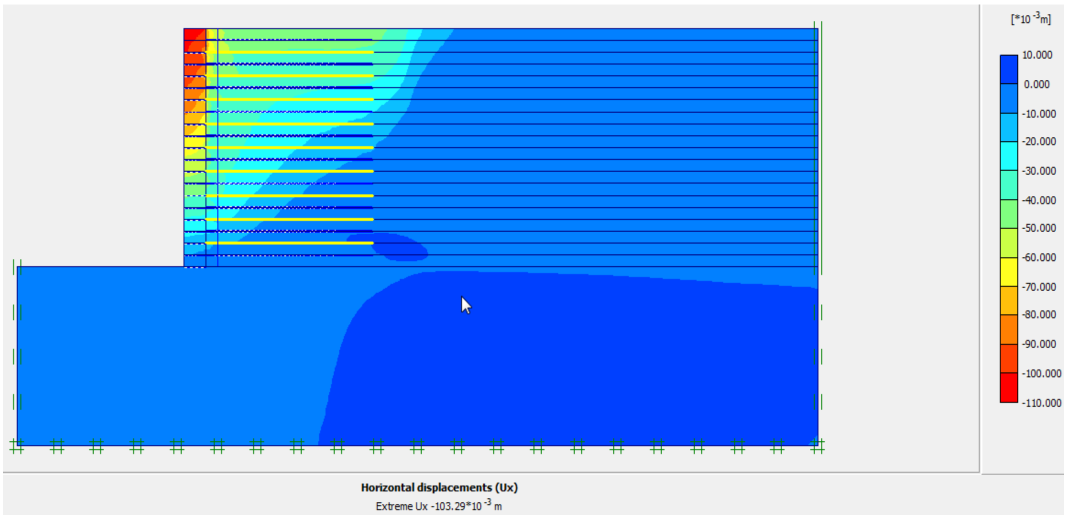

Figure 3. 2 Horizontal Displacement of GRS Wall with Soft Clay Backfill

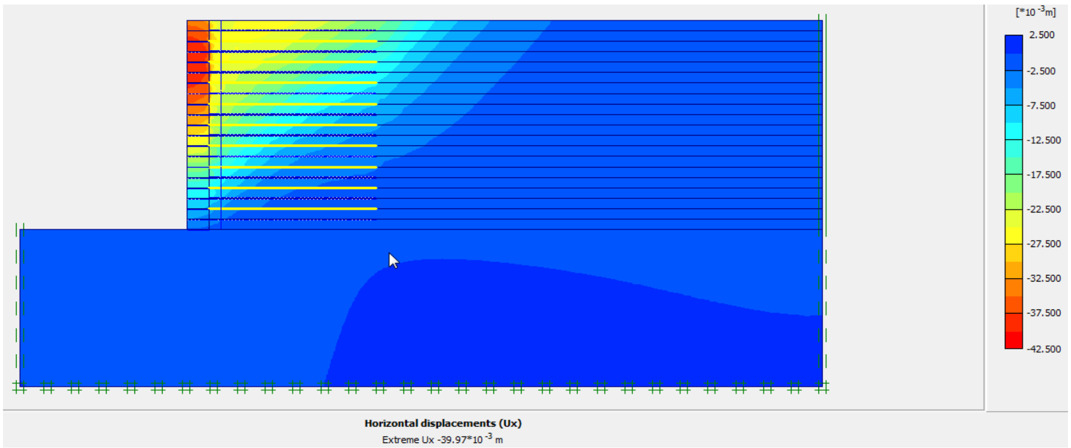

Figure 3. 3 Horizontal Displacement of GRS Wall with Medium Sand Backfill

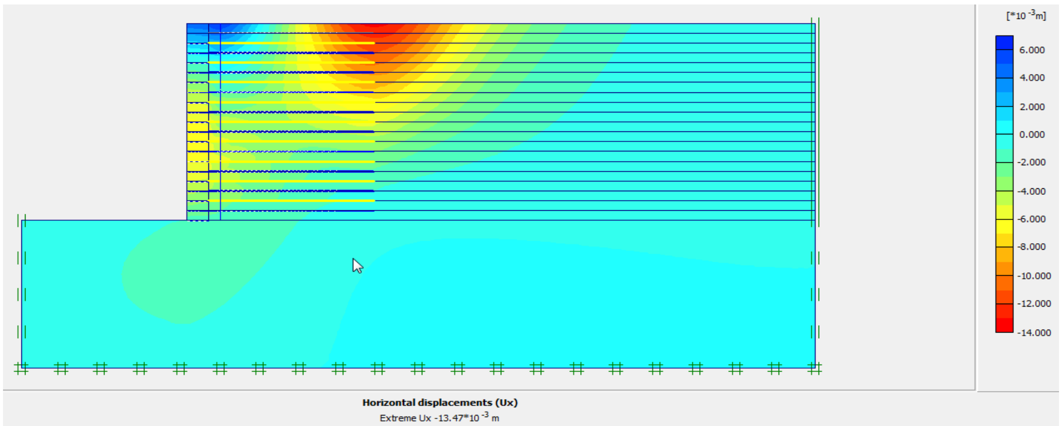

Figure 3. 4 Horizontal Displacement of GRS Wall with Stiff Clay Backfill

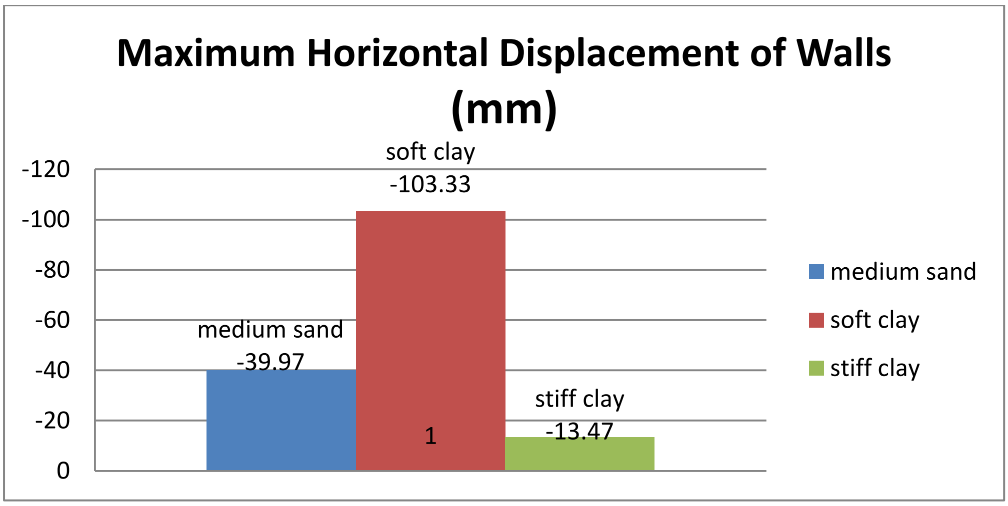

Figure 3. 5 Maximum Horizontal Displacements of GRS Walls

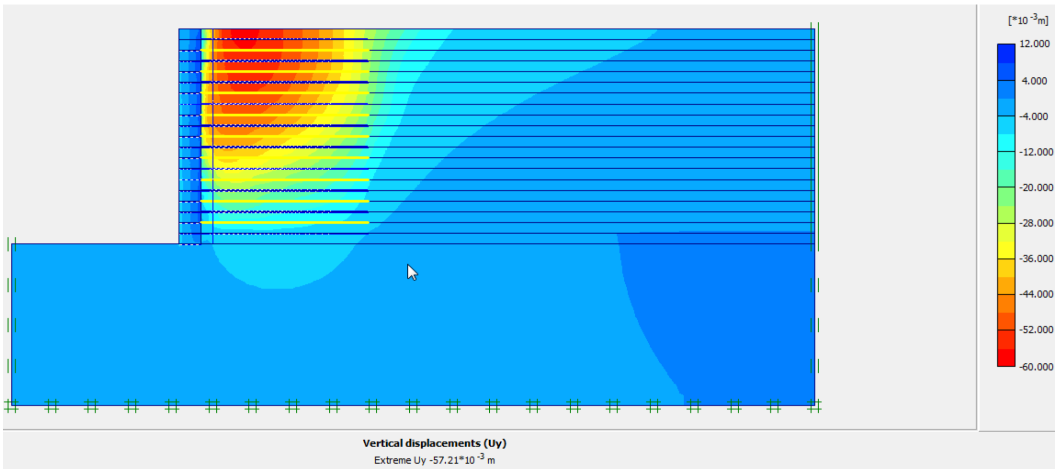

Figure 3. 6 Vertical Displacement of GRS Wall with Soft Clay Backfill

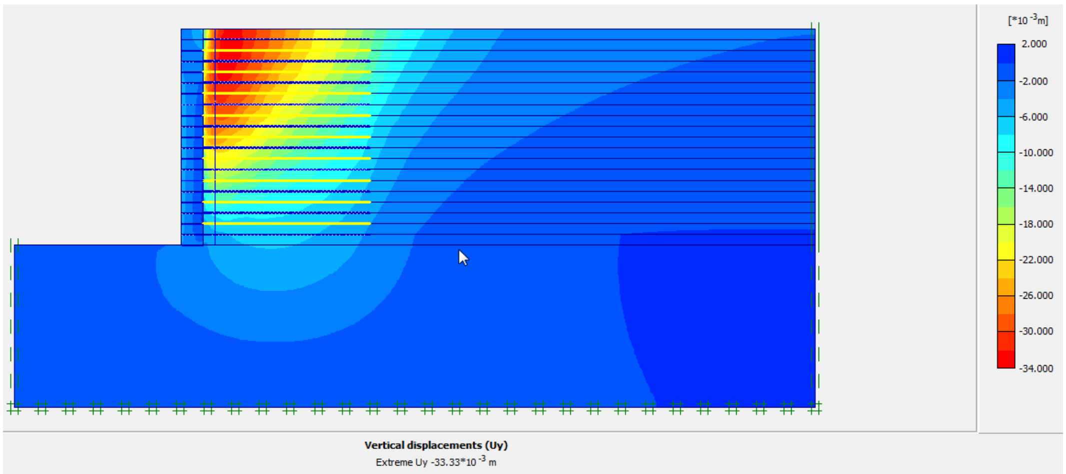

Figure 3. 7 Vertical Displacement of GRS Wall with Medium Sand Backfill

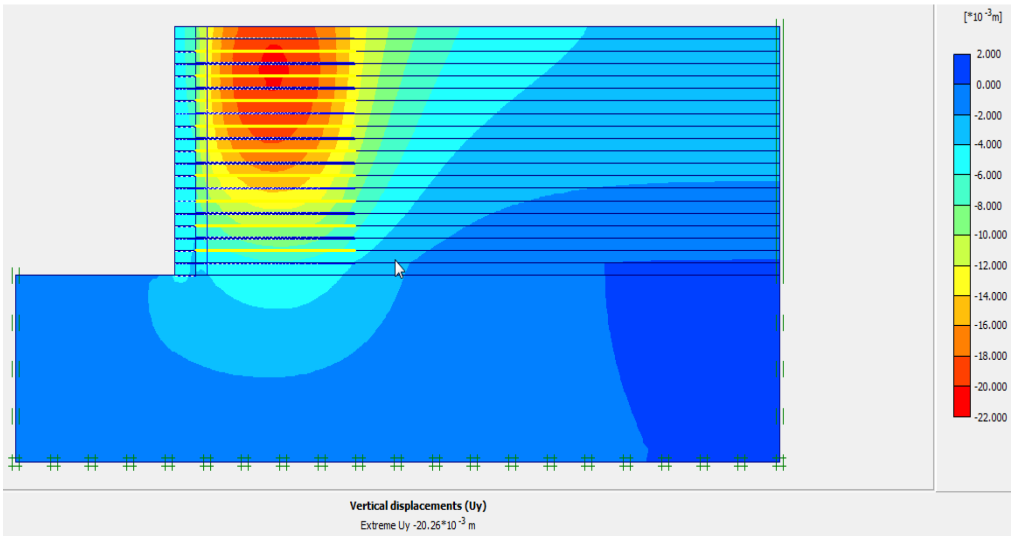

Figure 3. 8 Vertical Displacement of GRS Wall with Stiff Clay Backfill

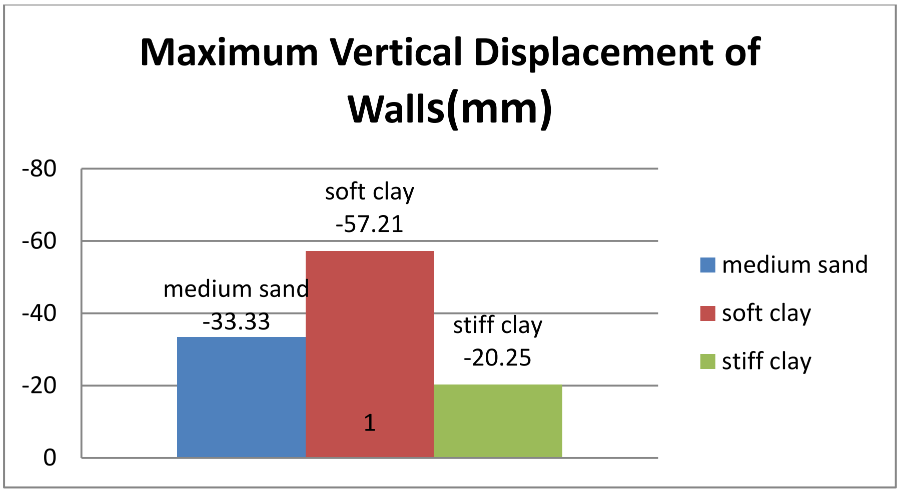

Figure 3. 9 Maximum Vertical Displacements of GRS Walls

Table 3. 11 Facing wall displacements

Elevation(m)	Horizontal displacement (mm)			Vertical displacement (mm)		
	Soft clay	Medium sand	Stiff clay	Soft clay	Medium sand	Stiff clay
0	-3.18	-2.21	-1.62	-4.48	-3.94	-4.61
1	-35.75	-16.2	-5.66	-6.23	-5.17	-5.49
2	-64.6	-30.2	-6.16	-6.05	-5.31	-5.31
3	-90.6	-39.4	-2.3	-5.16	-4.49	-4.9
4	-103.3	-33.6	-4.87	-3.07	-2.23	-4.56

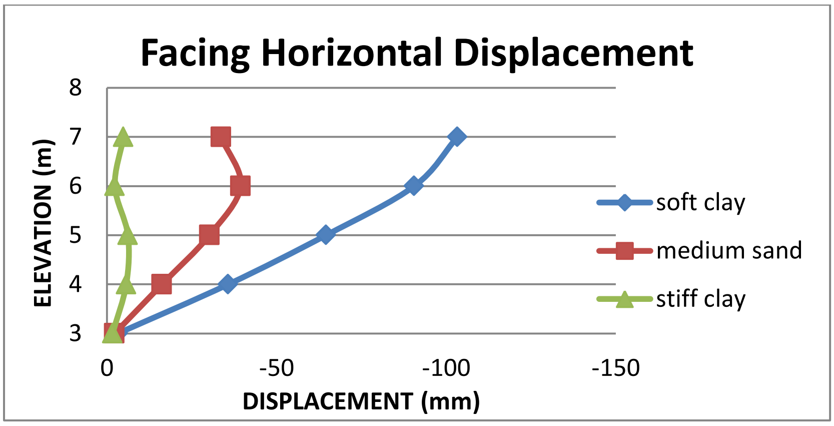

Figure 3. 10 GRS Wall Facing Horizontal Displacements

Observation

Figure 3.10 clearly shows that all backfill materials have minimum horizontal displacement at the bottom of the wall facing and they have nearly the displacements. But when we go from bottom to top of the wall the horizontal displacement varies for each backfill materials. Soft clay backfill displaces more than others and it have maximum displacement at the wall top, the medium sand backfill is displaced more at around 6m elevation.

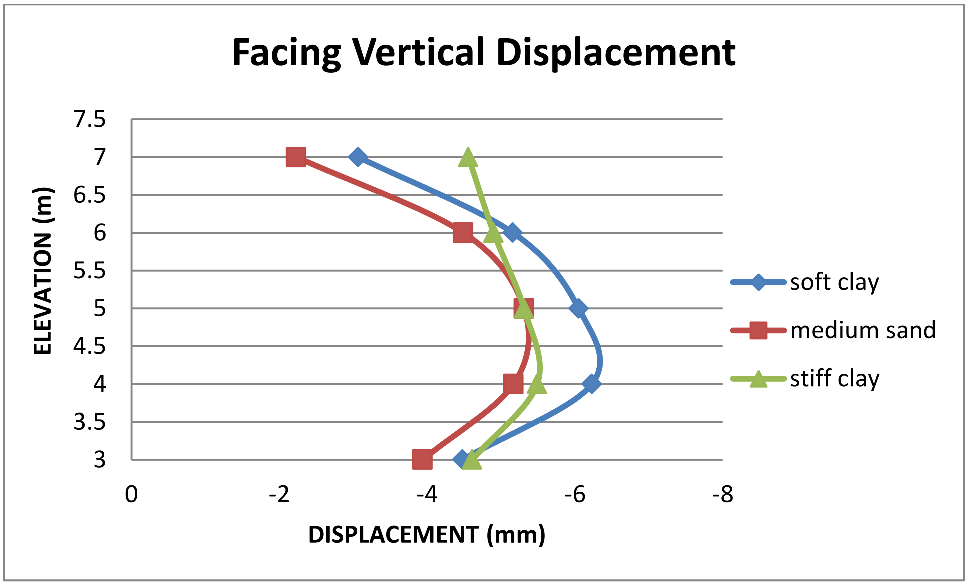

Figure 3. 11 GRS Wall Facing Vertical Displacements

In Figure3.11all backfill materials have maximum vertical facing deformation around the mid height of the wall. Medium sand shows less vertical displacement at the top face and stiff clay exhibits larger deformation at the wall top facing.

Major factors influencing lateral displacements during construction includes compaction intensity, reinforcement to soil stiffness ratio, reinforcement length, deformability of facing system, reinforcement to facing connection and also Interaction between reinforcement/ Geogrid and the soil material determines the displacement response of the wall system (Oyegible 2011). Basically backfill strength properties i.e. angle of internal friction and cohesion has significant effect on the result. So we can see that cohesive soils exhibit low displacement relative to the less cohesive materials. When we see medium sand and stiff clay 66.3%average difference in displacement values and their respective cohesion values are 2 kN/m^2 and 20 kN/m^2.

3.4.5 Geogrid Displacements and forces

The geogrid imbedded in side of the backfill material exhibits displacements and forces were developed due to the triggering effects of the soil movement under pressure.

Table 3. 12 Geogrid displacements

Layer	Elevation (m)	horizontal displacement(mm)			Vertical displacement(mm)		
		Soft clay	Medium sand	Stiff clay	Soft clay	Medium sand	Stiff clay
1	3.4	-10.59	-5.25	-3.19	-10.57	-7.56	-7.33
2	3.8	-20.14	-9.97	-4.68	-20.13	-12.05	-10.26
3	4.2	-26.61	-13.4	-5.43	-29.77	-17	-13.05
4	4.6	-30.8	-16.8	-5.43	-37.79	-20.9	-15.5
5	5	-33.4	-19.3	-5.26	-44	-26.1	-17.47
6	5.4	-33.8	-21.7	-6.9	-48.54	-28.6	-18.87
7	5.8	-38.9	-23.5	-8.57	-52.19	-30.9	-19.76
8	6.2	-46.3	-24.7	-10.21	-54.7	-32.9	-20.18
9	6.6	-54.3	-25.4	-11.69	-56	-33.2	-20.12

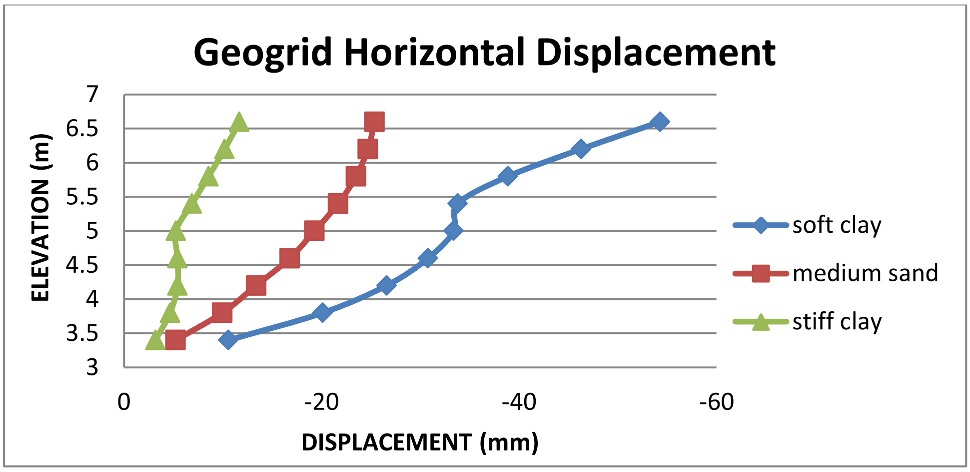

Figure 3. 12 Maximum Geogrid Horizontal Displacements

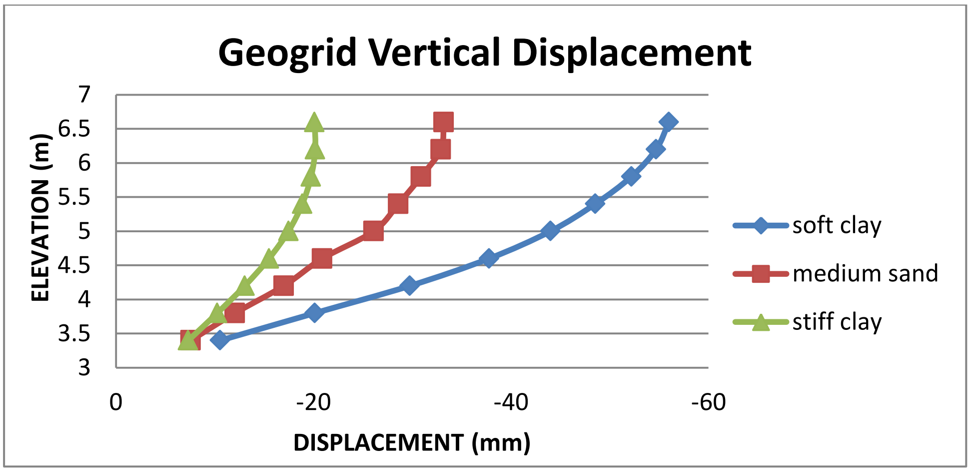

Figure 3. 13 Maximum Geogrid Vertical Displacements

Table 3. 13 Maximum Geogrid forces

Layer	Elevation (m)	Force (kN/m)		
		Soft clay	Medium sand	Stiff clay
1	3.4	10.043	7.561	1.465
2	3.8	17.553	13.679	3.313
3	4.2	19.293	12.959	4.007
4	4.6	18.015	13.158	4.143
5	5	16.296	11.805	4.179
6	5.4	12.958	10.025	3.973
7	5.8	8.862	8.212	3.238
8	6.2	4.737	6.257	2.158
9	6.6	1.623	4.014	1.19

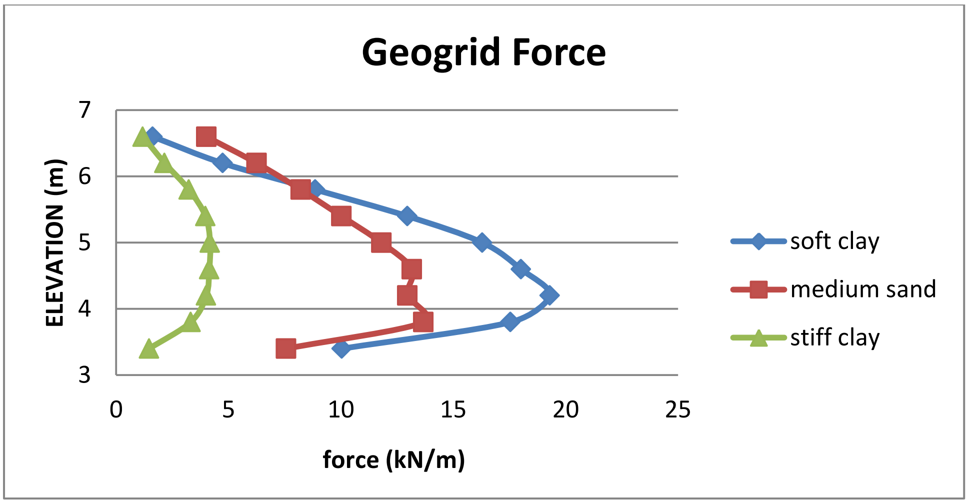

Figure 3. 14 GRS Walls Maximum Geogrid Forces

Observation

The magnitude and distribution of maximum reinforcement force in each layer within the reinforced soil zone for the model walls were examined. The maximum tension force which is maximum force at the Geogrid was the result obtained from software output program that is the maximum axial force for each Geogrid. From Figure 3.14Geogrid of soft clay backfill have maximum force at the third layer, Geogrid force for medium sand backfill have maximum load at the second layer and Geogrid of stiff clay backfill have maximum force at the mid layer of the wall. geogrid forces are greater for the walls with weaker backfills (Khalid Farrag 2004). It is also observed that the distribution of maximum load along the wall height varies between a parabolic shape, for the cases with a relatively cohesion less backfill, as observed in medium sand and a more linear shape when the backfill is more cohesive as observed in stiff clay backfill. But cohesion of a material alone does not govern this.

3.5 Validation

Numerical modeling attempts can be classified into two major groups on the basis of whether or not numerical results were compared with measurements from physical models, including field-instrumented walls (Bathrust 2001). Many of the studies reviewed by the authors investigated the response of idealized reinforced soil wall models. Relatively fewer studies are available in the literature that report direct comparisons of numerical results and experimentally measured results from full-scale instrumented walls. In the few cases where direct comparisons are reported, there are often significant discrepancies in magnitude and trends between predicted and measured values. In this thesis direct comparison of results from laboratory or full scale tests were not presented due to the model material property dissimilarity from the available full scale or laboratory studies in this type of walls. So that I just tried to validate our model results mainly facing wall displacements and geogrid forces from nearly similar available case study which is (PARAMETRIC ANALYSIS OF REINFORCED SOIL WALLS WITH DIFFERENT BACKFILL MATERIAL PROPERTIES) by Kianoosh Hatami School of Civil Engineering and Environmental Science University of Oklahoma, Norman, OK, USA Richard J. Bathurst, 2005

Wall construction

Wall was constructed with layers to satisfy the AASHTO requirement that the reinforcement spacing not exceed twice the toe to heel dimension of the modular blocks and to meet the minimum permitted reinforcement length to height ratio of L/H = 0.7.

Facing lateral displacement

The predicted facing lateral displacement of model walls with different backfill strength properties. As may be expected, the plots show that facing deflections diminish in magnitude as soil strength increases due to an increase in friction angle or increase in soil cohesion or both. In this thesis also as shown in Figure 3.15the soils of better strength showed less displacement. The pattern of deflected shape is also influenced by the addition of soil cohesion. An increase in soil cohesion moves the location of maximum wall deflection lower down the wall and is particularly effective in reducing deflections at the wall crest. However many other factors including soil modulus has effects on the performance of walls constructed with different backfill materials.

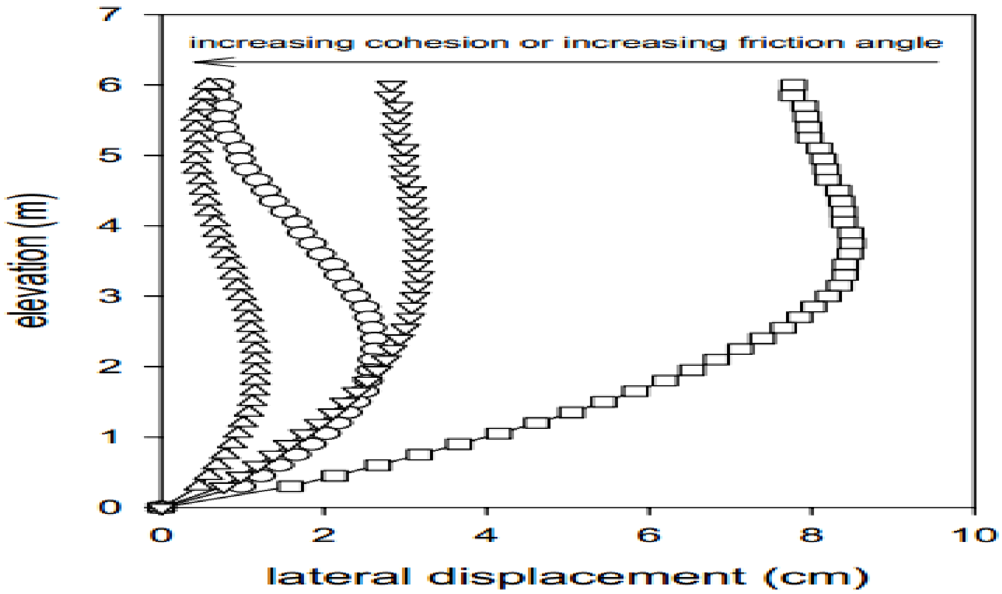

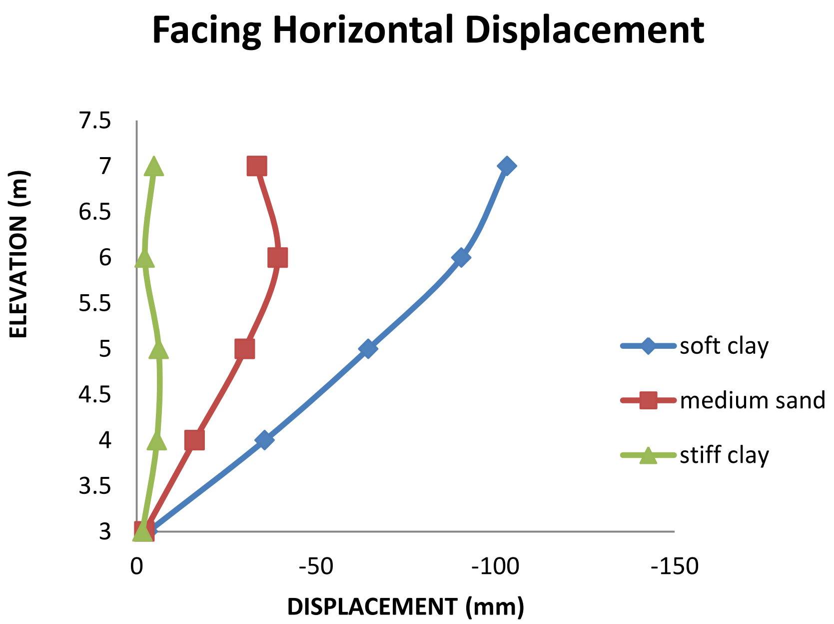

Figure 3. 15 Facing Wall Displacements for Validation

Geogrid force

Geogrid forces are greater for the walls with weaker backfills. It is also observed that the distribution of maximum load along the wall height varies between parabolic shapes as seen in Figure 3.16.

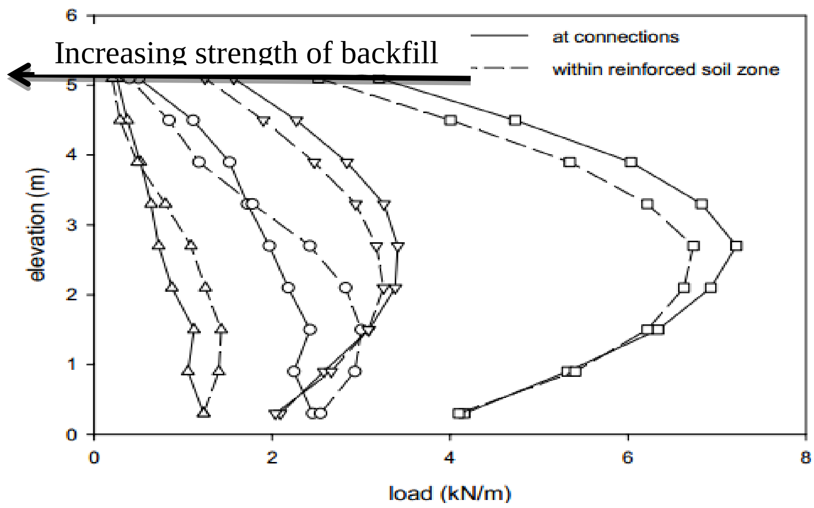

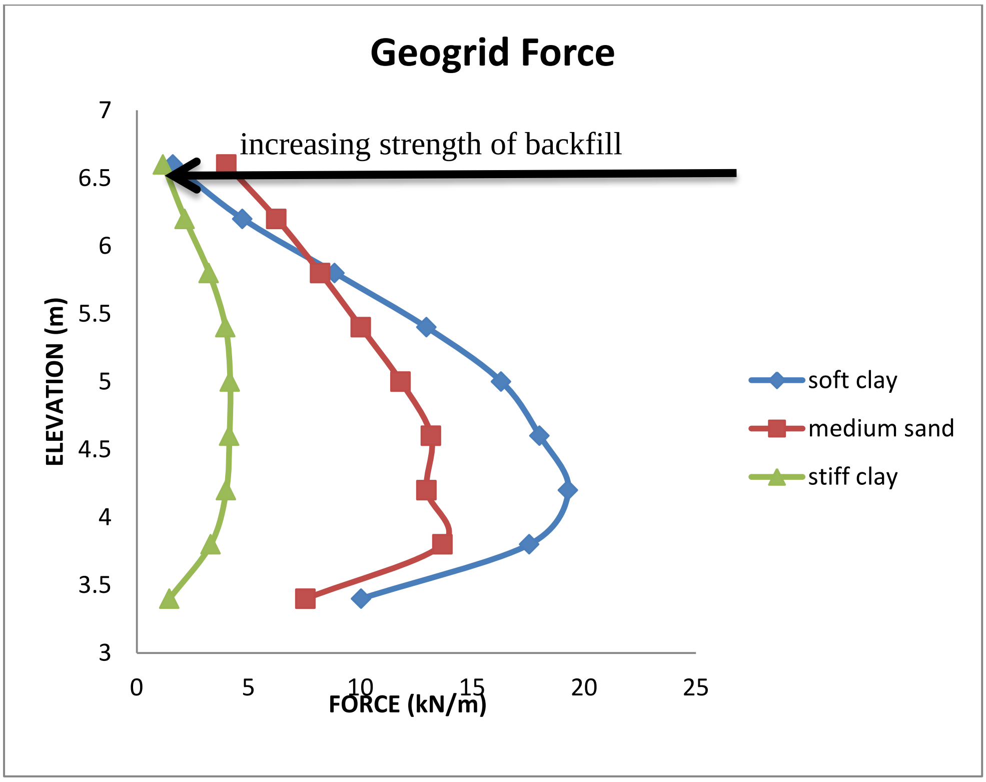

Figure 3. 16 Geogrid Forces for Validation

3.6 Influence of Backfill Material on the Behavior of Reinforced Earth Retaining Structures

The influence of backfill type and material properties on the performance of reinforced soil segmental retaining walls at the end of construction was investigated using a numerical model. The Plaxis input model is shown in Figure 3.1 the design parameters for the different soil cases are shown in Table 3.10. The modular facing block wall and Geogrid parameters are shown in Table 3.11 and Table3.12 respectively.

Table 3. 14 Soil data parameters

Mohr Coulomb		Model 1	Model 2	Model 3
		Soft Clay	Medium Sand	Stiff Clay
Type		Drained	Drained	Drained
γunsat [κN/m3]		16	18	17
γsat [κN/m3]		18	20	19
kx [m/day]		0.001	0.001	0.001
ky [m/day]		0.001	0.001	0.001
Eref [kN/m²]		25000	50000	30000
ν [–]		0.25	0.3	0.2
Cref [kN/m²]		10	2	20
φ [°]		20	34	28
ψ [°]		0	2	0
Rinter. [-]		0.5	0.67	0.5

Table 3. 15 Reinforcement data parameters

Reinforcement	EA [kN/m]	Sz [m]
Geogrid	1500	0.4

Foundation

In order not to allow any failure inside the foundation soil, a high cohesion (c = 200 kN/m2) and internal friction angle (phi = 35) were assigned to the foundation soil. The elastic moduli of the foundation soil were taken as 50000 kN/m^2.

3.7 Influence of Reinforcement Stiffness on the Behavior of Reinforced Earth Retaining Walls

Here in this analysis the reinforcement stiffness of the retaining walls were varied for the three backfill materials (i.e. soft clay, medium sand and stiff clay). Similar geometry, backfill material property and reinforcement spacing was used as the first analysis for the current case, while the reinforcement stiffness were varied.

Models covered under this sub topic was Model 4, model 5 and model 6; and all this models have similar soil data property with the first three models model 1, model 2, and model 3 respectively.

Table 3. 16 Reinforcement data parameters

Reinforcement	EA [kN/m]	Sz[m]
Geogrid	Varied	0.4

The stiffness of Geogrid reinforcements were 1500 KN/m and 750 KN/m.

3.8 Influence of Reinforcement Vertical Spacing on the Behavior of Earth Retaining Walls

In this analysis the reinforcement spacing of the retaining walls were varied for the three backfill materials (i.e. soft clay, medium sand and stiff clay). Similar geometry, backfill material and reinforcement stiffness were used as the first analysis for the current case, while the reinforcement spacing were varied.

Models covered under this sub topic was model 7, model 8 and model 9; and all this models have similar soil data property with the first three models model 1, model 2, and model 3 respectively

Table 3. 17 Reinforcement data parameters

Reinforcement	EA [kN/m]	Sz [m]
Geogrid	1500	Varied

The vertical spacing of Geogrid reinforcements was 0.4m and 0.2m.

3.9 Influence of Reinforcement Length on the Behavior of Earth Retaining Walls

In this analysis the reinforcement length of the retaining walls were varied for the three backfill materials (i.e. soft clay, medium sand and stiff clay). Similar backfill material and reinforcement stiffness and spacing were used as the first analysis for the current case, while the reinforcement lengths were varied.

Models covered under this sub topic was Model 10, model 11 and model 12; and all this models have similar soil data property with the first three models model 1, model 2, and model 3 respectively.

Table 3. 18 Reinforcement data parameters

Reinforcement	EA [kN/m]	Sz [m]	Length[m]
Geogrid	1500	0.4	Varied

The length of Geogrid reinforcements was 3m and 4m.

3.10 Influence of Surcharge Pressure on the Behavior of Earth Retaining Walls

In this analysis the wall performance after the end of construction and application of surcharge pressure were analyzed for the three backfill materials (i.e. soft clay, medium sand and stiff clay). Similar geometry, backfill material and reinforcement stiffness were used for the three models. But the surcharge loads were varied.

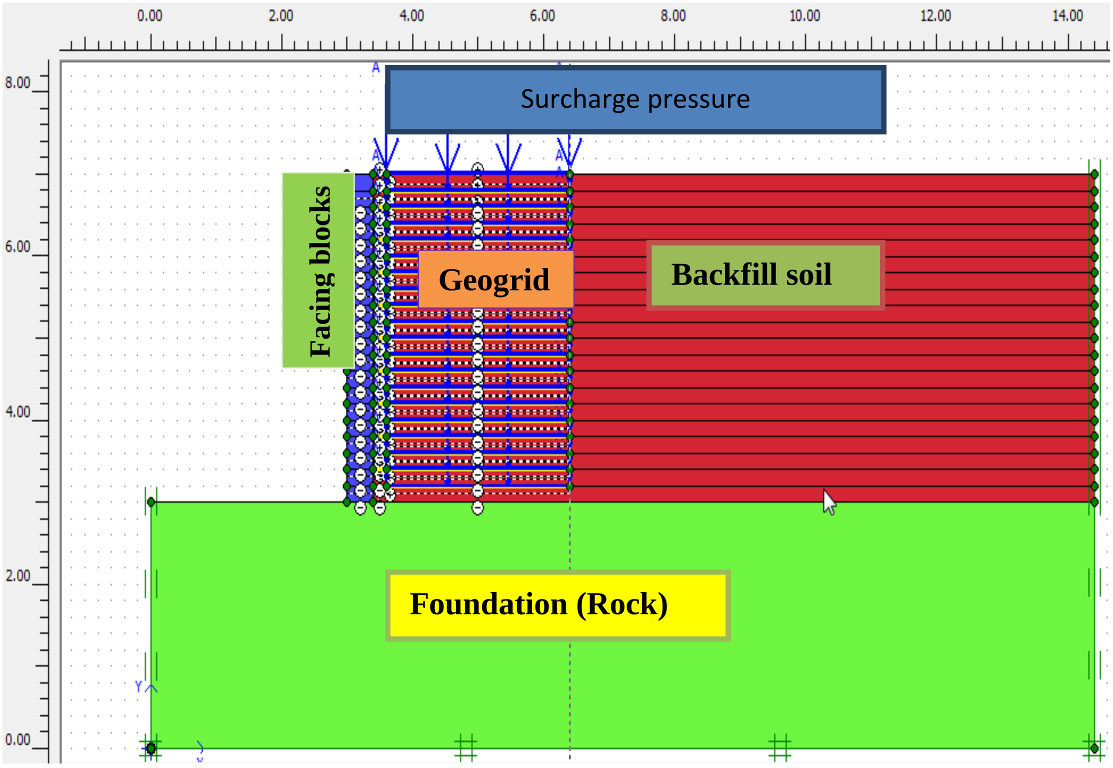

Figure 3. 17 Reinforced Soil Wall Model

Models covered under this sub topic was Model 13/16, model 14/17 and model 15/18; and all this models have similar soil data property with the first three models model 1, model 2, and model 3 respectively

Table 3. 19 Reinforcement data parameters

Reinforcement	EA [kN/m]	Sz [m]	Length [m]	Applied load
Geogrid	1500	0.2	3	Varied

The applied surcharge load on the wall was 20 kN/m^2 and 40 kN/m^2.

All models to be analyzed was under different influencing factors in order to understand the effects of such parameters on the performance of geosynthetically reinforced earth retaining walls

Table 3. 20 Different study parameters of all models

Backfill type	Model type	Reinforcement			Surcharge (kN/m2)
		Stiffness kN/m	Vertical Spacing (m)	Length (m)	
soft clay	model 1	1500	0.4	3	0
	model 4	750	0.4	3	0
	model 7	1500	0.2	3	0
	model 10	1500	0.4	4	0
	model 13	1500	0.2	3	20
	model 16	1500	0.2	3	40
medium sand	model 2	1500	0.4	3	0
	model 5	750	0.4	3	0
	model 8	1500	0.2	3	0
	model 11	1500	0.4	4	0
	model 14	1500	0.2	3	20
	model 17	1500	0.2	3	40
stiff clay	model 3	1500	0.4	3	0
	model 6	750	0.4	3	0
	model 9	1500	0.2	3	0
	model 12	1500	0.4	4	0
	model 15	1500	0.2	3	20
	model 18	1500	0.2	3	40

CHAPTER 4

MODELING RESULTS AND DISCUSSION

4.1 General

A total of 18 runs are analyzed using the software PLAXIS 2D. The runs are based on different backfill property, surcharge pressure, reinforcement length, strength and spacing. Every model in PLAXIS 2D, before the beginning of any calculation phase, starts with the initial Phase. The initial phase consists of the soil clusters only in which all other structural parts are not activated. Therefore this stage calculates the stresses and deformations due to the soil clusters only by means of gravity loading. In any non-linear analysis where a finite number of calculation steps are used, there will be some drift from the exact solution. To limit this drift, tolerated error option is available in the PLAXIS 2D. The mesh size and maximum unbalanced force at the grid points (i.e. tolerated error) were selected based on a series of parametric analysis to concurrently optimize accuracy and computation speed. The tolerated error used in these runs for all phases except for some phases was 0.01. A tolerated error of 0.01 means the computed value differs from the exact solution by maximum of 1%.Therefore this error is considered to be within safe and working limits.

The results of all runs were indicated the influence of different parameters in the performances of reinforced earth retaining walls at the end of construction. End of construction represents a working stress (i.e. serviceability) condition that is the operational condition. Finite element analysis was carried out using commercial software PLAXIS version 8.5 for the three backfill material types mentioned in the previous chapter. The results are compared and reported here in this chapter. Behavior of reinforced earth retaining walls were investigated for different backfill material, geogrid length, surcharge pressure, geogrid stiffness and geogrid spacing through facing lateral displacements, vertical deformations, geogrid movements and forces.

4.2 influence of Backfill Materials on the Behavior of Reinforced Earth Retaining Walls

The analysis results compared and reported here shown in the Figure 4.1 was the maximum horizontal displacement and Figure 4.2 shows maximum vertical deformations.

4.2.1 GRS wall Displacements

Wall horizontal and vertical displacements after the end of construction were observed using charts for the three of backfill material types.

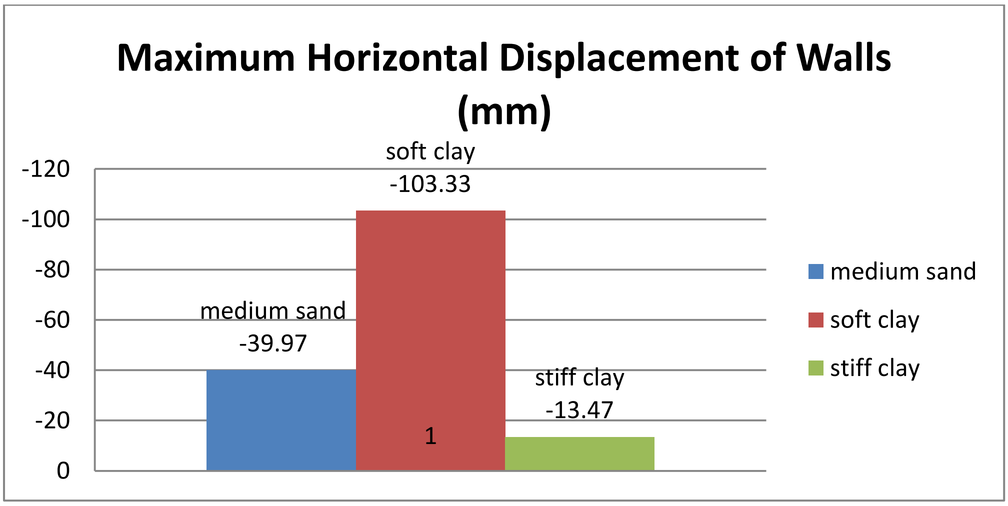

Figure 4. 1 Maximum Horizontal Displacements of GRS Walls

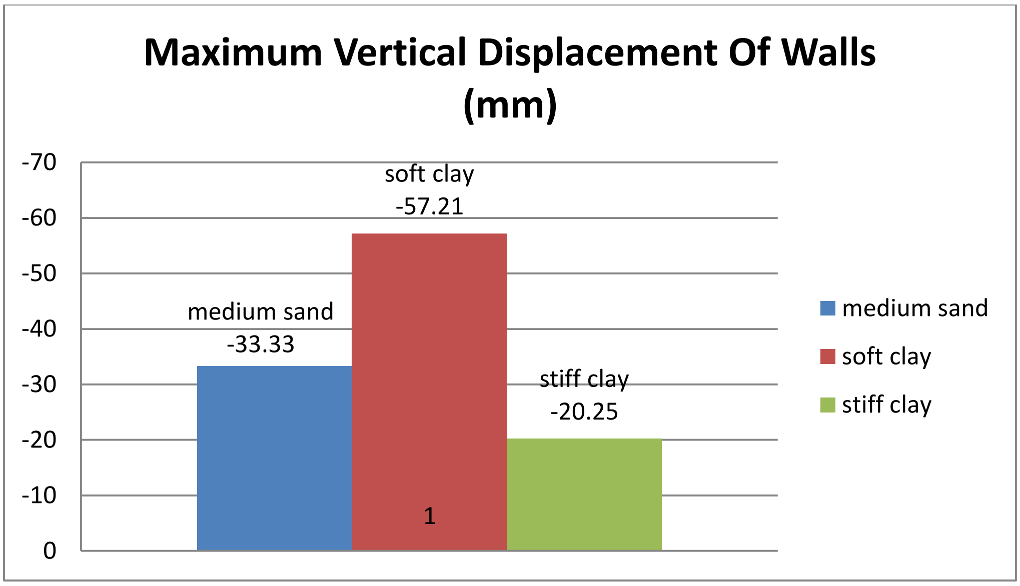

Figure 4. 2 Maximum Vertical Displacements of GRS Walls

Table 4. 1 Facing wall displacements

Elevation(m)	Horizontal displacement (mm)			Vertical displacement (mm)		
	Soft clay	Medium sand	Stiff clay	Soft clay	Medium sand	Stiff clay
3	-3.18	-2.21	-1.62	-4.48	-3.94	-4.61
4	-35.75	-16.2	-5.66	-6.23	-5.17	-5.49
5	-64.6	-30.2	-6.16	-6.05	-5.31	-5.31
6	-90.6	-39.4	-2.3	-5.16	-4.49	-4.9
7	-103.3	-33.6	-4.87	-3.07	-2.23	-4.56

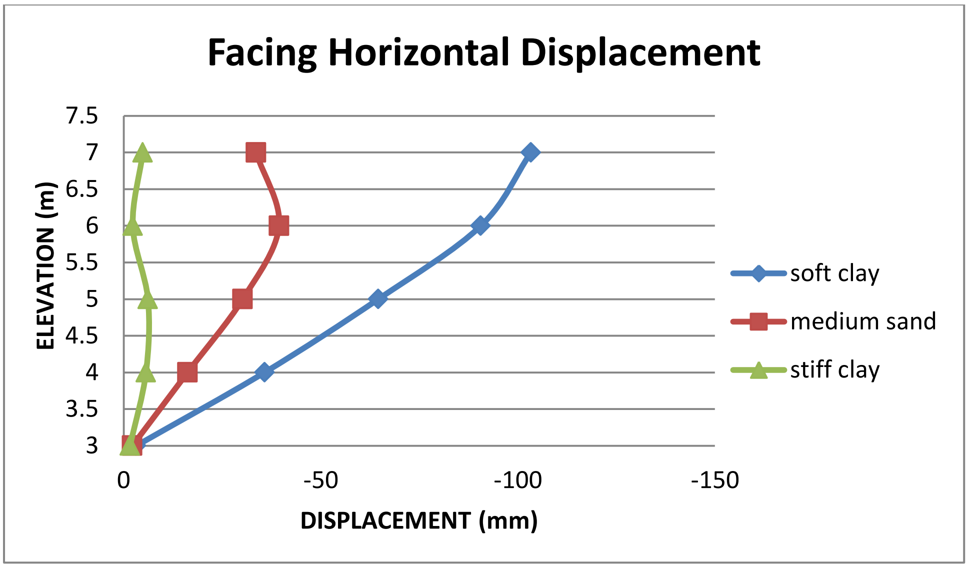

Figure 4. 3 GRS Wall Facing Horizontal Displacements

Observation

Figure 4.3 clearly shows that all backfill materials have minimum horizontal displacement at the bottom of the wall facing and they have nearly the displacements. But when we go from bottom to top of the wall the horizontal displacement varies for each backfill materials. Soft clay backfill displaces more than others and it have maximum displacement at the wall top, the medium sand backfill is displaced more at around 6m elevation.

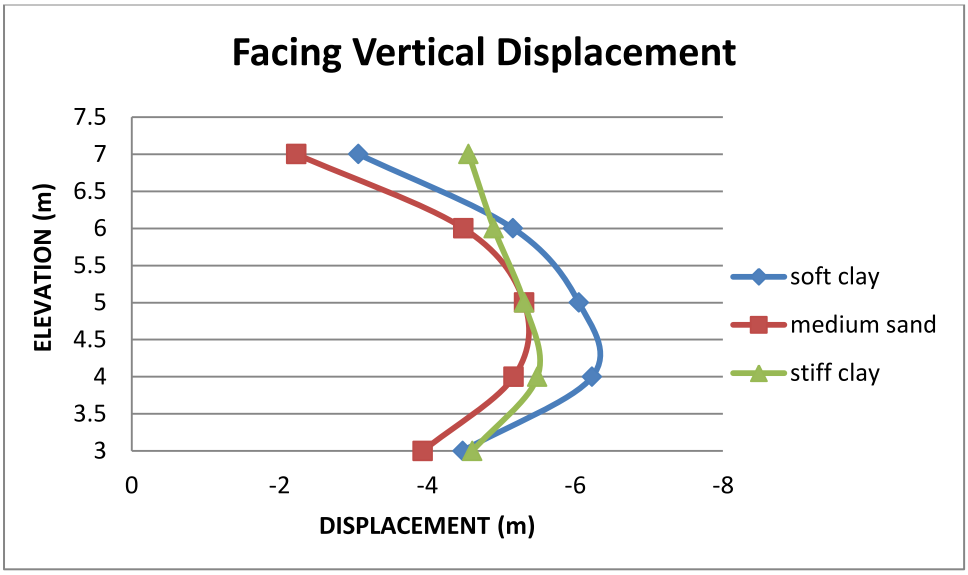

Figure 4. 4 GRS Wall Facing Vertical Displacements

In Figure 4.4all backfill materials have maximum vertical facing deformation around the mid height of the wall. Medium sand shows less vertical displacement at the top face and stiff clay exhibits larger deformation at the wall top facing.

Major factors influencing lateral displacements during construction includes compaction intensity, reinforcement to soil stiffness ratio, reinforcement length, deformability of facing system, reinforcement to facing connection and also Interaction between reinforcement/ Geogrid and the soil material determines the displacement response of the wall system (Oyegible 2011). Basically backfill strength properties i.e. angle of internal friction and cohesion has significant effect on the result. So we can see that cohesive soils exhibit low displacement relative to the less cohesive materials. When we see medium sand and stiff clay 66.3%average difference in displacement values and their respective cohesion values are 2 kN/m^2 and 20 kN/m^2.

4.2.2 Geogrid Displacements and forces

The geogrid imbedded in side of the backfill material exhibits displacements and forces were developed due to the triggering effects of the soil movement under pressure.

Table 4. 2 Geogrid displacements

Layer	Elevation(m)	horizontal displacement(mm)			Vertical displacement(mm)		
		Soft clay	Medium sand	Stiff clay	Soft clay	Medium sand	Stiff clay
1	3.4	-10.59	-5.25	-3.19	-10.57	-7.56	-7.33
2	3.8	-20.14	-9.97	-4.68	-20.13	-12.05	-10.26
3	4.2	-26.61	-13.4	-5.43	-29.77	-17	-13.05
4	4.6	-30.8	-16.8	-5.43	-37.79	-20.9	-15.5
5	5	-33.4	-19.3	-5.26	-44	-26.1	-17.47
6	5.4	-33.8	-21.7	-6.9	-48.54	-28.6	-18.87
7	5.8	-38.9	-23.5	-8.57	-52.19	-30.9	-19.76
8	6.2	-46.3	-24.7	-10.21	-54.7	-32.9	-20.18
9	6.6	-54.3	-25.4	-11.69	-56	-33.2	-20.12

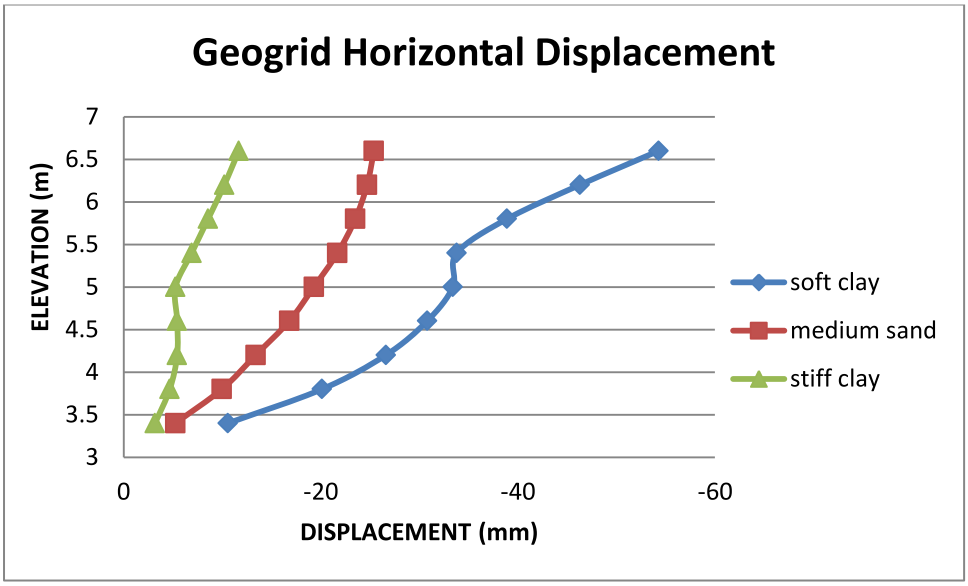

Figure 4. 5 Maximum Geogrid Horizontal Displacement

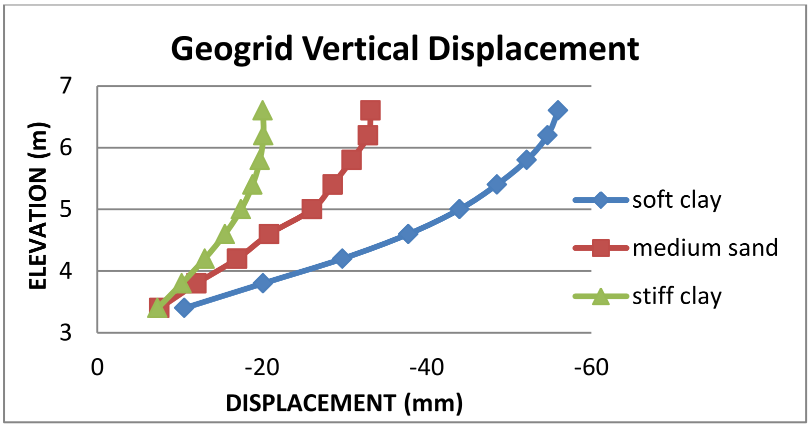

Figure 4. 6 Maximum Geogrid Vertical Displacement

Observation

The horizontal displacement and vertical displacement of the reinforcing material (i.e. Geogrid) were tabulated in Table 4.3 the horizontal displacement of geogrid reinforcing soft clay backfill was greater, the geogrid imbedded in stiff clay backfill shows less lateral displacement. As in Figure 4.5 all backfill soils geogrid were maximum horizontal displacement at the top facing of the wall.

Similarly the vertical displacements of the geogrid for all backfill materials were increased from wall bottom to top.

Table 4. 3 Maximum geogrid force

Layer	Elevation (m)	Force (kN/m)		
		Soft clay	Medium sand	Stiff clay
1	3.4	10.043	7.561	1.465
2	3.8	17.553	13.679	3.313
3	4.2	19.293	12.959	4.007
4	4.6	18.015	13.158	4.143
5	5	16.296	11.805	4.179
6	5.4	12.958	10.025	3.973
7	5.8	8.862	8.212	3.238
8	6.2	4.737	6.257	2.158
9	6.6	1.623	4.014	1.19

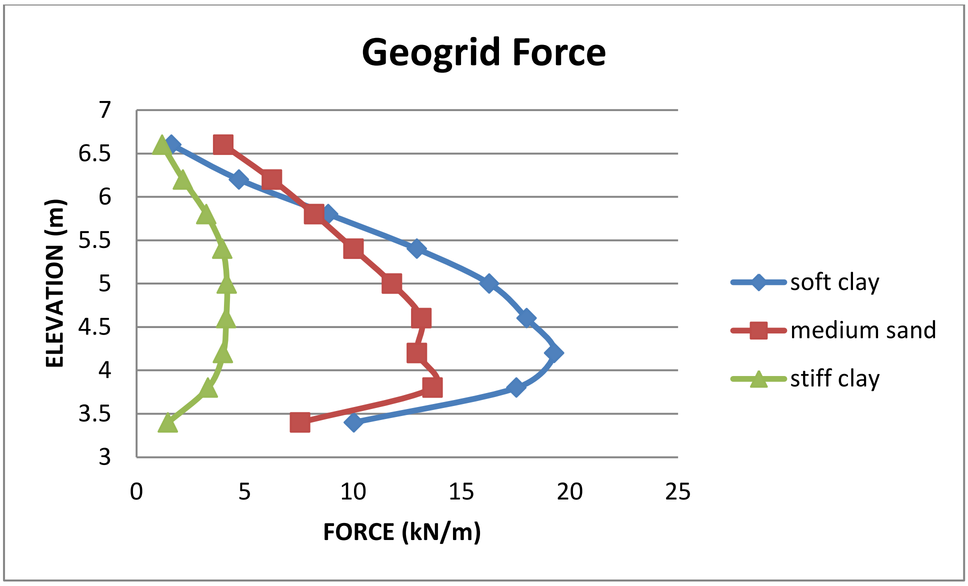

Figure 4. 7 GRS Walls Maximum Geogrid Forces

Observation

The magnitude and distribution of maximum geogrid force in each layer within the reinforced soil zone for the model walls were examined. The maximum tension force which is maximum force at the geogrid was the result obtained from software output program that is the maximum axial force for each geogrid. From Figure 4.7geogrid of soft clay backfill have maximum load at the third layer, geogrid force for medium sand backfill have maximum force at the second layer and geogrid of stiff clay backfill have maximum force at the mid layer of the wall.

Geogrid forces are greater for the walls with weaker backfills (Khalid Farrag 2004). It is also observed that the distribution of maximum load along the wall height varies between a parabolic shape, for the cases with a relatively cohesion less backfill, as observed in medium sand and a more linear shape when the backfill is more cohesive as observed in stiff clay backfill for in this case. But cohesion of a material alone does not govern the distribution of maximum force in the geogrid obviously.

Table 4. 4 Location of maximum geogrid force

soft clay geogrid force		medium sand geogrid force	stiff clay geogrid force
layer	Max. load location	Max. load location	Max. load location
1	4.197	3.854	3.951
2	4.356	3.854	3.4
3	4.279	3.854	3.4
4	4.585	3.918	3.4
5	4.585	3.982	3.4
6	4.728	3.982	3.4
7	4.871	4.172	3.4
8	5.385	4.172	3.5
9	5.443	4.427	3.5

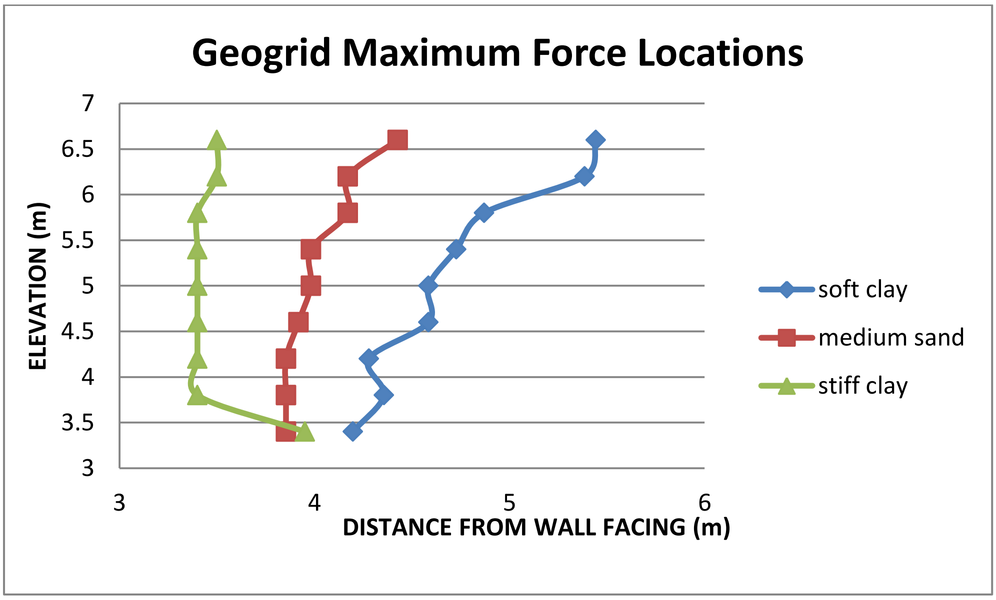

Figure 4. 8 Maximum Geogrid Force Location along the Wall Height

Table 4.5presented the maximum geogrid forces at locations along the length of the geogrid layers within the reinforced soil zone.

The most critical slip surface in reinforced earth retaining walls were assumed to concede with the maximum tensile force lines, (FHWA 1990). Figure 4.8 shows the most critical failure surfaces of each backfill materials.

4.3 Influence of Reinforcement Stiffness on the Behavior of Earth Retaining Structures

The strength of reinforcement material has a significant effect on the performance of earth retaining structures. The engineering performance of weak soil materials can be improved by incorporation of reinforcing elements like geogrid. Hence these reinforcements improve strength and deformation properties of structures over the unreinforced once.

Geogrid strength of 1500 KN/m was analyzed in different backfill materials above and we got verities of results i.e. facing horizontal movements, geogrid displacements, and geogrid forces at different critical locations of the reinforced earth wall. Now in the following sections the behavior of GRS wall was analyzed for different reinforcement stiffness and compared with the previous one.

4.3.1 Soft clay backfill

All the material properties of the soil (i.e. Soft Clay backfill Geogrid 1500 kN/m/ **model 1**and Soft Clay Backfill Geogrid 750 kN/m/**model 4**) was not changed only the axial stiffness of the reinforcing material/Geogrid was changed.

The maximum horizontal and vertical displacements of model 1 and model 4 were shown below in Figure 4.9indicated that, both models have greater horizontal displacements than vertical displacements. When the Geogrid stiffness of soft clay backfill material reinforced wall reduced in half (i.e. from 1500 KN/m to 750 KN/m) the maximum horizontal displacement was approximately increased by 8%. Similarly the maximum vertical displacement of the wall increased by 22.5%.

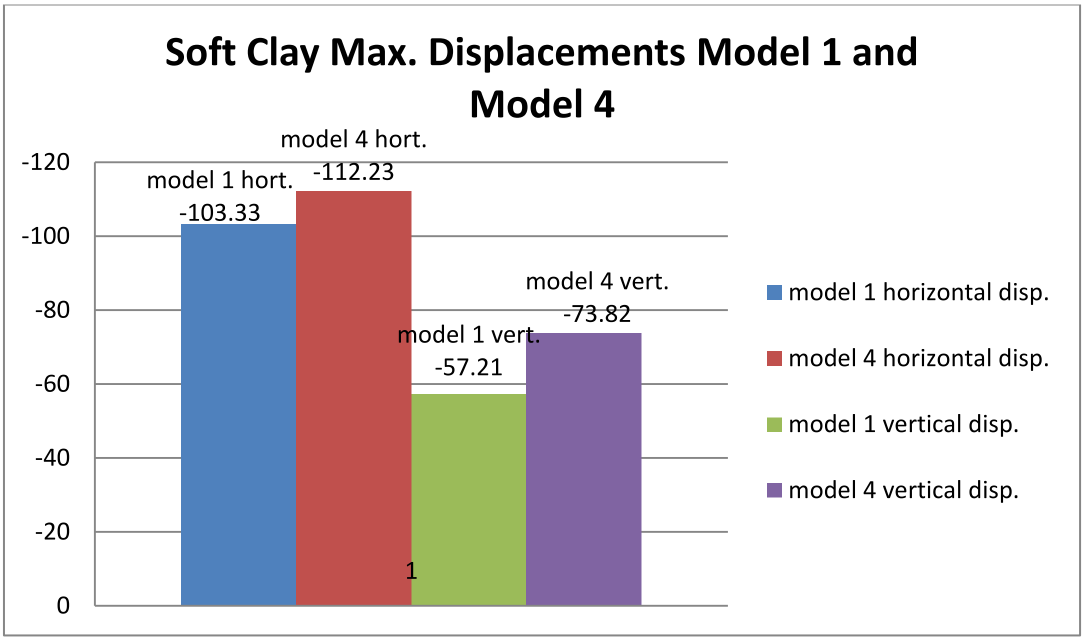

Figure 4. 9 Maximum Displacement GRS Wall with Soft Clay Backfill Geogrid Stiffness Influence

Observation

Figure 4.9below shows the facing wall displacements for model 1 and model 4. Horizontal deflection of facing wall for model 1 is less than model 4. The vertical displacement of model 1 is greater at the mid height of the wall than model 4. While model 1 has lesser vertical deformation than model 4 at the facing wall top.

Table 4. 5 Soft clay facing displacements of varying Geogrid stiffness

	Facing Displacements(mm)			
	model 1		model 4	
elevation	horizontal	vertical	horizontal	vertical
3	-3.18	-4.48	-3.37	-4.66
4	-35.75	-6.23	-53.3	-7.37
5	-64.6	-6.05	-95.7	-3.78
6	-90.6	-5.16	-106.4	-5.25
7	-103.3	-3.07	-102.8	-10.32

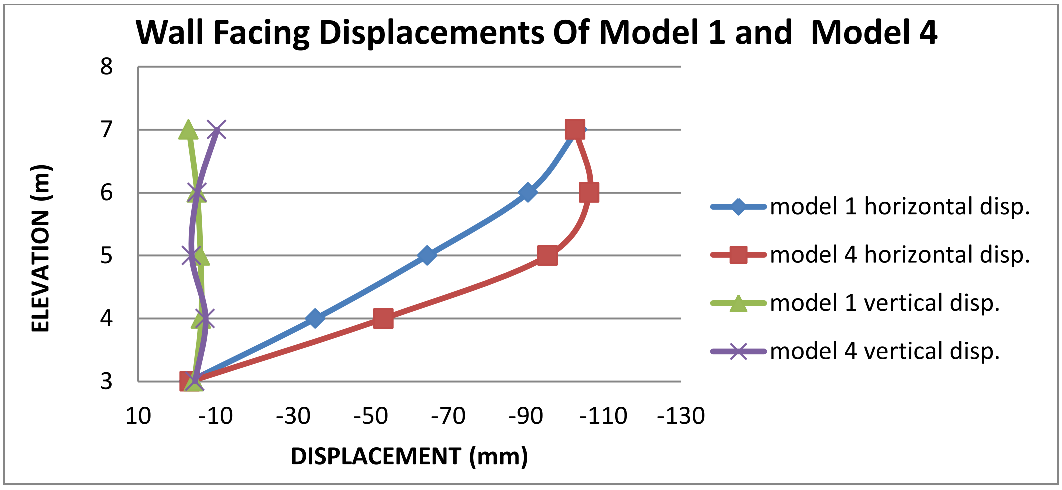

Figure 4. 10 GRS wall with soft clay backfill facing displacement Geogrid stiffness influence

Observation

The maximum horizontal displacement of geogrid for model 1 and model 4 have s-shaped deflection, comparing the displacement values model 4 which is smaller geogrid stiffness has greater displacements for both vertically and horizontally. In figure 4.10, geogrid vertical displacement of model 4 above the mid height of the wall was greater than the Geogrid horizontal displacement. Likewise the vertical displacement of geogrid for model 1 is greater than horizontal displacement of geogrid throughout the wall height.

Table 4. 6 Maximum Geogrid displacements soft clay backfill Geogrid stiffness influence

maximum Geogrid displacement(mm)				
	model 1		model 4	
elevation	horizontal	vertical	horizontal	Vertical
3.4	-10.59	-10.57	-17.99	-11.84
3.8	-20.14	-20.13	-34.22	-22.81
4.2	-26.61	-29.77	-45.28	-36.01
4.6	-30.8	-37.79	-51.8	-47.8
5	-33.4	-44	-54.5	-57.03
5.4	-33.8	-48.54	-53.9	-64.7
5.8	-38.9	-52.19	-52.7	-70.24
6.2	-46.3	-54.7	-53.7	-73.16
6.6	-54.3	-56	-59.9	-73.78

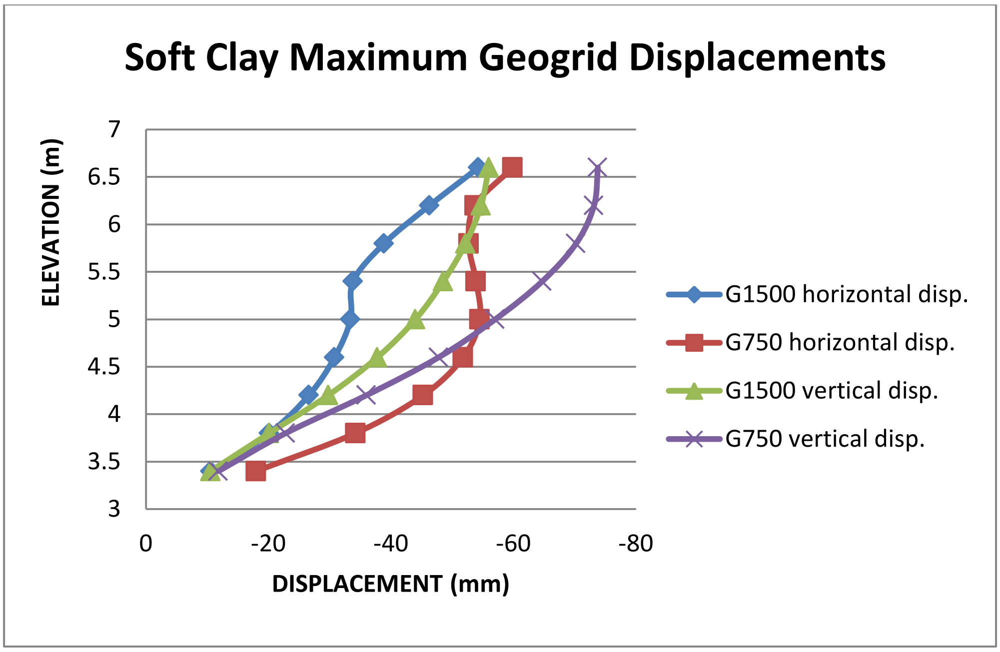

Figure 4. 11 Maximum Geogrid Displacement of GRS Wall with Soft Clay Backfill Geogrid Stiffness Influence

In Figure 4.11 the maximum force of geogrid observed throughout the wall height is within 0.25H to 0.5H range. Model 1 has greater geogrid tension load than model 4.

Table 4. 7 Maximum Geogrid force of GRS wall with soft clay backfill

maximum Geogrid force (kN/m)			
	model 1	model 4	
elevation	force	force	
3.4	10.043	9.463	
3.8	17.553	14.678	
4.2	19.293	15.99	
4.6	18.015	16.1306	
5	16.296	14.347	
5.4	12.958	11.486	
5.8	8.862	7.743	
6.2	4.737	3.985	
6.6	1.623	2.1334	

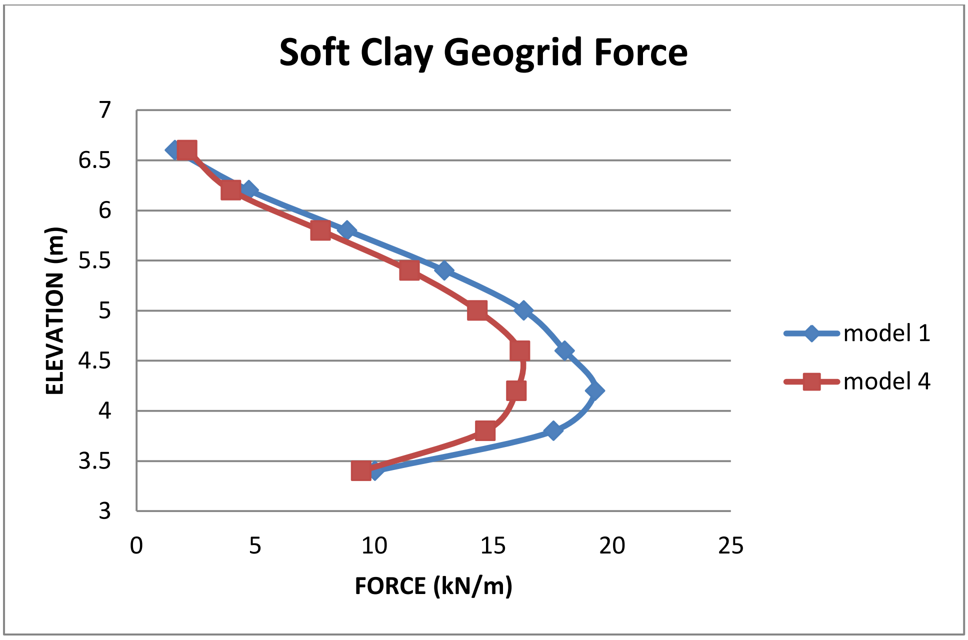

Figure 4. 12 Maximum Geogrid Force of GRS Wall with Soft Clay Backfill

Table 4. 8 Maximum Geogrid force location

	Max. force location	
elevation	model 1	model 4
3.4	4.197	4.0667
3.8	4.356	4.0667
4.2	4.279	4.4166
4.6	4.585	4.533
5	4.585	4.65
5.4	4.728	4.883
5.8	4.871	5
6.2	5.385	5.4667
6.6	5.443	3.6

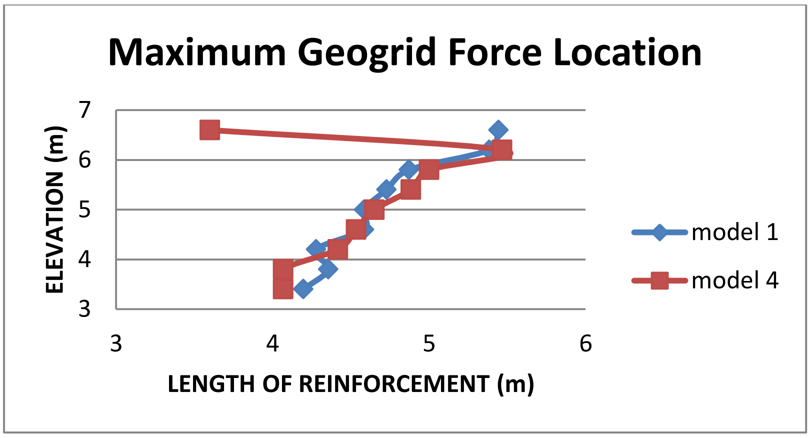

Figure 4. 13 Maximum Geogrid Force Location Geogrid Stiffness Influence

As in Figure 4.13the location of maximum tension load throughout the length of Geogrid for each layer was observed. Almost similar maximum load location was observed for model 1 and model 4.

4.3.2 Medium sand backfill

All the material properties of the soil were not changed only the axial stiffness of the reinforcing material/Geogrid was changed from 1500 kN/m to 750 kN/m which is reduced in half.

- GRS wall with Geogrid stiffness 1500 kN/m (**model 2**).
- GRS wall with Geogrid stiffness 750 kN/m (**model 5**).

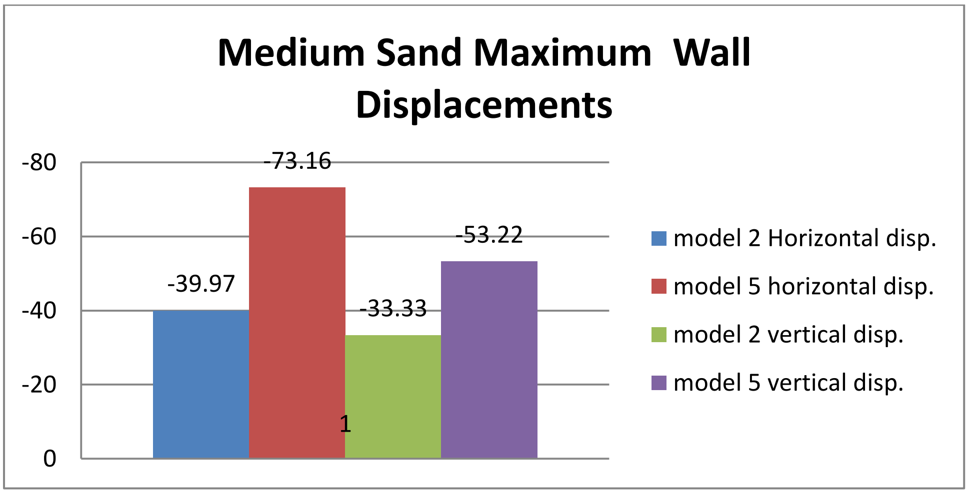

Figure 4. 14 Maximum Displacement of Wall with Medium Sand Backfill Geogrid Stiffness Influence

Observation

As we can understand from Figure 4.14, the maximum horizontal and vertical displacements of model 5 (i.e. geogrid stiffness of 750 kN/m) is greater than model 2(i.e. geogrid stiffness of 1500 kN/m). The vertical and horizontal displacement of model 2 was small differences which are about 16.6%. Rather the vertical and horizontal displacements differences of the GRS wall model 5 were about 27%.

Table 4. 9 Medium sand facing displacement

facing displacement [mm]				
	model 2		model 5	
elevation	Horizontal	vertical	horizontal	vertical
3	-2.21	-3.94	-2.34	-3.97
4	-16.2	-5.17	-27.07	-5.77
5	-30.2	-5.31	-53.03	-5.92
6	-39.4	-4.49	-71.71	-4.51
7	-33.6	-2.23	-63.5	-0.36

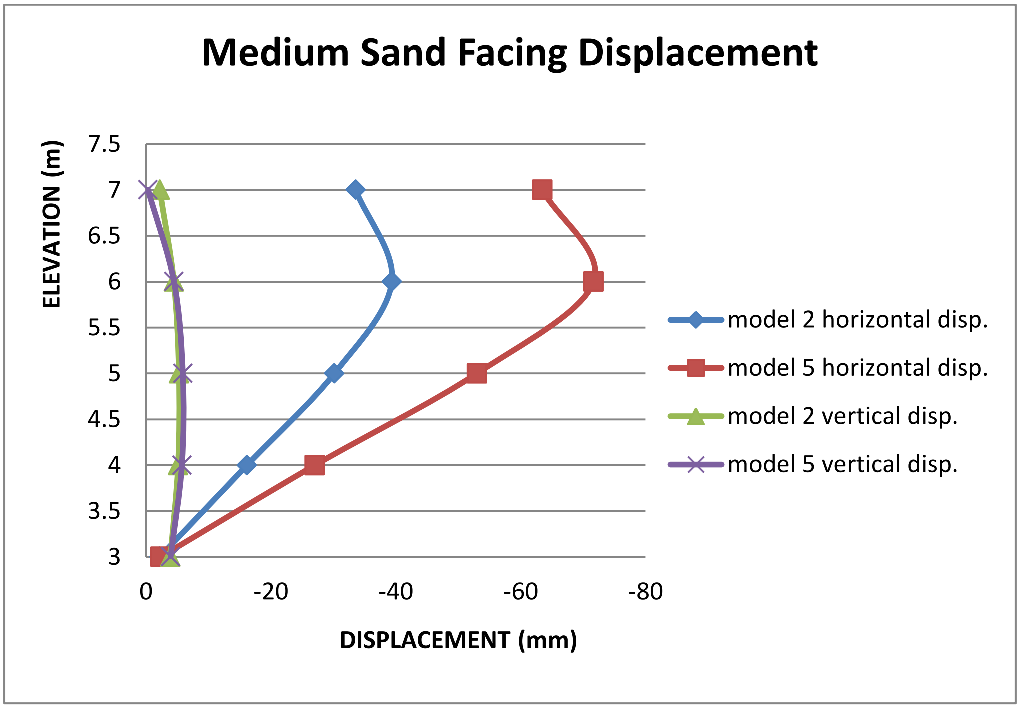

Figure 4. 15 Facing Displacement of GRS Wall with Medium Sand Backfill

Observation

GRS wall with different reinforcement strength for medium sand backfill was analyzed. Figure 4.15shown that wall facing vertical displacements of model 2 and model 5 have almost the same throughout the wall height, means that varying geogrid stiffness does not lead to significant effect in vertical deformation of the facing wall. But the horizontal movement of facing wall was larger for model 5 than model 2. The maximum horizontal displacement for both models was occurred at 0.75H.

Table 4. 10 Medium sand maximum Geogrid displacements

maximum Geogrid displacement [mm]				
	model 2		model 5	
elevation	horizontal	vertical	horizontal	vertical
3.4	-5.25	-7.56	-7.5	-8.32
3.8	-9.97	-12.05	-16.02	-15.65
4.2	-13.4	-17	-23.21	-23.35
4.6	-16.8	-20.9	-29.19	-31.84
5	-19.3	-26.1	-34.46	-39.01
5.4	-21.7	-28.6	-39.54	-44.89
5.8	-23.5	-30.9	-43.15	-48.23
6.2	-24.7	-32.9	-47.02	-51.4
6.6	-25.4	-33.2	-48.64	-53

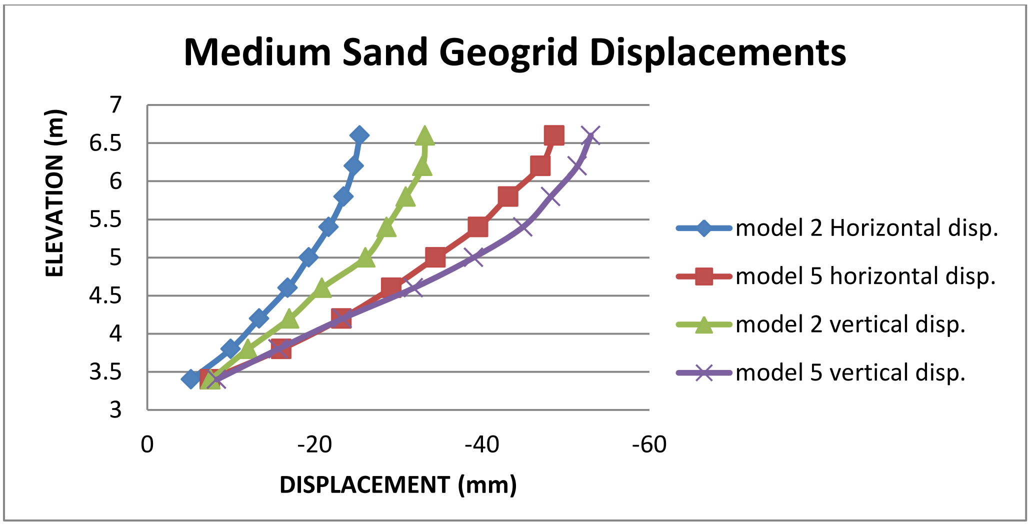

Figure 4. 16 Maximum Geogrid Displacement Medium Sand Backfill

Observation

Figure 4.16shown that maximum geogrid displacements of model 5 was greater than model 2, this is due to the stiffness reduction of geogrid. For model 2 vertical displacements has greater than horizontal displacement. But the reverse was true for model 5. So using reduced geogrid stiffness results high deformation on GRS walls with medium sand backfill.

Table 4. 11 Medium sand Geogrid force

Geogrid force		
	model 2	model 5
Elevation	force	force
3.4	7.561	7.77
3.8	13.679	12.253
4.2	12.959	13.328
4.6	13.158	13.086
5	11.805	11.833
5.4	10.025	10.585
5.8	8.212	8.676
6.2	6.257	6.073
6.6	4.014	4.101

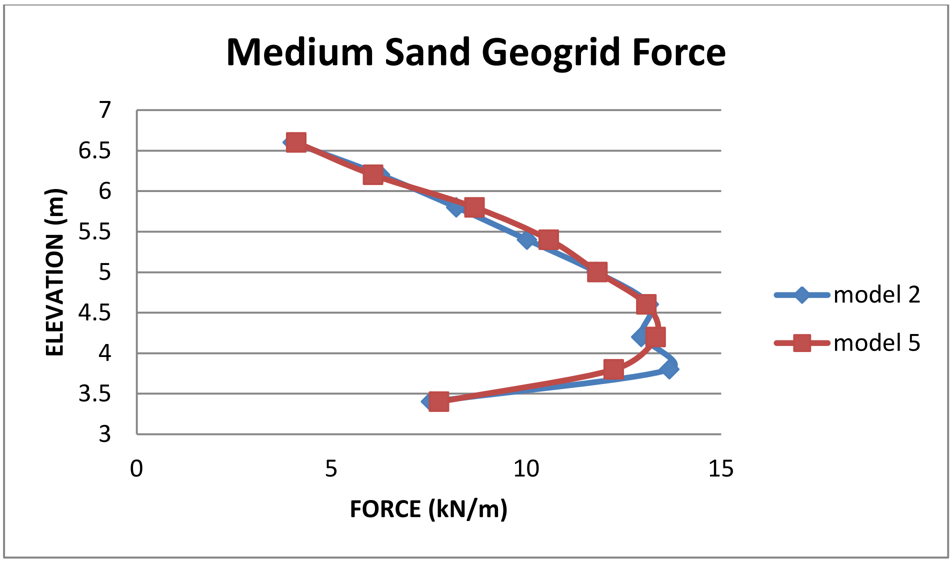

Figure 4. 17 Maximum Geogrid Force Medium Sand Backfill

Observation

Geogrid forces are tensile forces developed within the stressed geogrid along the reinforcement length. Figure 4.17shown that the distribution of maximum force along the wall height varied between parabolic shapes. Maximum geogrid forces were occurred around 0.3H of the wall height.

Table 4. 12 Medium sand maximum geogrid force location

	Max. force location	
Elevation	model 2	model 5
3.4	3.854	3.854
3.8	3.854	3.854
4.2	3.854	3.918
4.6	3.918	3.981
5	3.982	3.981
5.4	3.982	3.981
5.8	4.172	4.363
6.2	4.172	4.618
6.6	4.427	4.872

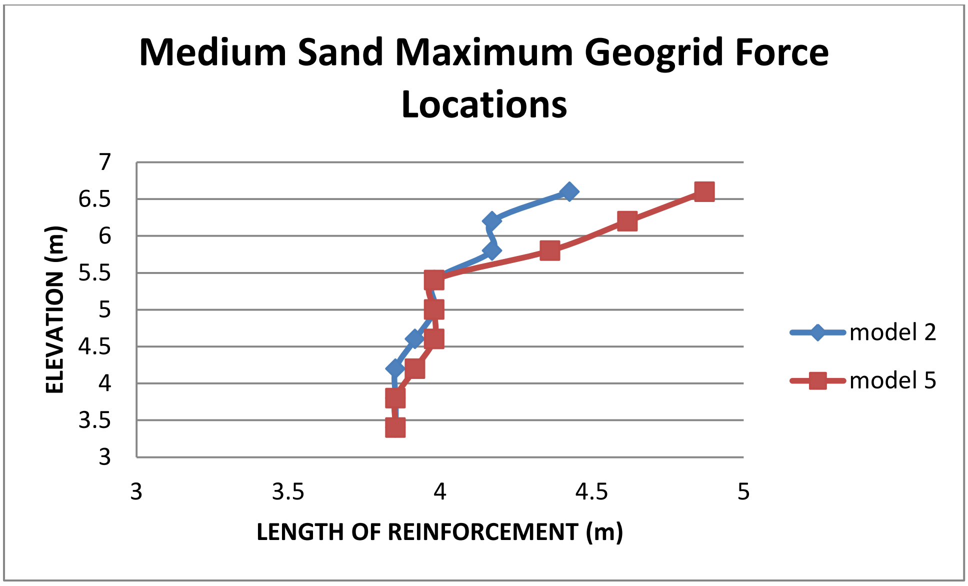

Figure 4. 18 Maximum Geogrid Force Location Medium Sand Backfill

Observation

The maximum geogrid load locations along the reinforcement length for each layer were investigated here in Figure 4.18. For both model 2 and model 5 maximum geogrid loads of the first 6 layers out of 9 layers from bottom up of wall height were occurred near to the face of wall.

4.3.3 Stiff Clay Backfill

All the material properties of the soil were not changed only the axial stiffness of the reinforcing material/geogrid was changed from 1500 kN/m to 750 kN/m which is reduced in half.

- GRS wall with geogrid stiffness 1500 kN/m (model 3)
- GRS wall with geogrid stiffness 750 kN/m (model 6)

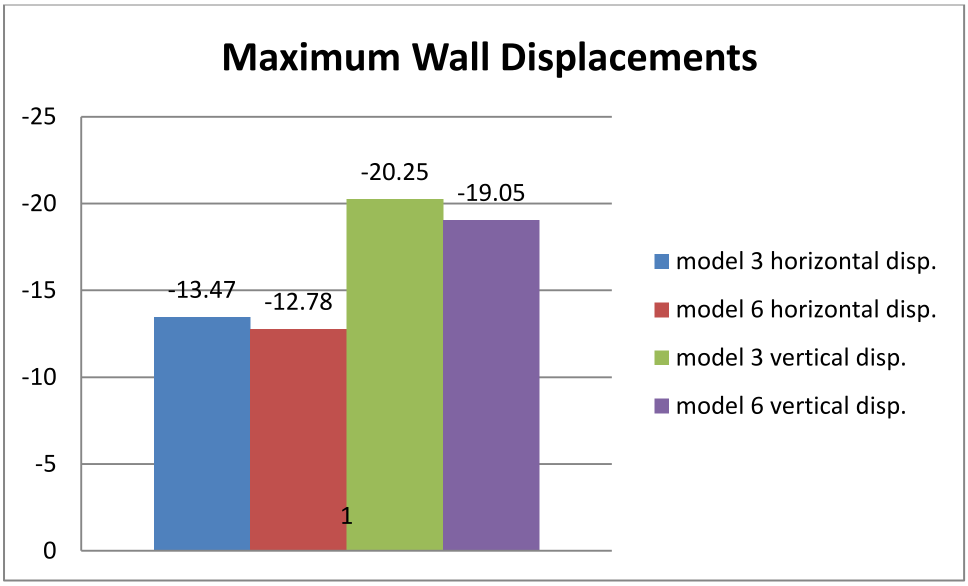

Figure 4. 19 Maximum Wall Displacements Stiff Clay Backfill

Observation

GRS wall with stiff clay backfill material maximum displacements shown in Figure 4.19described that the maximum vertical displacement of the wall was greater than the maximum horizontal displacement for both geogrid stiffness's (i.e. model 3 and model 6). The variation in the geogrid stiffness(i.e. half reduction in stiffness) have less improvement in the performance of GRS wall with stiff clay backfill material; which is around 5% for horizontal displacement and 6% for vertical displacements.

Table 4. 13 Stiff clay facing displacement

facing displacement				
	model 3		model 6	
elevation	horizontal	vertical	horizontal	vertical
3	-1.62	-4.61	-1.68	-4.57
4	-5.66	-5.49	-5.94	-5.46
5	-6.16	-5.31	-6.83	-5.26
6	-2.3	-4.9	-2.81	-4.61
7	-4.87	-4.56	-4.886	-4.24

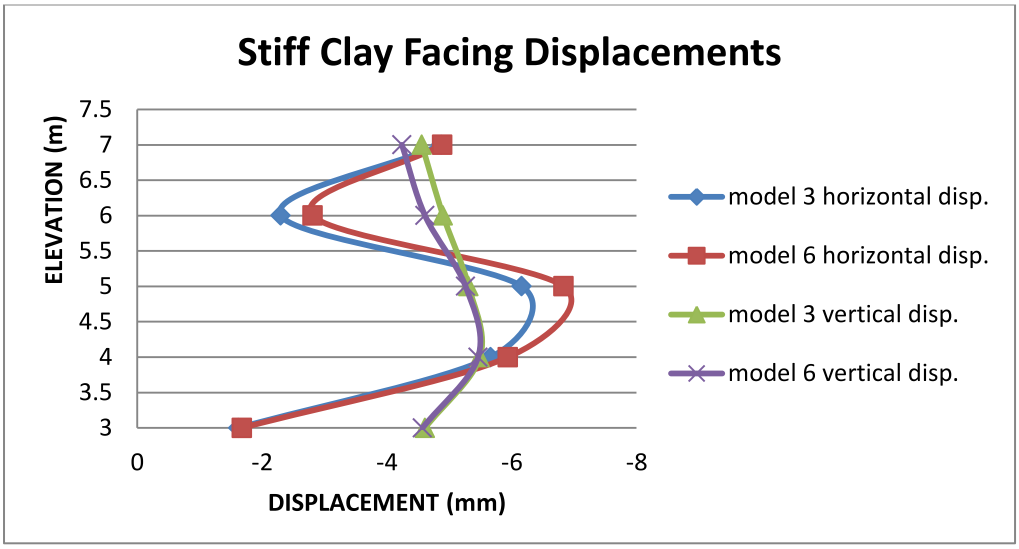

Figure 4. 20 Wall Facing Displacements Stiff Clay Backfill

Observation

The facing modular block wall of GRS wall with stiff clay backfill in different geogrid stiffness was examined. As in Figure 4.20shown above the horizontal deflection of facing was s-shaped and which is maximum at the mid height of the wall. Vertical deformation of the wall facing is nearly similar for both models and which is maximum between 0.3H and 0.5H.

Table 4. 14 Stiff clay maximum Geogrid displacements

maximum Geogrid displacement [mm]				
	model 3		model 6	
elevation	horizontal	vertical	horizontal	Vertical
3.4	-3.19	-7.33	-3.35	-7.18
3.8	-4.68	-10.26	-4.97	-9.81
4.2	-5.43	-13.05	-6.06	-12.38
4.6	-5.43	-15.5	-6.33	-14.71
5	-5.26	-17.47	-5.64	-16.63
5.4	-6.9	-18.87	-6.66	-17.93
5.8	-8.57	-19.76	-8.31	-18.69
6.2	-10.21	-20.18	-9.93	-19.01
6.6	-11.69	-20.12	-11.39	-18.87

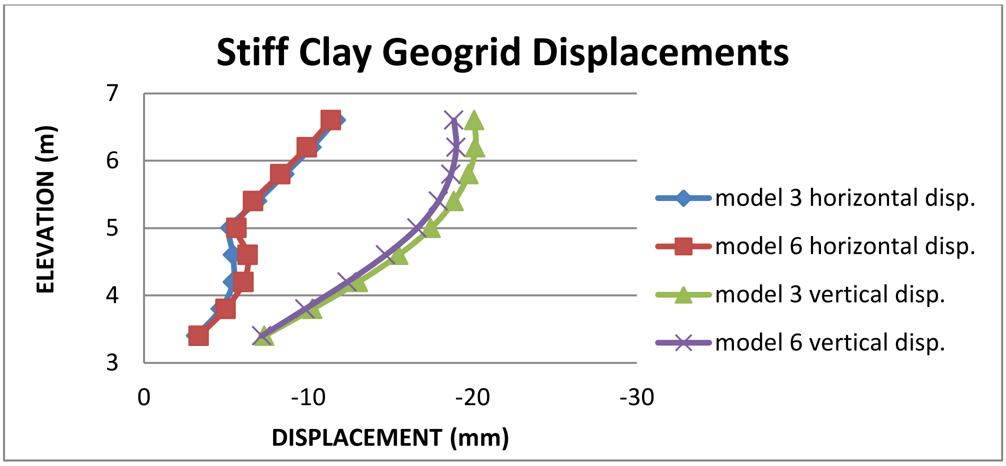

Figure 4. 21 Maximum Geogrid Displacements Stiff Clay Backfill

Observation

The Figure 4.21 shown that the displacements of reinforcement material geogrid for GRS wall with stiff clay backfill, like wall displacements geogrid have greater vertical displacements than horizontal displacements. From the displacements of GRS wall, facing displacements and geogrid displacements there is a little bit difference in the displacements for model 3 and model 6. Therefore, once state of equilibrium between the geogrid stiffness and backfill soil angle of internal friction has to be reached the GRS wall to be stable. Further additional stiffness becomes unnecessary and uneconomical.

Table 4. 15 Stiff clay maximum geogrid force

Maximum geogrid force		
	model 3	model 6
elevation	force	force
3.4	1.465	1.647
3.8	3.313	3.235
4.2	4.007	4.635
4.6	4.143	5.213
5	4.179	5.1315
5.4	3.973	4.804
5.8	3.238	3.796
6.2	2.158	2.58
6.6	1.19	1.095

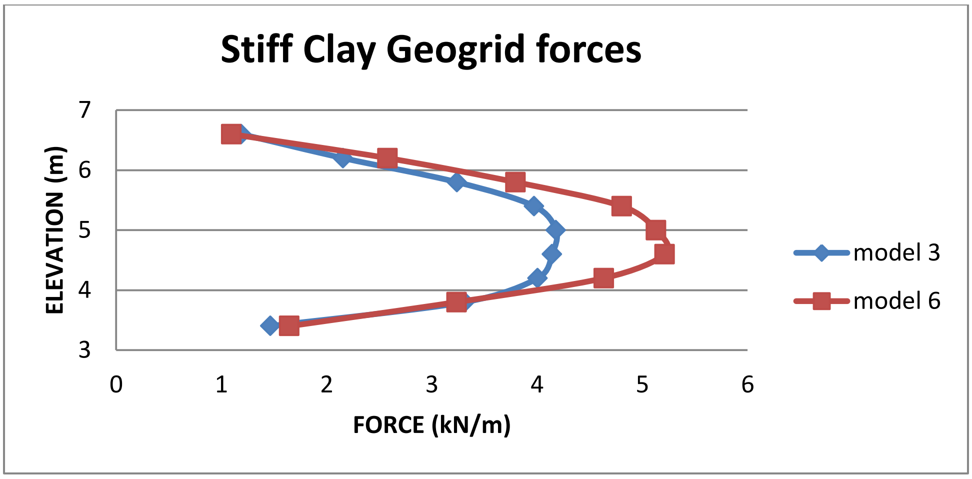

Figure 4. 22 Maximum Geogrid Force of Stiff Clay Backfill

Observation

The maximum geogrid force of the wall with small geogrid stiffness has greater than the geogrid of high relative stiffness. Following that the maximum tension forces developed in the geogrid is higher for model 6 than model 3. Within the height of the wall maximum loads in the geogrid was occurred at the mid layers of geogrid. Geogrid forces are relatively small at the wall bottom; this is due to the influence foundation.

Table 4. 16 Stiff clay maximum geogrid force location

Maximum geogrid force location		
	model 3	model 6
Elevation	distance from facing	distance from facing
3.4	3.951	3.4
3.8	3.4	3.4
4.2	3.4	3.4
4.6	3.4	3.4
5	3.4	3.4
5.4	3.4	3.4
5.8	3.4	3.4
6.2	3.5	3.4
6.6	3.5	3.6

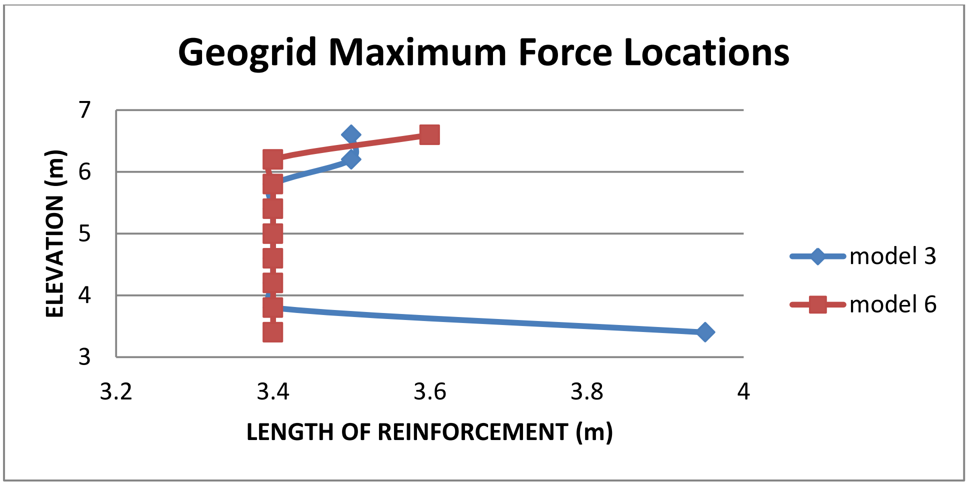

Figure 4. 23 Maximum Geogrid Force Locations of Stiff Clay Backfill

Observation

For both models maximum geogrid forces are obtained at the early length of the geogrid i.e. just behind the facing wall. Variation in soil properties and construction methods results in shifting of the position of maximum tensile forces away from the failure plane. It also depends on the length and stiffness of reinforcements (Oyegible 2011). Lateral restraint of wall facing results maximum tensile forces maximum at the back of the facing and decreases to the end of reinforcement. Jewell (1988) stated that the locus of maximum tensile force (*T*) would always be inclined to (45°+Ø/2) the horizontal if the soil-reinforcement interface is sufficiently bonded, otherwise, the locus will move towards the facing.

<u>4.3.4 Compression of Model Responses for Geogrid Stiffness Variation Influence</u>

All models of GRS wall performances from facing displacements (i.e. Figure 4.24 and figure4.25), geogrid displacements (i.e. Figure 4.26 and Figure4.27), geogrid loads (i.e. Figure 4.28) and maximum load locations (i.e. Figure4.29) were compared.

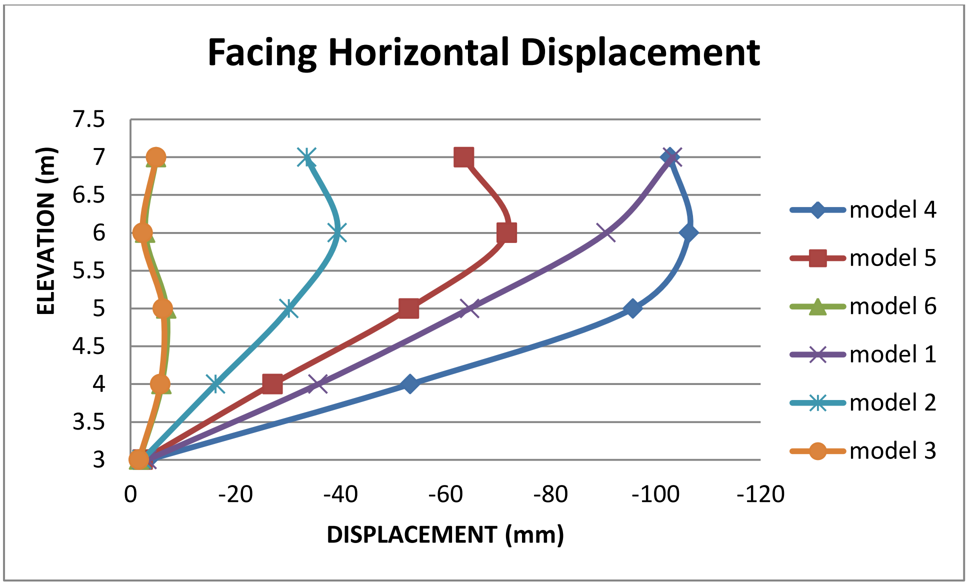

Figure 4. 24 Influence of Geogrid Stiffness on Wall Facing Horizontal Displacements

Observation

As shown in Figure 4.24soft clay have maximum horizontal displacement for both geogrid stiffness's. Medium sand and soft clays have significantly influenced by the geogrid stiffness in the horizontal displacement rather stiff clays have a little bit influenced by geogrid stiffness in lateral movement of facing wall.

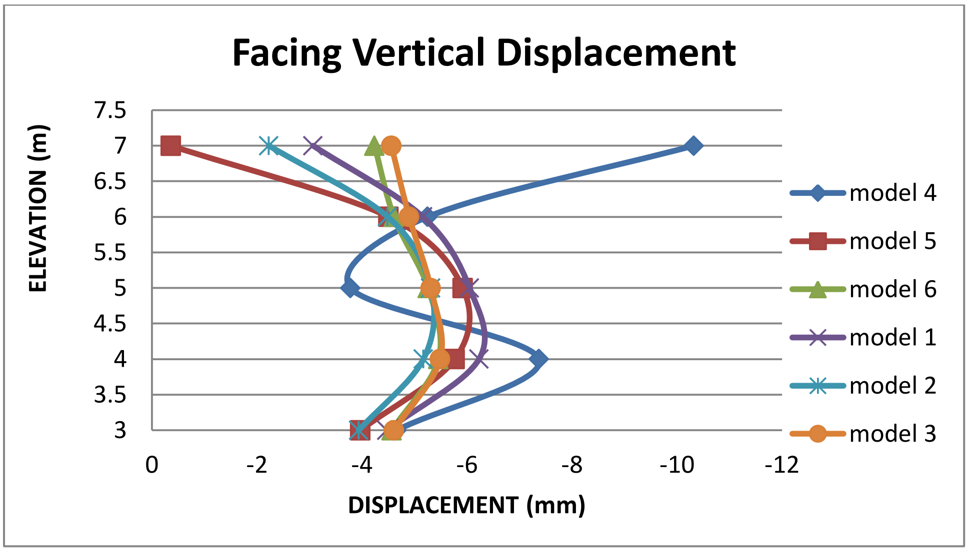

Figure 4. 25 Influence of Geogrid Stiffness on Wall Vertical Displacements

Observation

Similar to the horizontal displacements vertical displacements of facing for stiff clay with both geogrid stiffness have small variation. As Figure 4.25vertical deformations of soft clays are larger than others. Stiff clays have almost uniform vertical displacements throughout the height of facing wall.

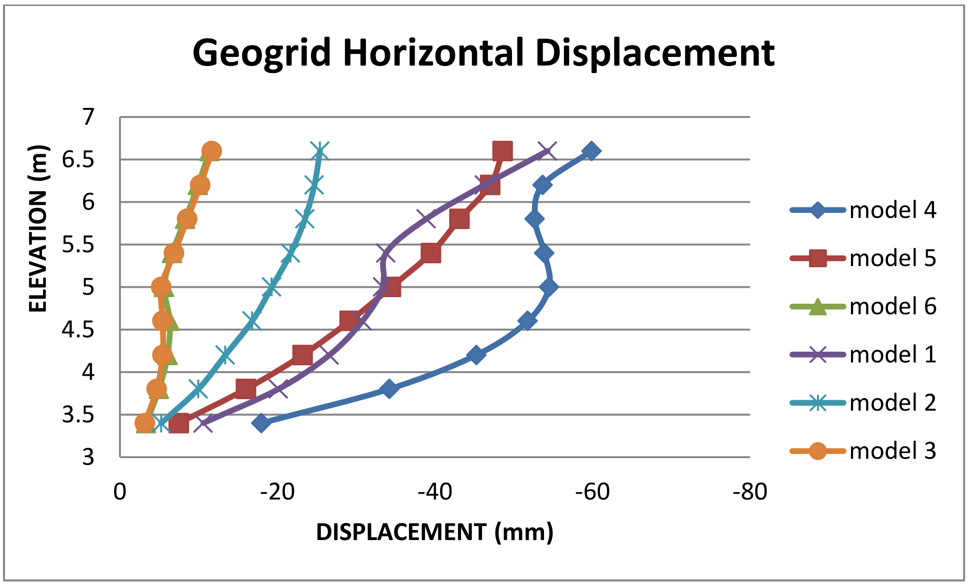

Figure 4. 26 Influence of Geogrid Stiffness on Geogrid Horizontal Displacements

Observation

Displacement of the reinforcing material basically influenced by the strength of the material and interaction of reinforcement and the soil here in this analysis result shown in Figure 4.26 for all models bottom geogrid layers have minimum horizontal displacements and top geogrid have maximum lateral movements.

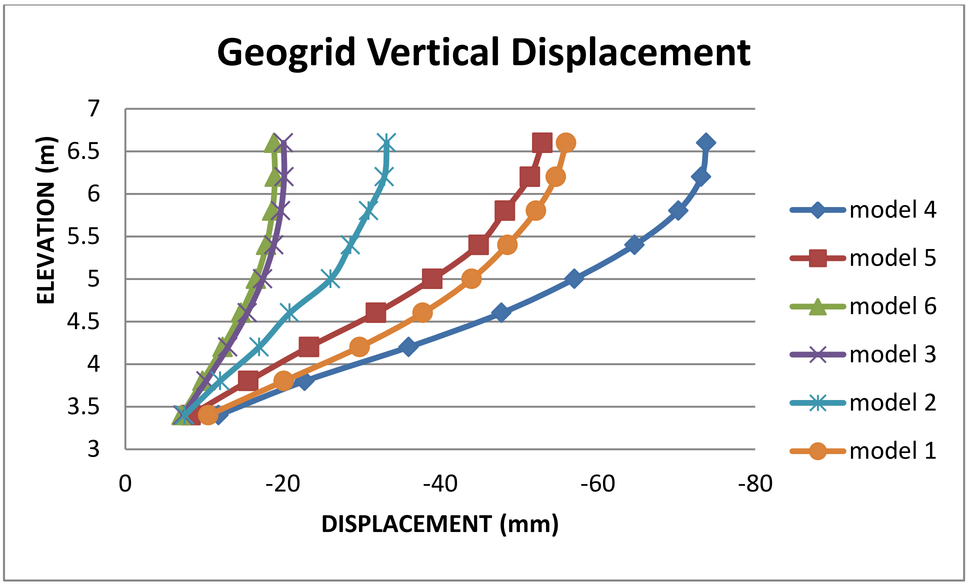

Figure 4. 27 Influence of Geogrid Stiffness on Geogrid Vertical Displacements

The vertical displacement of geogrid for all models was greater at the top wall and linearly decreased to the bottom.

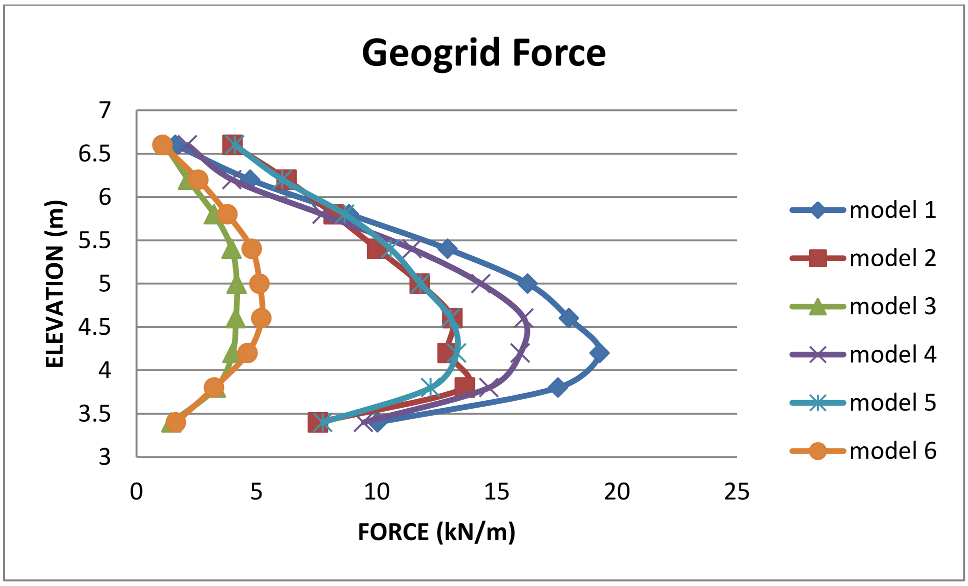

Figure 4. 28 Influence of Geogrid Stiffness on Geogrid Force

Figure 4.28shown that loads developed in the geogrid to take the GRS wall at equilibrium were maximum at 0.3H to 0.5H intervals for all models. Relatively Weak GRS walls have higher geogrid force.

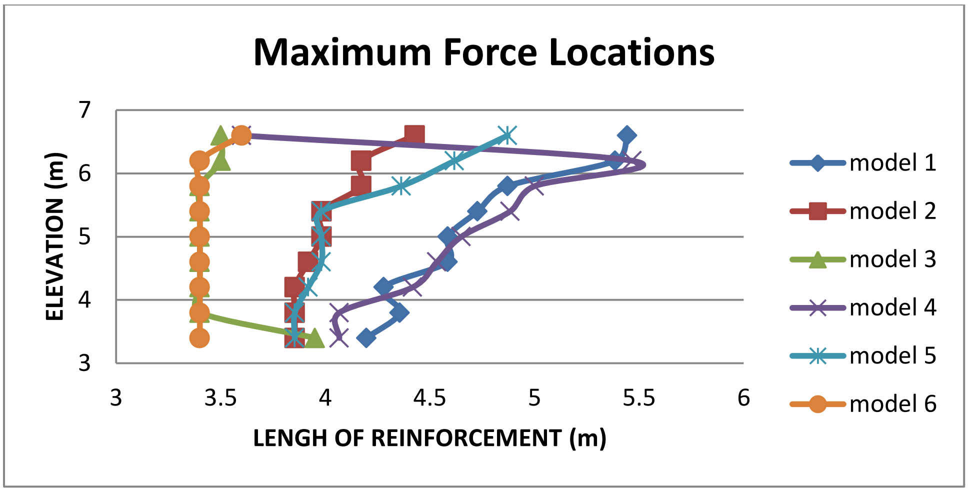

Figure 4. 29 Influence of Geogrid Stiffness on Maximum Geogrid force Location

Since the most critical slip surface of GRS wall was assumed to concede with maximum geogrid tensile forces line. As shown in the Figure 4.29stiff clay maximum geogrid forces occurred just at the back of facing wall. From Mohr coulomb failure criterion the most critical failure plane was (45^{o}+Ø/2) from the horizontal.

4.4 Influence of Geogrid Spacing on the Behavior of Earth Retaining Structures

Reinforcement spacing is one of the design parameter in the GRS wall design. Therefore it is crucial to investigate the influence of spacing on the behavior of GRS walls. Model 1, model 2 and model 3 were their geogrid spacing of 0.4m and the coming models (i.e. model 7, model 8 and model 9) were geogrid spacing of 0.2m has been compared.

4.4.1 Soft clay backfill

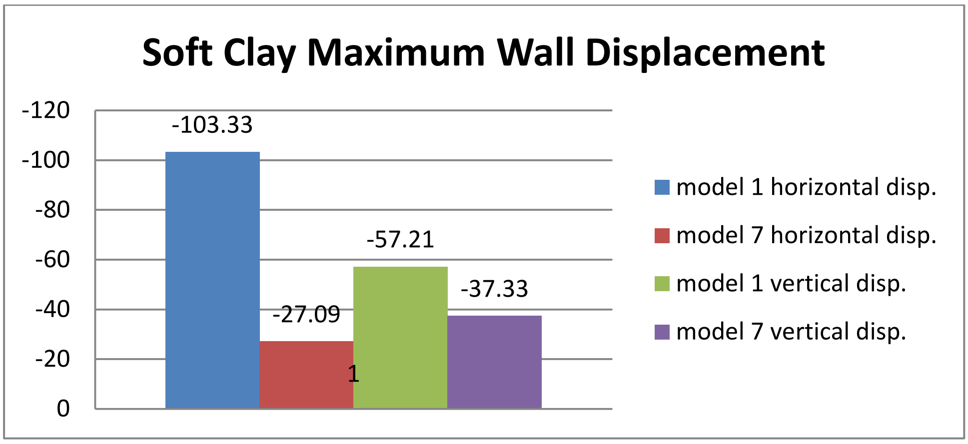

Figure 4. 30 Maximum Displacement of Wall with Soft Clay Backfill Geogrid Spacing Influence

Observation

The maximum horizontal and vertical displacements of model 1 and model 7 was shown above in Figure 4.30 indicated that, the horizontal displacement of the wall for geogrid spacing variation from 0.4 m to 0.2 m was reduced by 73.78% and the vertical displacement was reduced by 34.74%. From the previous case study we could see that, when the geogrid stiffness of soft clay backfill material reinforced wall reduced in half (i.e. from 1500 kN/m to 750 kN/m) the maximum horizontal displacement was approximately increased by 8%. the maximum vertical displacement of the wall increased by 22.5%.

Table 4. 17 Wall facing displacements soft clay backfill

	Facing Displacements [mm]			
	model 1		model 7	
elevation	horizontal	vertical	horizontal	vertical
3	-3.18	-4.48	-2.72	-4.98
4	-35.75	-6.23	-17.09	-6.12
5	-64.6	-6.05	-24.78	-5.27
6	-90.6	-5.16	-26.48	-4.35
7	-103.3	-3.07	-21.29	-3.44

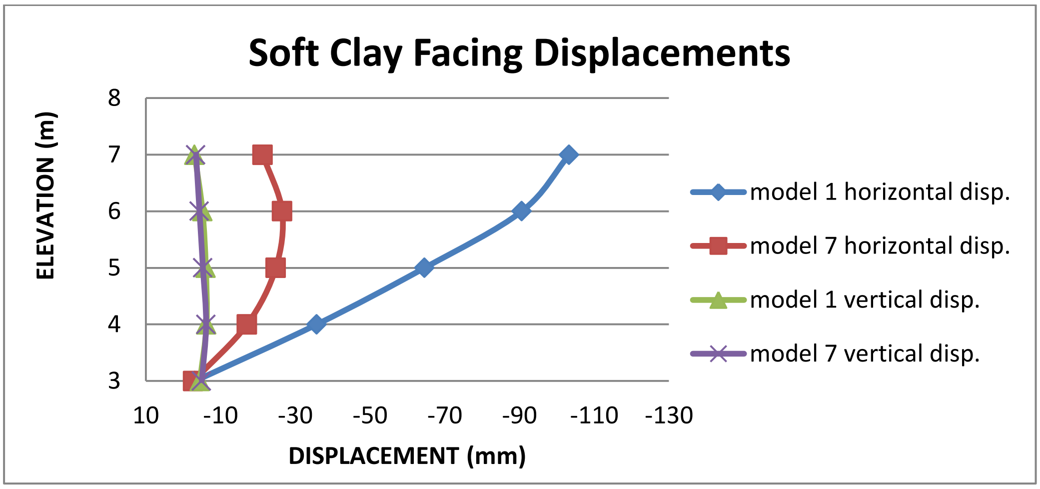

Figure 4. 31 Wall Facing Displacements of Soft Clay Influence of Geogrid Spacing

Observation

As shown in Figure 4.31there was significant reduction in the horizontal displacement of the facing wall as the vertical spacing of the geogrid reduced. But small variation was observed in the vertical deformation of the facing wall, In addition vertical displacement of facing wall show small change for the geogrid stiffness and spacing variation.

Table 4. 18 Maximum geogrid displacement soft clay backfill

maximum geogrid displacement [mm]				
	model 1		model 7	
elevation	horizontal	vertical	horizontal	vertical
3.4	-10.59	-10.57	-7.8	-9.57
3.8	-20.14	-20.13	-12.6	-15.24
4.2	-26.61	-29.77	-15.34	-20.86
4.6	-30.8	-37.79	-16.46	-26
5	-33.4	-44	-16.3	-30.34
5.4	-33.8	-48.54	-15.04	-33.68
5.8	-38.9	-52.19	-16.28	-35.93
6.2	-46.3	-54.7	-20.08	-37.07
6.6	-54.3	-56	-23.61	-37.28

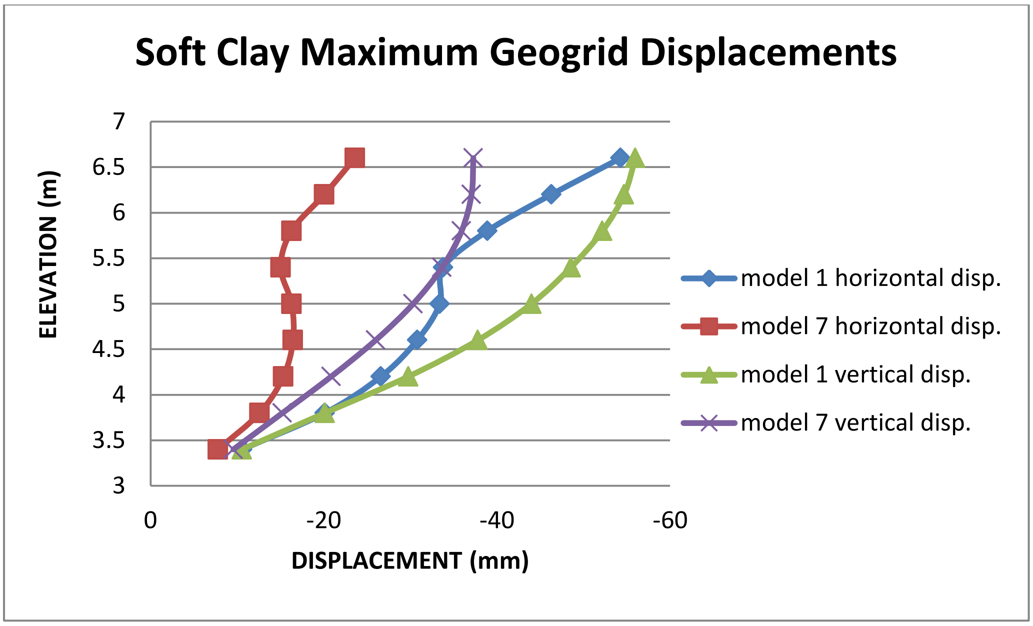

Figure 4. 32 Maximum Geogrid Displacement Soft Clay Backfill Geogrid Spacing Influence

Geogrid displacements of the GRS wall with soft clay backfill material in case of spacing variation shown in Figure 4.32above were reduced as geogrid spacing reduced from 0.4 m to 0.2 m.

Table 4. 19 Maximum Geogrid force soft clay backfill

Maximum geogrid force [kN/m]		
	model 1	model 7
elevation	load	load
3.4	10.043	5.86
3.8	17.553	7.64
4.2	19.293	8.147
4.6	18.015	7.602
5	16.296	6.365
5.4	12.958	4.777
5.8	8.862	3.025
6.2	4.737	1.351
6.6	1.623	1.801

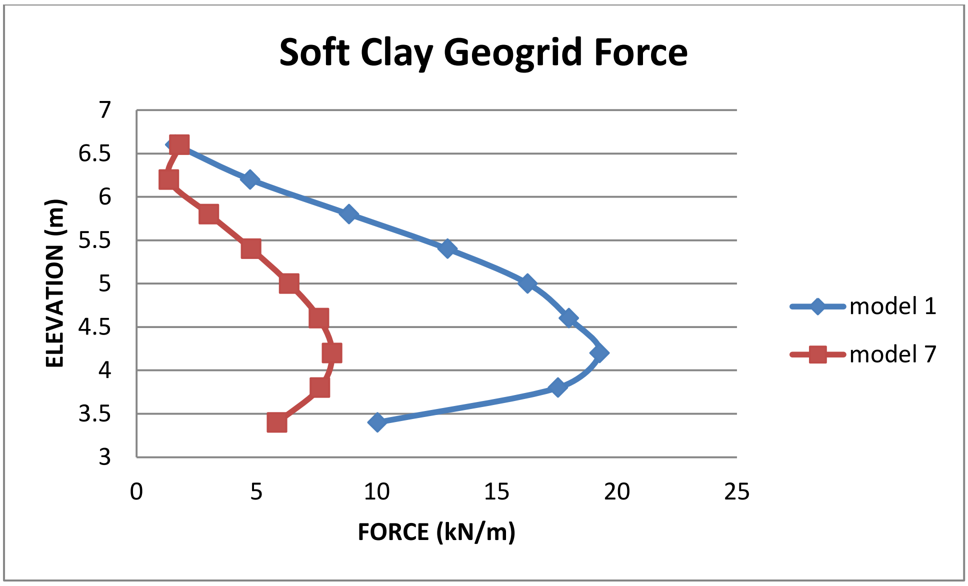

Figure 4. 33 Maximum Geogrid Load of Soft Clay Backfill Geogrid Spacing Influence

Reducing the vertical spacing of the geogrid was effective in maximum geogrid force reduction as compared with that of increasing geogrid stiffness for such backfill soil materials as shown in Figure 4.33.

Table 4. 20 Maximum geogrid force location soft clay backfill

	Max. load location	
elevation	model 1	model 7
3.4	4.197	4.162
3.8	4.356	4.337
4.2	4.279	4.337
4.6	4.585	4.559
5	4.585	4.665
5.4	4.728	4.559
5.8	4.871	4.559
6.2	5.385	5.686
6.6	5.443	3.6

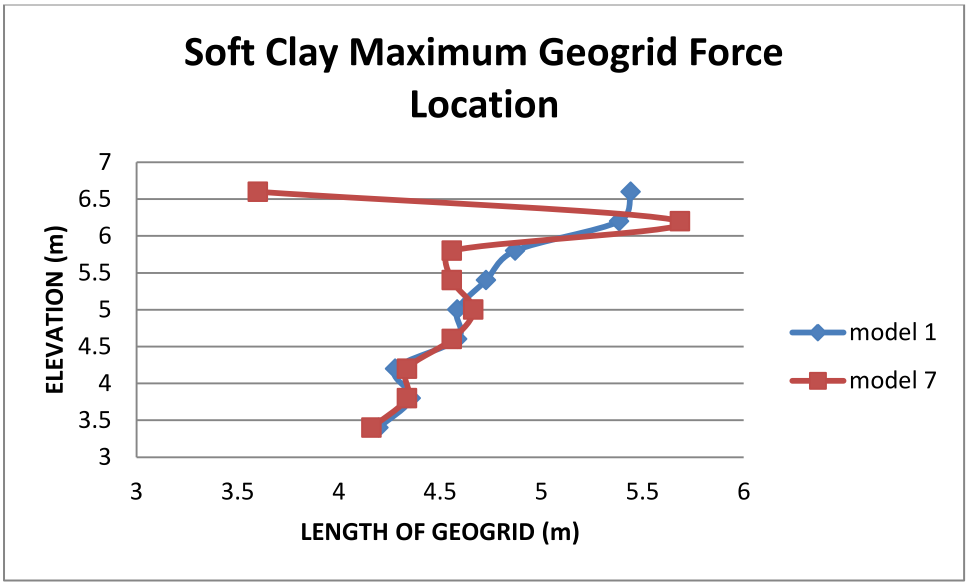

Figure 4. 34 Maximum Geogrid Force Location of Soft Clay Backfill Geogrid Spacing Influence

Bottom layers of Geogrid have maximum force location of near to the facing wall and gone far from the facing as we go up to the top geogrid layers see Figure 4.34 above.

4.4.2 Medium sand backfill

All the material properties of the soil were not changed only the geogrid vertical spacing was changed from 0.4 m to 0.2 m which is reduced in half.

- GRS wall with geogrid spacing 0.4 m (**model 2**).
- GRS wall with geogrid spacing 0.2 m (**model 8**).

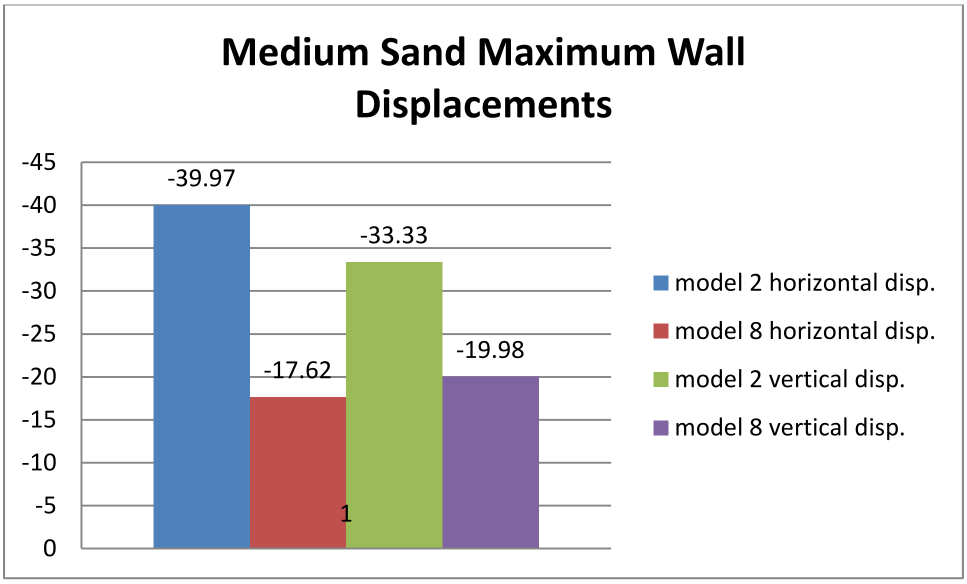

Figure 4. 35 Maximum Wall Displacements of Medium Sand Backfill Geogrid Spacing Influence

Observation

Due to the reduction of geogrid spacing from 0.4 m to 0.2 m which is in half, the maximum horizontal displacement of GRS wall reduced in 56% and the maximum vertical displacement of the wall also reduced in 40% as shown in Figure 4.35.

Table 4. 21 Medium sand facing displacements

facing displacement				
	model 2		model 8	
elevation	horizontal	vertical	horizontal	vertical
3	-2.21	-3.94	-2.08	-4.39
4	-16.2	-5.17	-9.46	-5.44
5	-30.2	-5.31	-15.34	-5.46
6	-39.4	-4.49	-17.58	-5
7	-33.6	-2.23	-12.05	-3.95

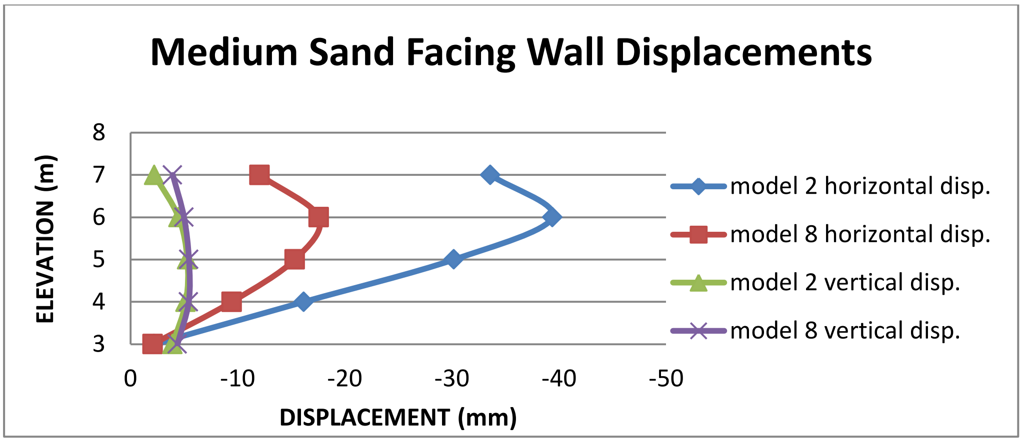

Figure 4. 36 Medium Sand Backfill Wall Facing Displacements Geogrid Spacing Influence

Observation

Figure 4.36shown that wall facing vertical displacements of model 2 and model 8 have almost the same throughout the wall height, means that varying geogrid vertical spacing does not lead to significant effect in vertical deformation of the facing wall. But the horizontal movement of facing wall was reduced for model 8 than model 2. The maximum horizontal displacement for both models was occurred at 0.75H.

Table 4. 22 Medium sand maximum geogrid displacements

Maximum geogrid displacement [mm]				
	model 2		model 8	
elevation	horizontal	vertical	horizontal	vertical
3.4	-5.25	-7.56	-4.51	-7.29
3.8	-9.97	-12.05	-6.83	-9.16
4.2	-13.4	-17	-8.5	-11.61
4.6	-16.8	-20.9	-9.66	-13.93
5	-19.3	-26.1	-10.29	-15.97
5.4	-21.7	-28.6	-10.57	-17.65
5.8	-23.5	-30.9	-10.59	-18.88
6.2	-24.7	-32.9	-10.61	-19.65
6.6	-25.4	-33.2	-12.17	-19.97

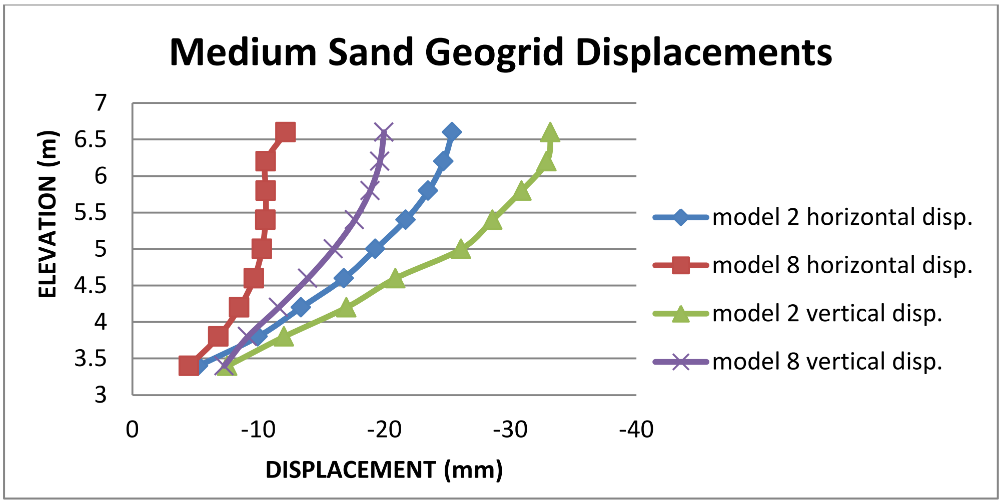

Figure 4. 37 Maximum Geogrid Displacements of Medium Sand Geogrid Spacing Influence

Observation

The maximum geogrid displacements for the selected layers were showed in Figure 4.37. Geogrid spacing variation cased significant difference in horizontal and vertical displacements of the geogrid for both models. Greater geogrid displacements were observed at the top layers of the wall.

Table 4. 23 Medium sand maximum geogrid forces

Geogrid Force		
	model 2	model 8
Elevation	force	force
3.4	7.561	4.266
3.8	13.679	5.063
4.2	12.959	5.278
4.6	13.158	5.315
5	11.805	4.561
5.4	10.025	3.738
5.8	8.212	2.816
6.2	6.257	1.764
6.6	4.014	0.76

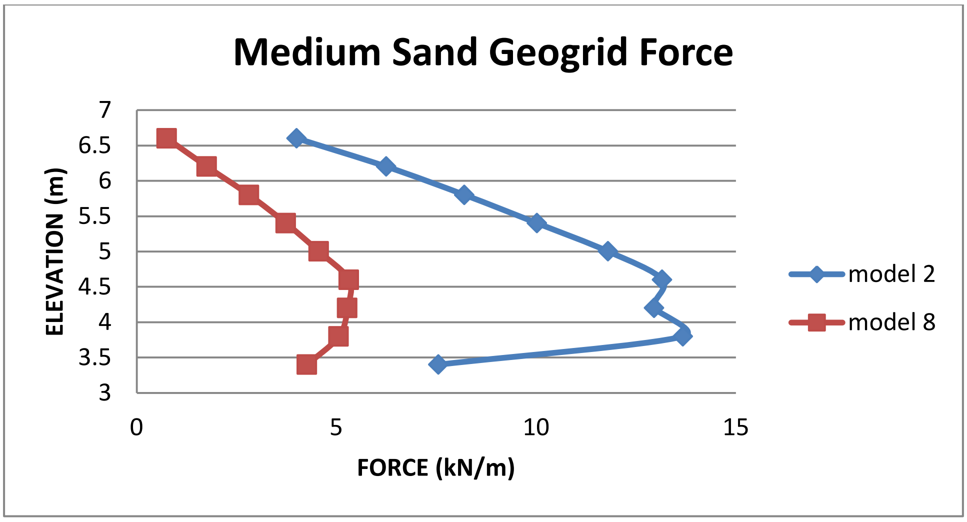

Figure 4. 38 Medium Sand Maximum Geogrid Force Geogrid Spacing Influence

Observation

Forces developed within the geogrid along its length as shown in Figure 4.38described that the distribution of maximum force along the wall height varied between parabolic shapes. Larger reduction in geogrid axial force observed in GRS wall with small vertical spacing.

Table 4. 24 Medium sand maximum geogrid force locations

	Max. force location	
Elevation	model 2	model 8
3.4	3.854	3.6
3.8	3.854	3.6
4.2	3.854	3.854
4.6	3.918	3.854
5	3.982	4.045
5.4	3.982	4.045
5.8	4.172	3.981
6.2	4.172	3.981
6.6	4.427	4.936

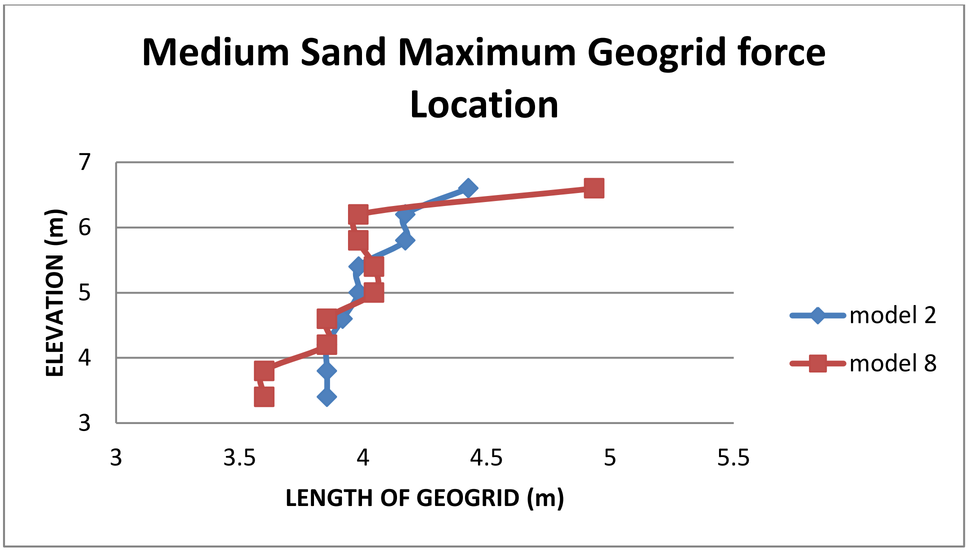

Figure 4. 39 Maximum Geogrid Force Locations of Medium Sand Backfill Geogrid Spacing Influence

Observation

The location of maximum forces in the geogrid for geogrid spacing variation was analyzed as shown in Figure 4.39. Bottom geogrid layers have maximum force location closest to the facing for model 8 than model 2.

4.4.3 Stiff Clay Backfill

All the material properties of the soil were not changed only the vertical spacing of the reinforcing material/geogrid was changed from 0.4 m to 0.2 m which is reduced in half.

- GRS wall with geogridspacing0.4 m (**model 3**)
- GRS wall with geogrid spacing 0.2 m (**model 9**)

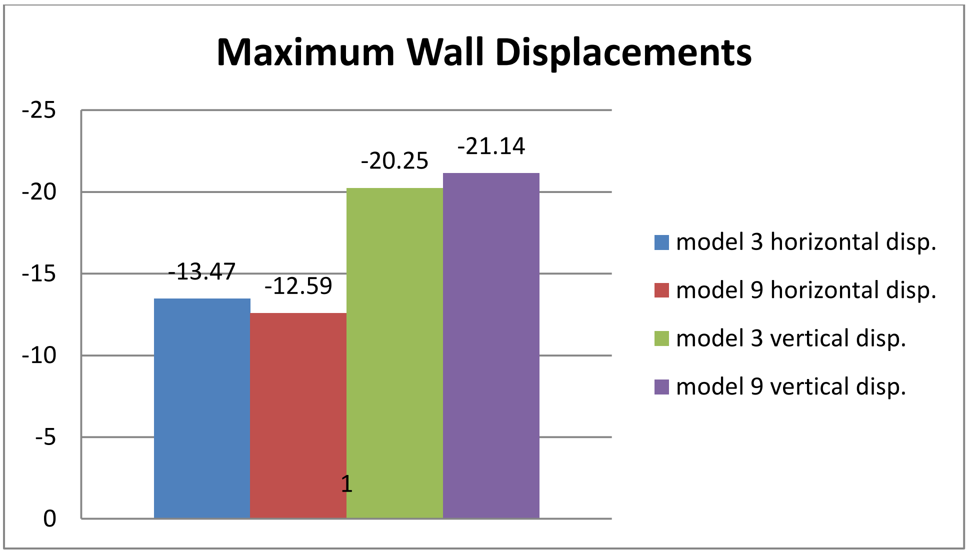

Figure 4. 40 Maximum Wall Displacement of Stiff Clay Backfill Geogrid Spacing Influence

Observation

As we seen in the previous case study which is geogrid stiffness influence, the variation of vertical spacing of reinforcing material has less effect in geogrid displacements of GRS wall with stiff clay backfill. The vertical displacement of geogrid was little bit increased for the reduction of geogrid spacing.

Table 4. 25 Stiff clay facing displacements

Facing displacement [mm]				
	model 3		model 9	
elevation	horizontal	vertical	horizontal	vertical
3	-1.62	-4.61	-1.6	-4.61
4	-5.66	-5.49	-4.79	-5.48
5	-6.16	-5.31	-4.22	-5.25
6	-2.3	-4.9	0.523	-4.83
7	-4.87	-4.56	7.603	-4.64

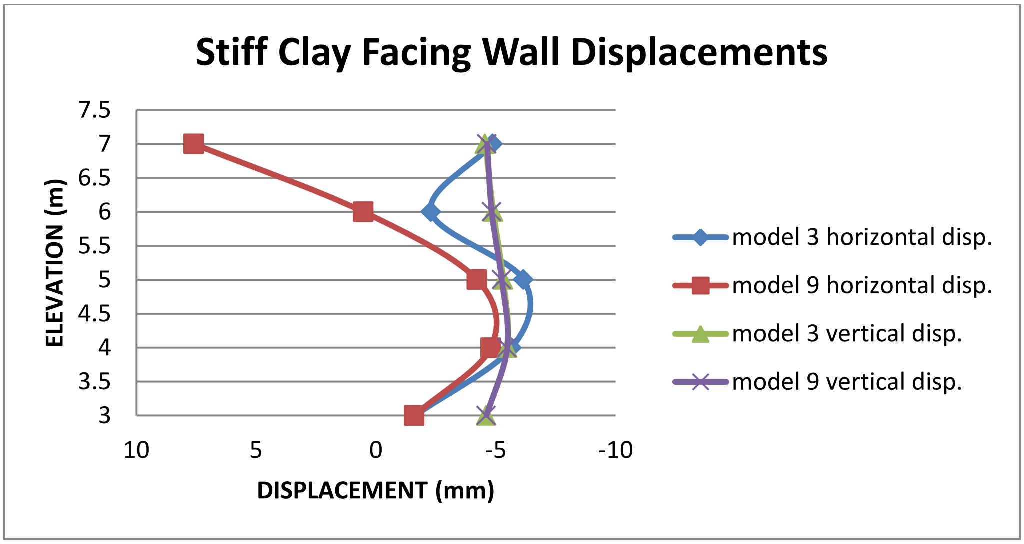

Figure 4. 41 Wall Facing Displacement of Stiff Clay Backfill Geogrid Spacing Influence

Observation

As seen in Figure 4.41the vertical deformations of the facing wall for both models was slight difference for the geogrid spacing variation influence. But there were variation in horizontal displacement of facing wall. Model 9 showed inward horizontal displacement of facing wall towards the backfill soil as we go to the top of the wall.

Table 4. 26 Stiff clay maximum geogrid displacements

Maximum geogrid displacement [mm]				
	model 3		model 9	
Elevation	horizontal	vertical	horizontal	Vertical
3.4	-3.19	-7.33	-2.99	-7.69
3.8	-4.68	-10.26	-4.12	-10.88
4.2	-5.43	-13.05	-4.69	-13.78
4.6	-5.43	-15.5	-4.53	-16.25
5	-5.26	-17.47	-5.39	-18.2
5.4	-6.9	-18.87	-6.9	-19.65
5.8	-8.57	-19.76	-8.45	-20.61
6.2	-10.21	-20.18	-9.94	-21.07
6.6	-11.69	-20.12	-11.21	-21

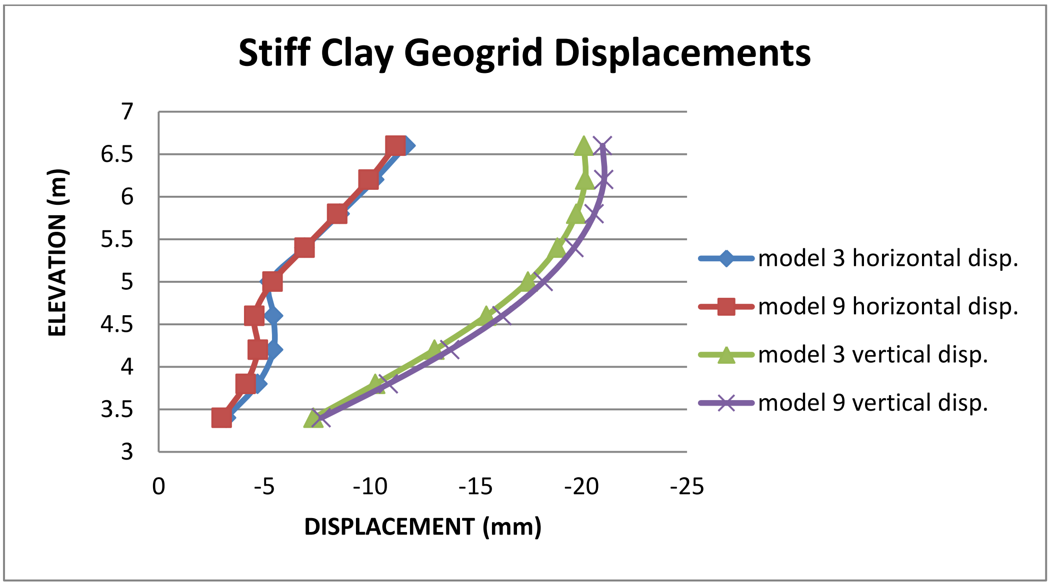

Figure 4. 42 Maximum Geogrid Displacement of Stiff Clay Backfill Geogrid Spacing Influence

Hence, the GRS wall model with stiff clay backfill was relatively stable for such serviceability condition; there were little difference in performance as geogrid spacing varied likewise in the variation of geogrid stiffness in previous case.

Table 4. 27 Stiff clay maximum geogrid forces

Maximum geogrid force[kN/m]		
	model 3	model 9
Elevation	force	force
3.4	1.465	1.221
3.8	3.313	2.009
4.2	4.007	2.994
4.6	4.143	3.281
5	4.179	3.076
5.4	3.973	2.522
5.8	3.238	1.746
6.2	2.158	1.147
6.6	1.19	0.65

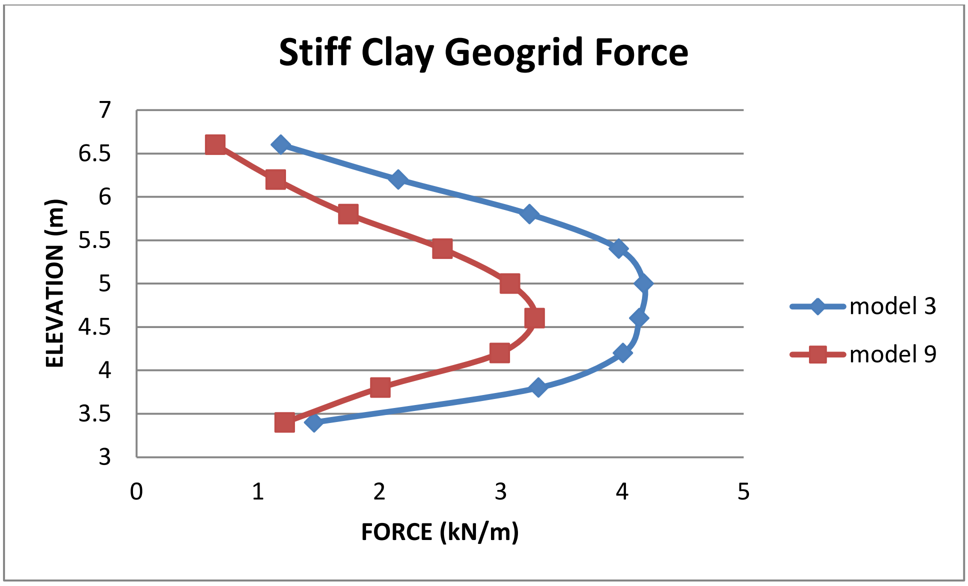

Figure 4. 43 Geogrid Forces of Stiff Clay Backfill Geogrid Spacing Influence

Observation

As shown in Figure 4.43the maximum force of the geogrid developed were reduced for each layer as the vertical spacing of geogrid reduced. Maximum geogrid forces were occurred at the mid height of the wall.

Table 4. 28 Stiff clay maximum geogrid force location

Maximum geogrid force location[kN/m]		
	Model 3	Model 9
Elevation	Distance from facing	Distance from facing
3.4	3.9	4.6
3.8	3.4	3.4
4.2	3.4	3.4
4.6	3.4	3.4
5	3.4	3.4
5.4	3.4	3.4
5.8	3.4	3.6
6.2	3.5	3.4
6.6	3.5	3.4

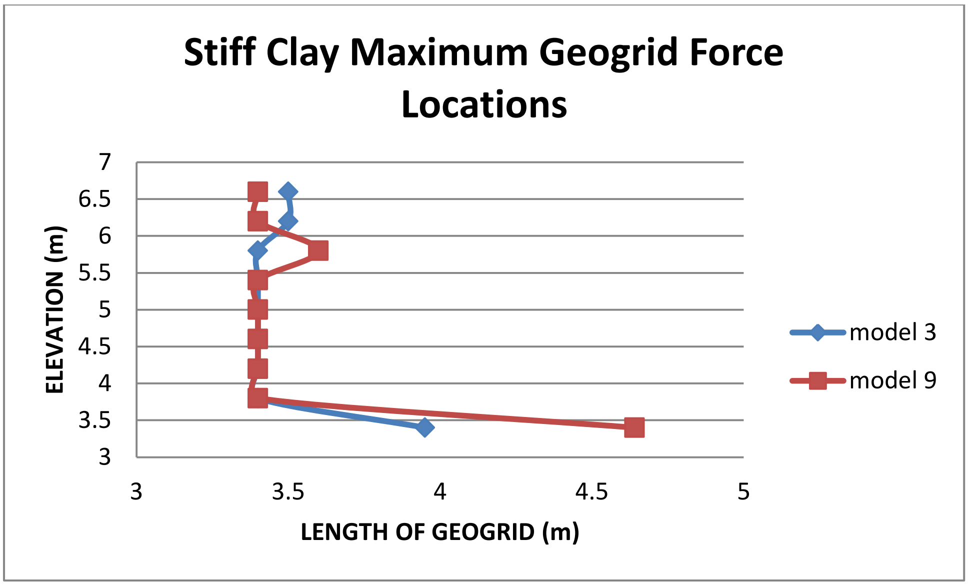

Figure 4. 44 Maximum Geogrid Load Locations Stiff Clay Backfill Geogrid Stiffness Influence

For both models maximum geogrid forces are obtained at the early length of the geogrid i.e. just behind the facing wall. Variation of geogrid spacing has small effect in the maximum geogrid force location.

4.4.4 Compression of Model Responses for Geogrid Vertical Spacing Variation Influence

The performance of GRS retaining wall model was evaluated and compared for different backfill material types with variation of geogrid vertical spacing. The results were illustrated in the table below.

Table 4. 29 Wall displacements for geogrid spacing influence with different backfill materials

spacing (m)	soft clay		medium sand		stiff clay	
	horizontal displacement (mm)	vertical displacement (mm)	horizontal displacement (mm)	vertical displacement (mm)	horizontal displacement (mm)	vertical displacement (mm)
0.2	-27.09	-37.33	-17.62	-19.98	-12.59	-21.14
0.4	-103.33	-57.21	-39.97	-33.33	-13.47	-20.25

All models of GRS wall performances from facing displacements (i.e. Figure 4.45 and Figure 4.46), Geogrid displacements (i.e. Figure 4.47 and Figure 4.48), geogrid forces (i.e. Figure 4.49) and maximum geogrid force locations (i.e. Figure 4.50) were compared.

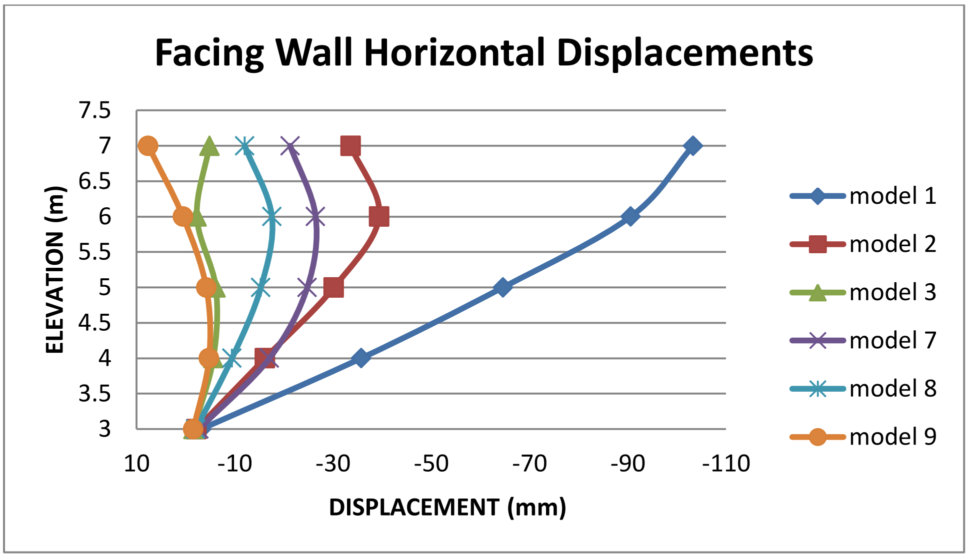

Figure 4. 45 Influence of Geogrid Spacing on Wall Facing Horizontal Displacements

Soft clay backfill wall with larger geogrid spacing have higher facing wall horizontal displacement. GRS wall with stiff clay backfill have smaller wall facing horizontal displacement than others even with larger geogrid vertical spacing.

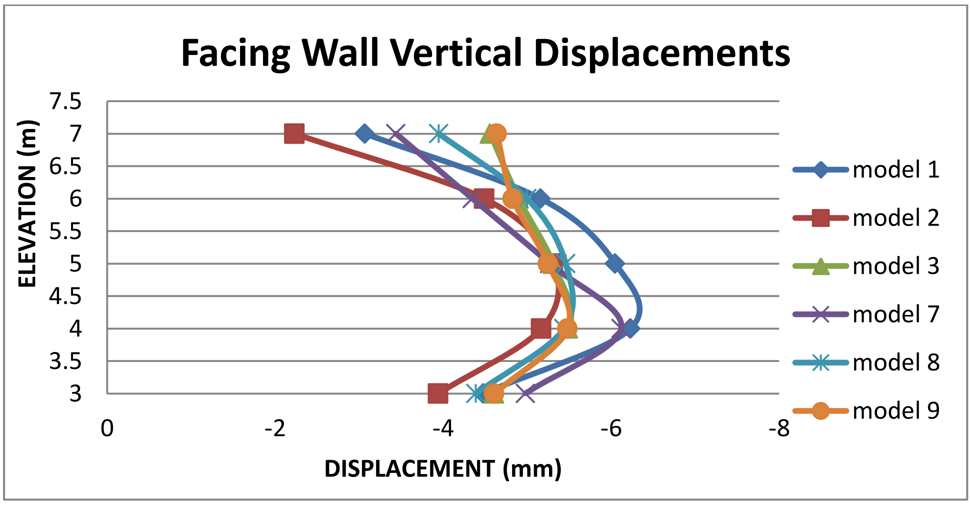

Figure 4. 46 Influence of Geogrid Spacing on Facing Vertical Displacements

Observation

At the wall facing top the vertical deformation of wall was maximum for GRS wall with stiff clay backfill and minimum facing deformation was observed in medium sand backfill with larger geogrid vertical spacing. At the wall mid height soft clay backfill with larger geogrid spacing showed larger vertical deformation at the wall facing.

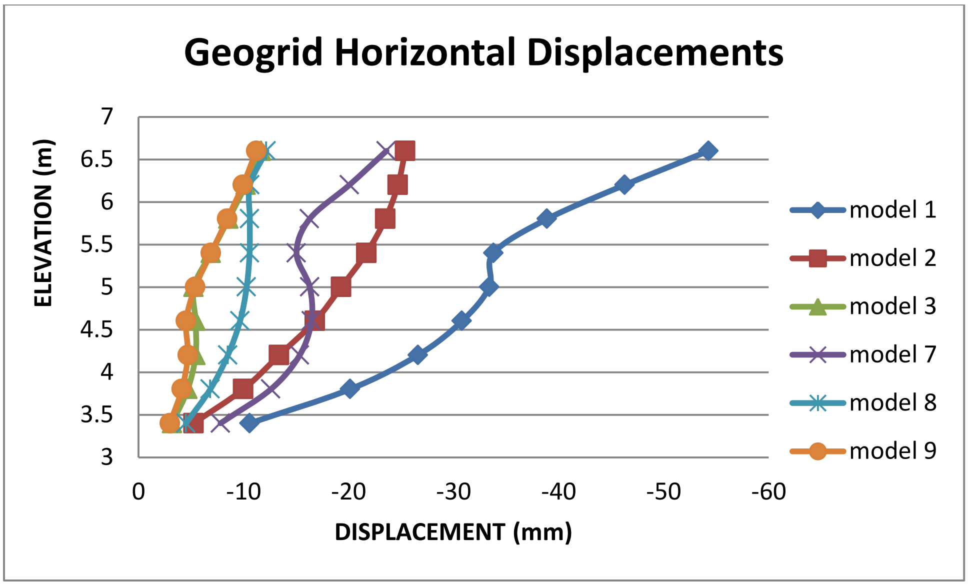

Figure 4. 47 Influence of Geogrid Spacing on Geogrid Horizontal Displacements

Except GRS wall with stiff clay backfill the other models have significant geogrid displacement variation as the geogrid vertical spacing varies.

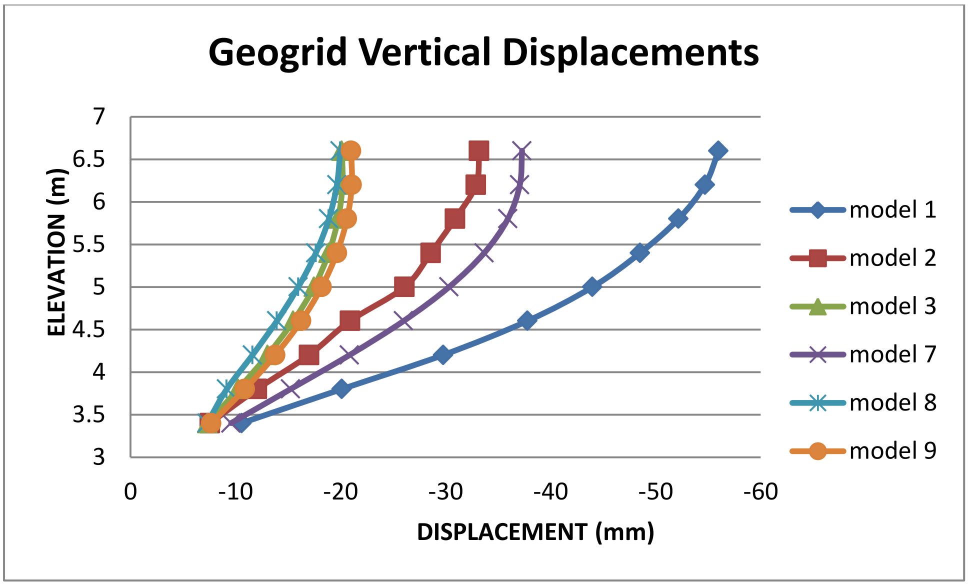

Figure 4. 48 Influence of Geogrid Spacing on Geogrid Vertical Displacements

Medium sand with minimum geogrid vertical spacing (model 8) has shown smaller vertical displacement of geogrid than other models.

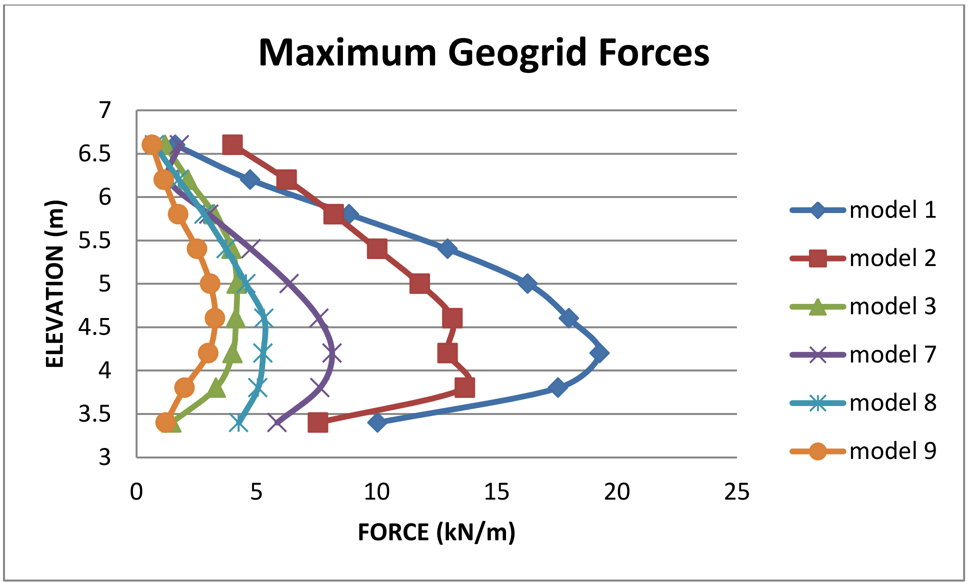

Figure 4. 49 Influence of Geogrid Spacing on Maximum Geogrid Forces

Observation

The maximum geogrid forces for the different backfill material and different geogrid vertical spacing were analyzed as shown in Figure 4.49and from this maximum geogrid force occurred within 0.3H-0.5H geogrid layers. Model 9 showed the minimum geogrid force and model 1 showed the maximum geogrid force relative to other models.

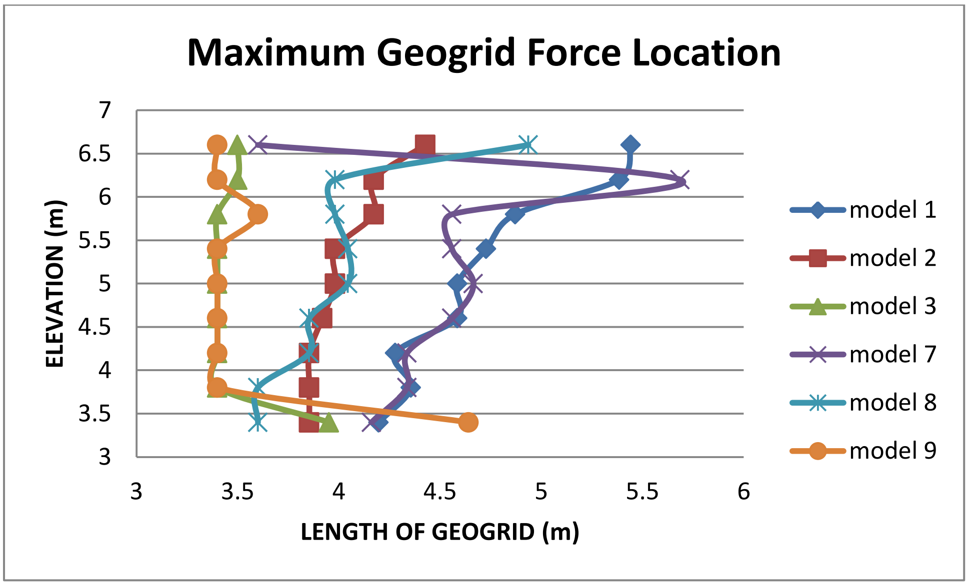

Figure 4. 50 Influence of Geogrid Spacing on the Maximum Geogrid Load Locations

Observation

GRS wall with stiff clay, medium sand and soft clay backfills maximum geogrid force location was analyzed with PLAXIS as shown in Figure above. Stiff clays for both geogrid vertical spacing showed maximum force location closest to the wall facing next we got medium sand and the last one was GRS wall with soft clay backfill.

4.5 Influence of Geogrid Length on the Behavior of Earth Retaining Structures

Reinforcement length have their own effect on the performance of earth retaining walls, in this study two types of geogrid length were used that is 3m and 4m. Wall performances of different backfill material for those geogrid lengths were investigated and the results are discussed below. All the model geometry, backfill material types' geogrid stiffness and boundary conditions were similar only the length of geogrid reinforcement was changed.

4.5.1 Soft Clay

- GRS wall with geogrid length3 m (**model 1**)
- GRS wall with geogrid length 4 m (**model 10**)

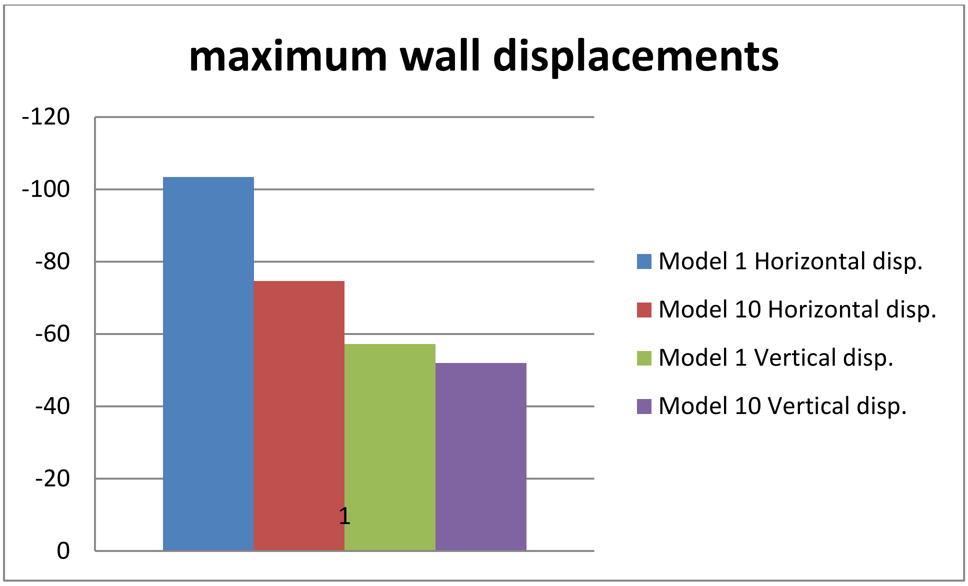

Figure 4. 51 Maximum Displacement of Wall with Soft Clay Backfill Geogrid Length Influence

Observation

GRS wall with soft clay backfill by different reinforcement length were analyzed. From Figure 4.51 the maximum wall displacements in the horizontal and vertical directions are presented. The horizontal and vertical displacements of the wall were decreased as we increase the geogrid length from 3 m to 4 m.

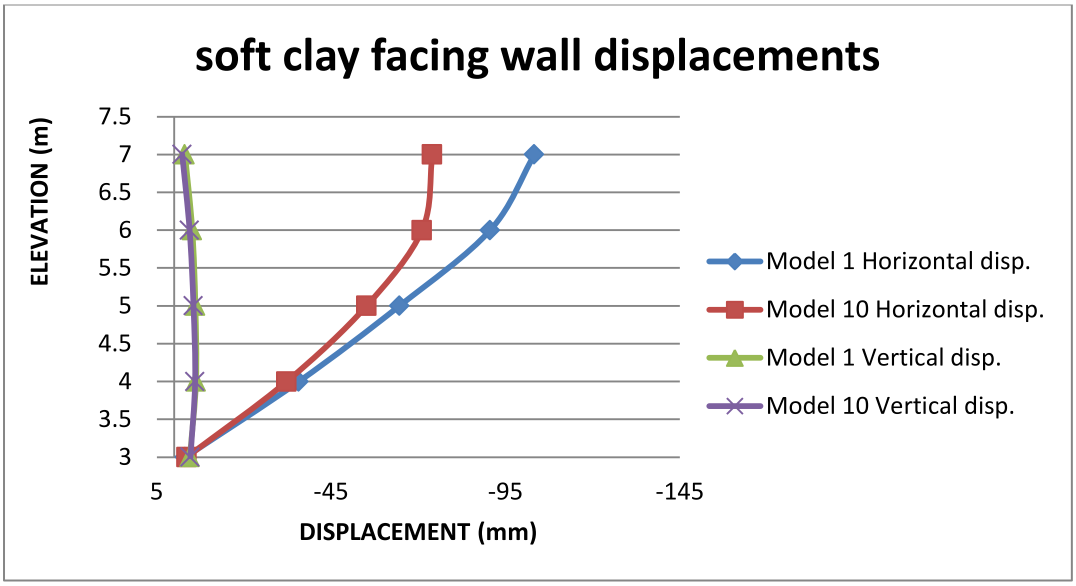

Figure 4. 52 Facing Wall Displacements with Soft Clay Backfill Geogrid Length Influence

Observation

The lateral movement of wall face as we go bottom up was significantly reduced for the increasing of geogrid length. Since the length of reinforcing material increases the contact of backfill material and reinforcement increases, so the development of friction resistance at the interface enhances the performance of the wall system.

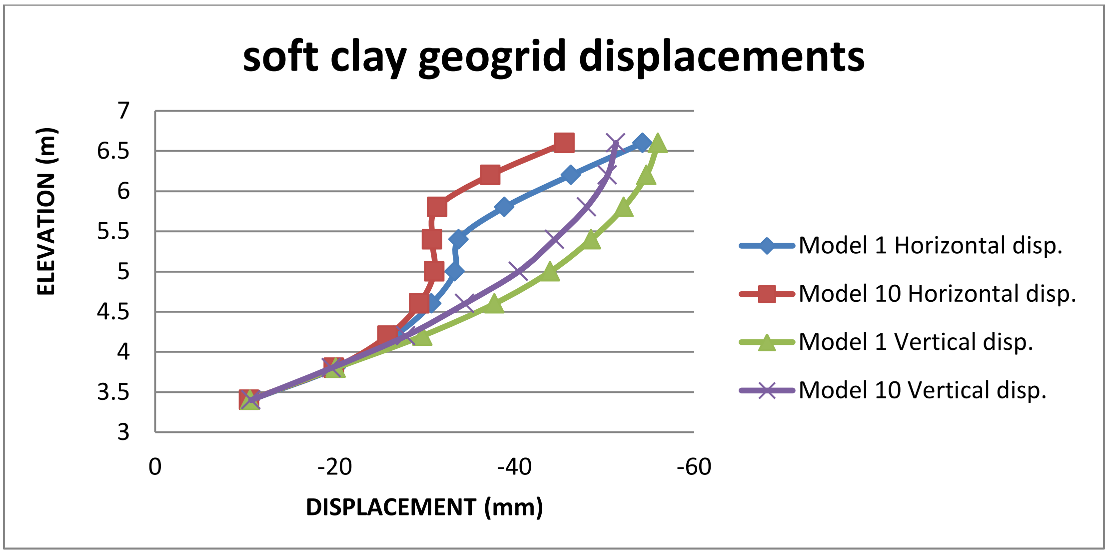

Figure 4. 53 Geogrid Displacement of Soft Clay Backfill with Geogrid Length Influence

Observation

The displacements of geogrid as increased the length of geogrid with in soft clay backfill material of GRS wall was decreased as seen in Figure 4.53.

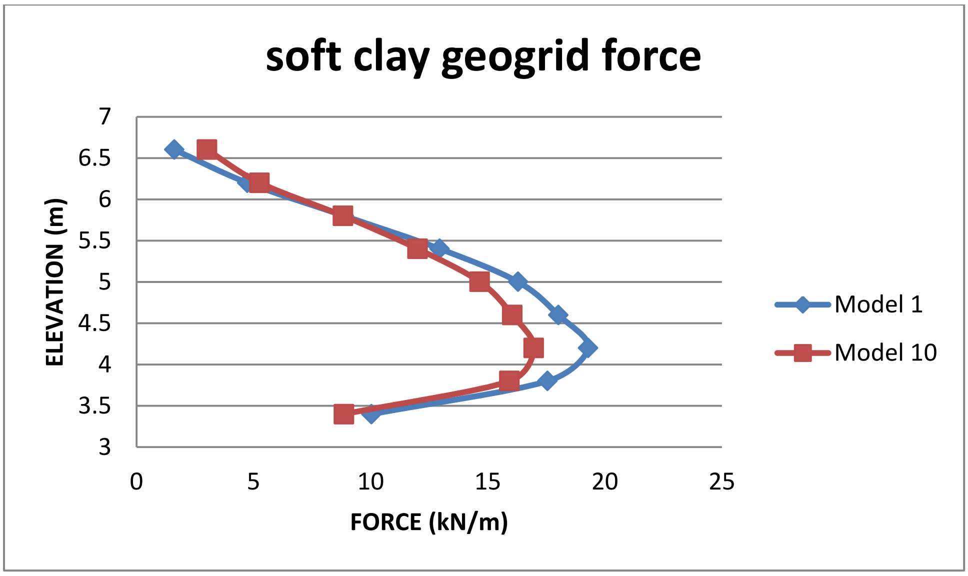

Figure 4. 54 Maximum Geogrid Forces of GRS Wall with Soft Clay Backfill of Geogrid Length Influence

The developed tension force within the geogrid was reduced when the geogrid length was increased. But at the top of the wall the inverse was observed from Figure 4.54.

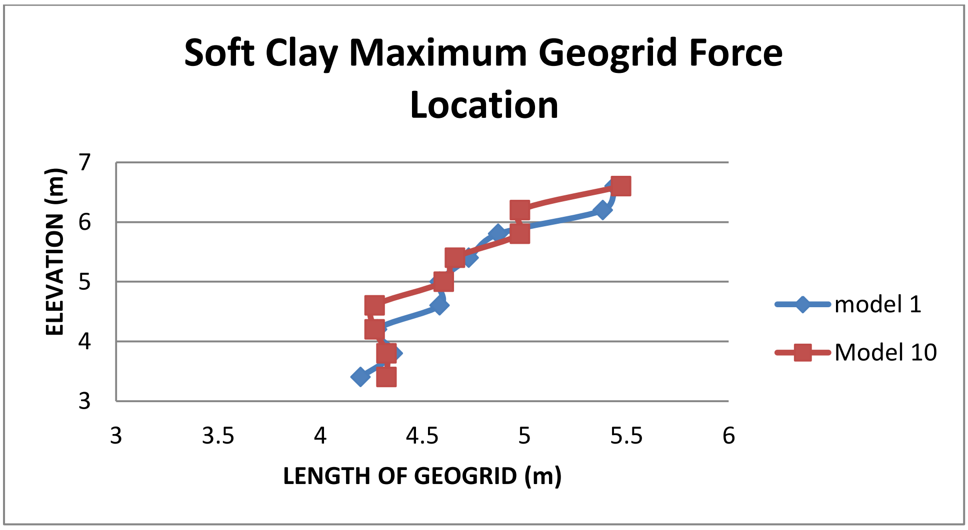

Figure 4. 55 Location of Maximum Force with In the Geogrid Influence of Geogrid Length

As the length increased from 3m to 4m the location of maximum geogrid force have a little bit deviation from one other. It's far from the facing as we go from bottom to top of the wall.

4.5.2 MEDIUM SAND

All the material properties of the soil were not changed only the geogrid length was changed from 3 m to 4 m.

- GRS wall with geogrid length 3 m (**model 2**).
- GRS wall with geogrid length 4 m (**model 11**).

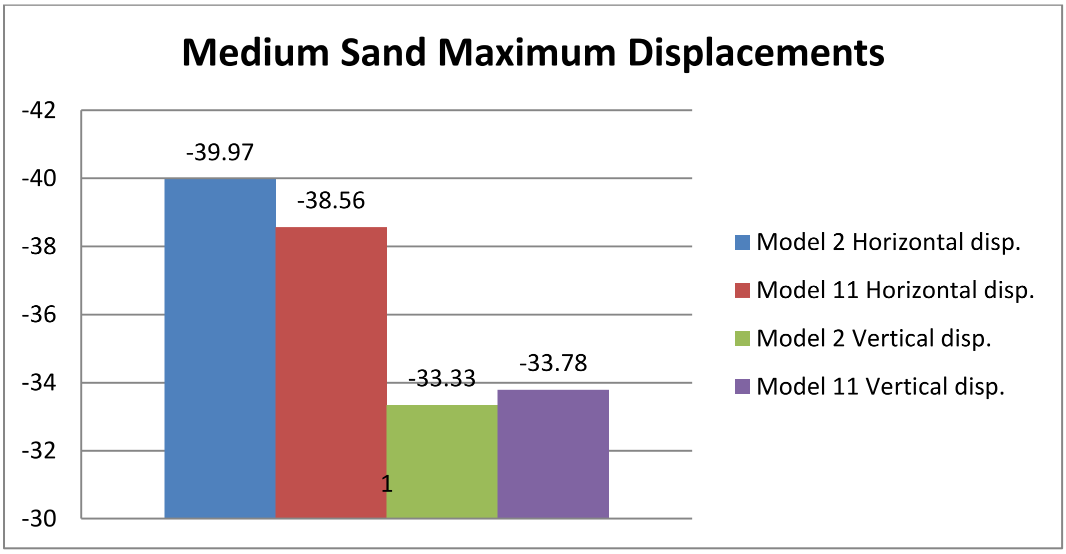

Figure 4. 56 Maximum Wall Displacements of Medium Sand Backfill with Geogrid Length Influence

Observation

The horizontal and vertical displacements of the wall with medium sand backfill material as seen in Figure 4.56 for both 3m and 4m geogrid length show small variations. This is due to the material property of backfill soil.

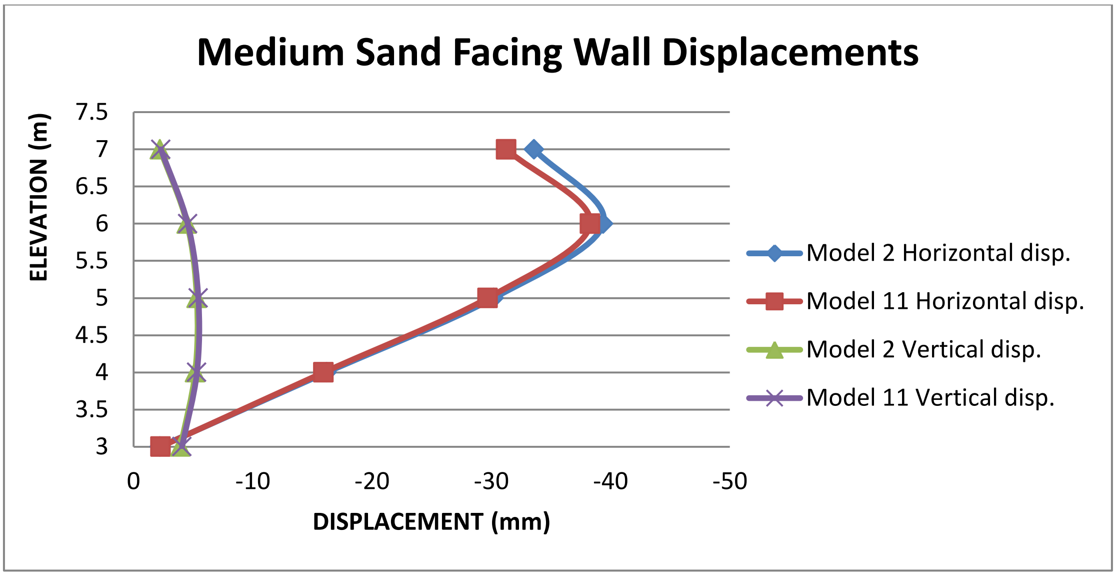

Figure 4. 57 Facing Wall Displacements of Medium Sand Backfill with Geogrid Length Influence

Observation

From Figure 4.57 indicated above the displacement of the wall facing for this backfill material as the length of geogrid increased shows little difference this indicates that further increasing the length of geogrid may be unnecessary.

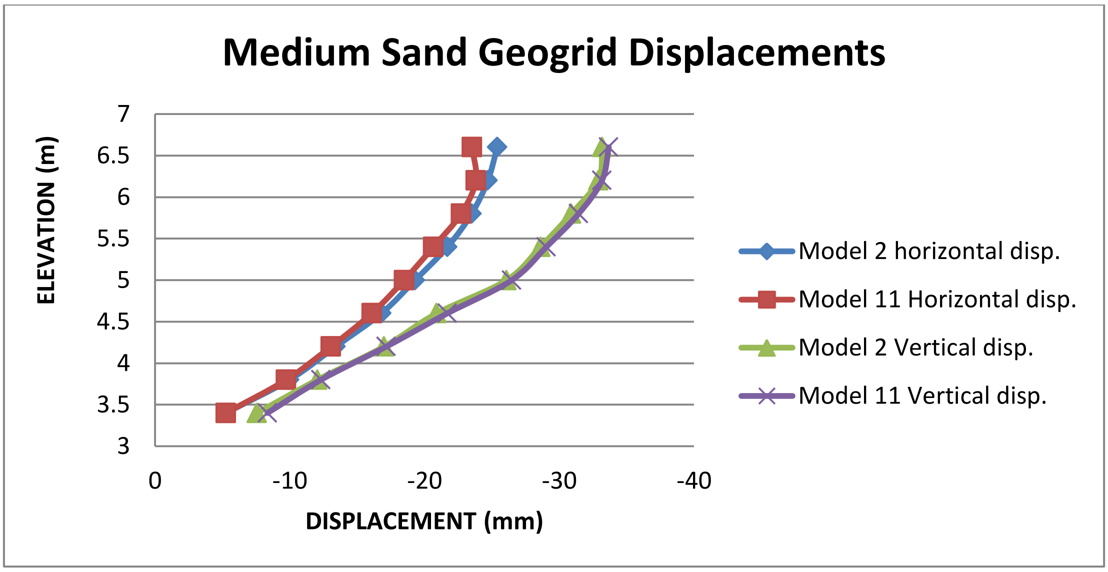

Figure 4. 58 Geogrid Displacements of Medium Sand Backfill with Geogrid Length Influence

Similar to the facing displacements geogrid displacement also have minimum variation as the length of geogrid increased by 1 m. the overall interaction of the backfill material with the geogrid results such condition.

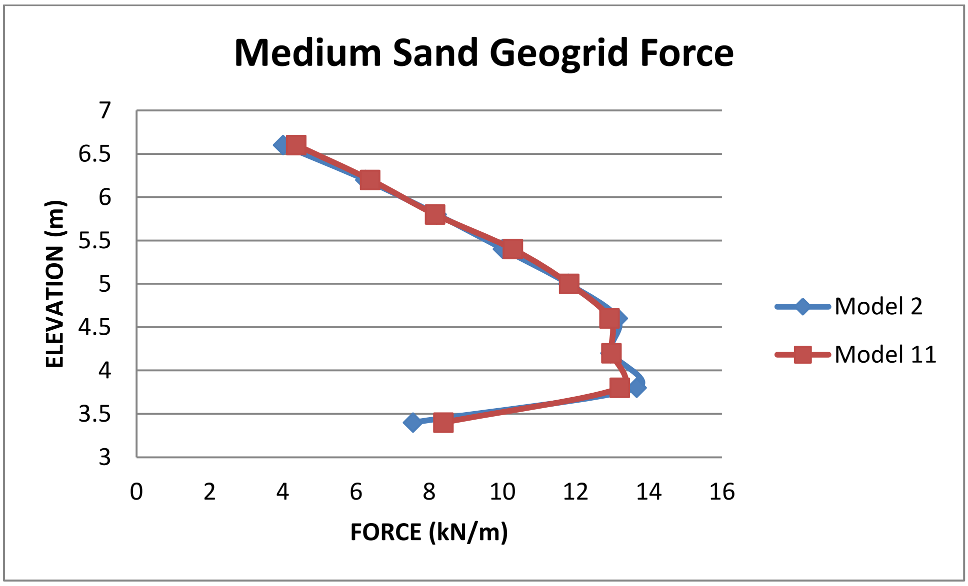

Figure 4. 59 Maximum geogrid load with in medium sand backfill with geogrid length influence

Figure 4.59 shown that there is no significant variation on the development of force within the geogrid for both models.

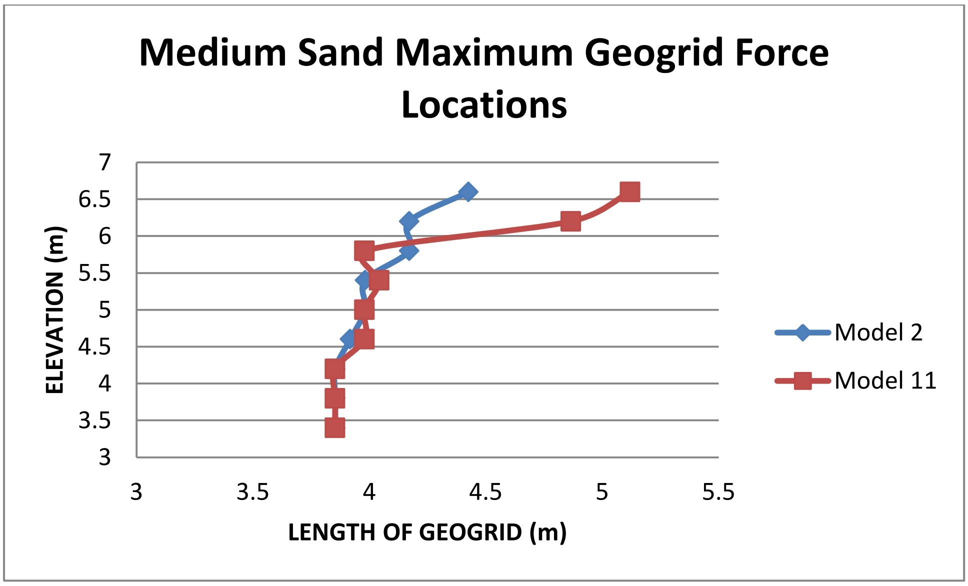

Figure 4. 60 Maximum Geogrid Force Location for Medium Sand Backfill with Geogrid Length Influence

The top two layers of geogrid show difference in the location of maximum geogrid force but as move down to the bottom of the wall the two models have nearly same maximum geogrid force location.

4.5.3 STIFF CLAY

All the material properties of the soil were not changed only the length of geogrid was changed from 3 m to 4 m which is reduced in half.

- GRS wall with geogrid length3 m (**model 3**)
- GRS wall with geogrid length 4 m (**model 12**)

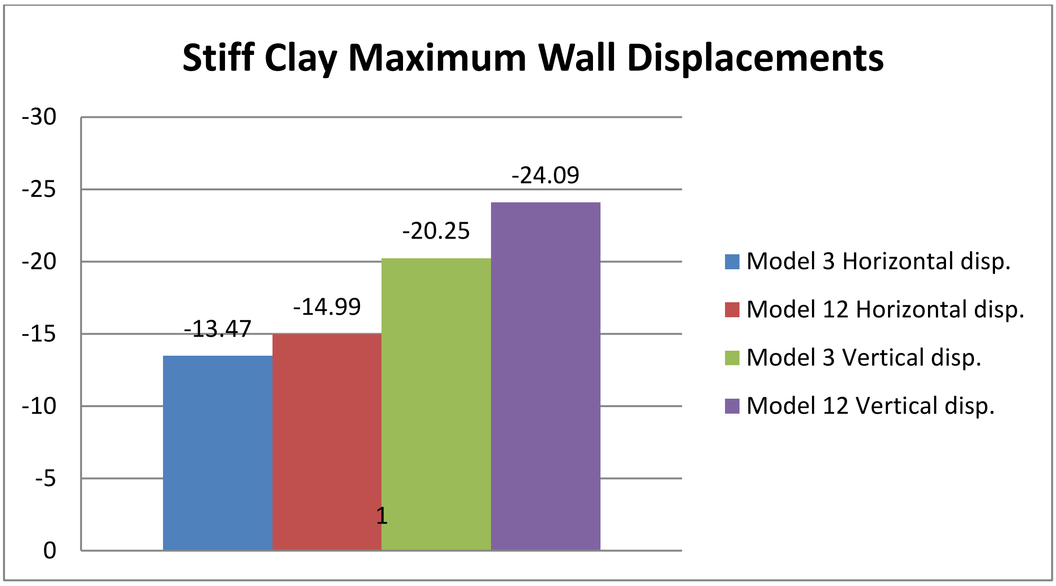

Figure 4. 61 Maximum wall displacements of stiff clay backfill geogrid length influence

Figure 4.61 indicated that as the length of geogrid increased from 3m to 4m the horizontal and vertical displacement of the wall were increased.

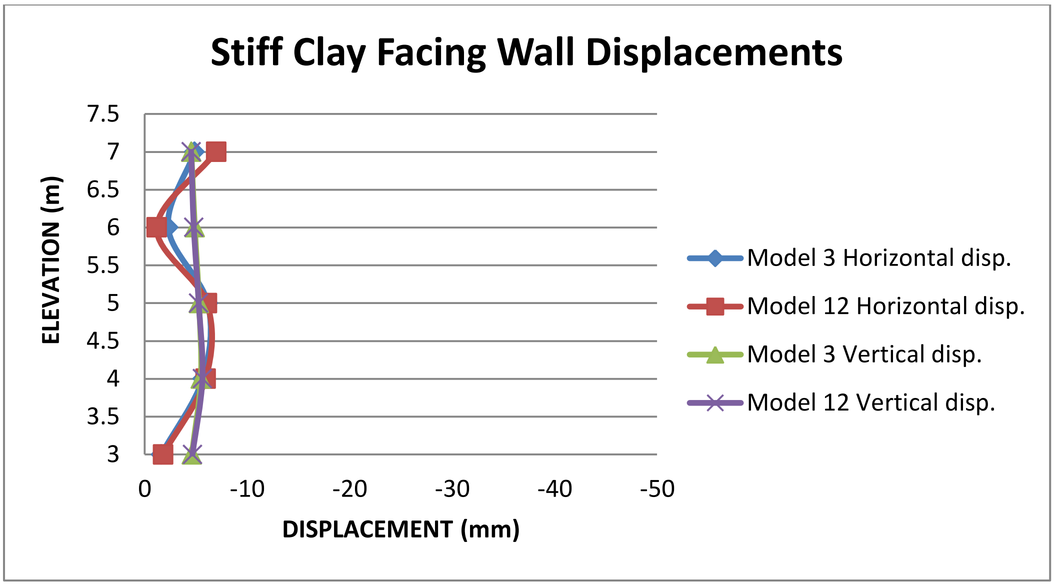

Figure 4. 62 Facing Wall Displacements of Stiff Clay Backfill with Geogrid Length Influence

Observation

As we seen in Figure 4.62 the lateral and vertical displacements of the facing wall in stiff clay backfill material in both reinforcement length shows minimum variation.

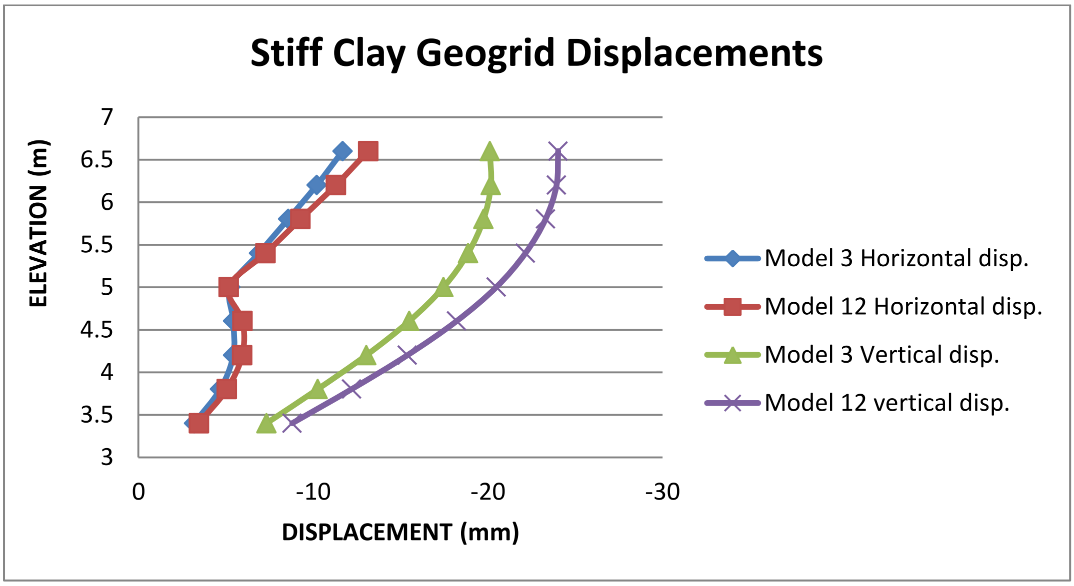

Figure 4. 63 Geogrid Displacements of the Stiff Clay Backfill Wall Geogrid Length Influence

Observation

When we see the displacement of geogrid the geogrid length of 4m show increased displacement as observed in the above facing wall displacements.

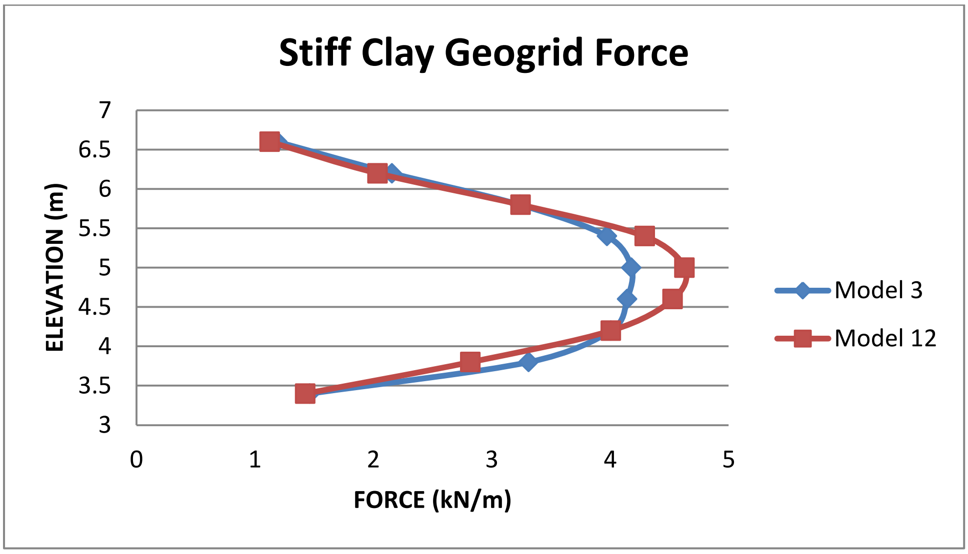

Figure 4. 64 Maximum Geogrid Load of Stiff Clay Backfill Geogrid Length Influence

Observation

maximum geogrid force for each layer was observed at the mid height of the wall and relative to 3m length of geogrid 4m length geogrid show maximum force in the geogrid.

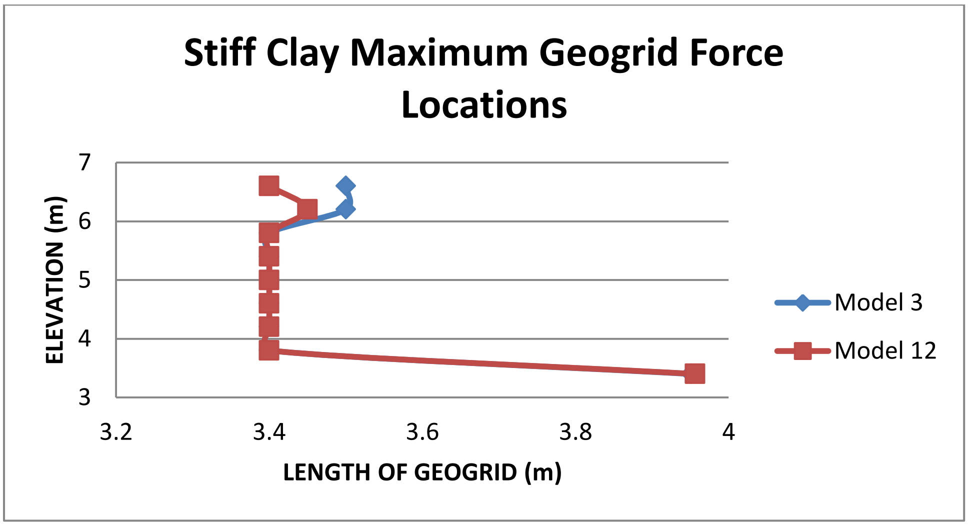

Figure 4. 65 Maximum Geogrid Force Locations of Stiff Clay with Geogrid Length

The influence of geogrid length was on the performance of different backfill material GRS retaining walls was tabulated here below.

Table 4. 30 Wall displacement for geogrid length influence with different backfill material

Length of geogrid (m)	**soft clay**		**medium sand**		**stiff clay**	
	Horizontal displ. (mm)	Vertical displ. (mm)	Horizontal displ. (mm)	Vertical displ. (mm)	Horizontal displ. (mm)	Vertical displ. (mm)
3	-103.33	-57.21	-39.97	-33.33	-13.47	-20.25
4	-74.56	-51.97	-38.56	-33.78	-14.99	-24.09

4.6 Influence of Surcharge Load on the Behavior of Earth Retaining Structures

Influence of surcharge load on the performance of reinforced earth retaining walls were involved through the application of a uniform pressure to the entire top surface of the soil from the back of the facing to the end of reinforced zone. Uniform pressure of20 kPa and 40 kPa were applied to the top surface of the uppermost layer of compacted soil after the construction sequence was completed. Three of backfill materials were analyzed and results were investigated at the end of construction and after application of surcharge pressure.

4.6.1 Soft Clay

All the material properties of the soil, reinforcement length and stiffness were not changed only the application of surcharge pressure after the end of construction was the difference between the three models model 7, model 13 and model 16.

- GRS wall at the end of construction/zero surcharge pressure (**model 7**)
- GRS wall after 20 kPa surcharge pressure applied (**model 13**)
- GRS wall after 40 kPa surcharge pressure applied (**model 16**)

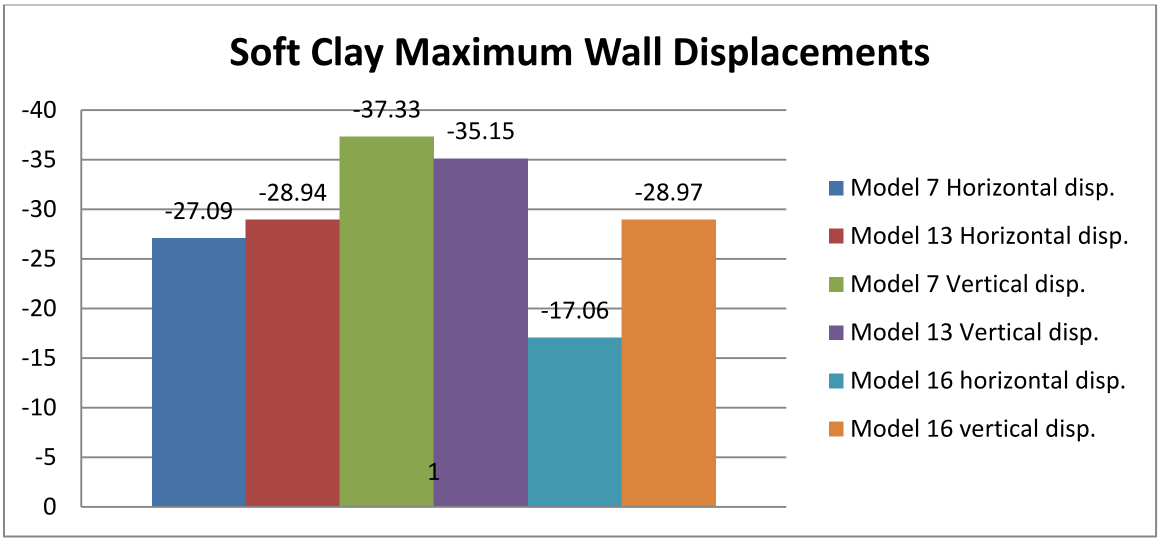

Figure 4. 66 Maximum Wall Displacements of Soft Clay Backfill Wall Surcharge Influence

Observation

When we apply a surcharge of 40 kPa we got relatively decreased horizontal and vertical displacements in the soft clay backfill wall. Due to compressibility of the backfill material the applied surcharge loads had significant effect in the reduction of displacements in the wall.

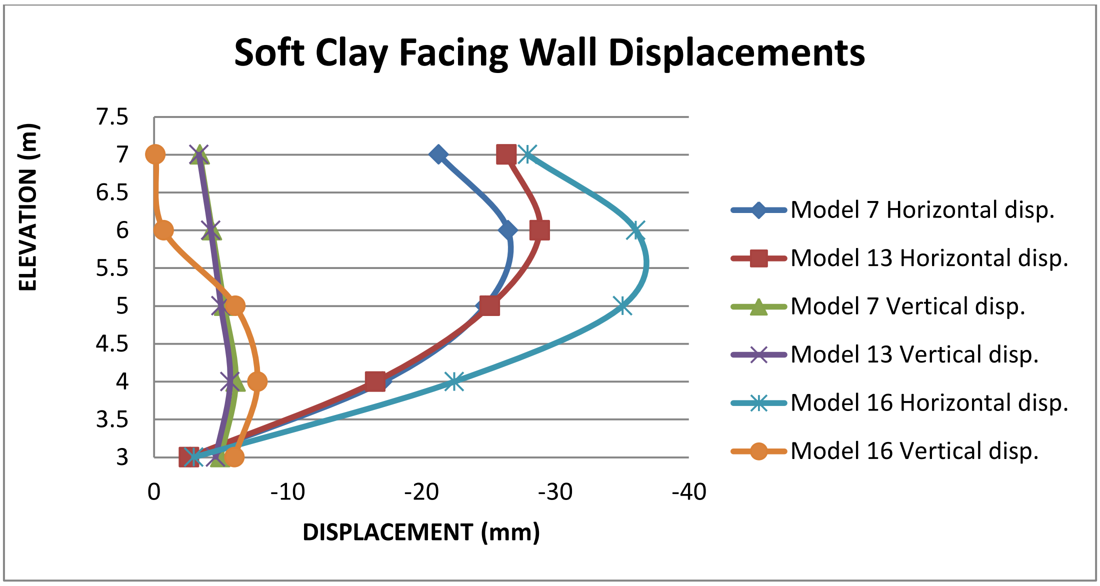

Figure 4. 67 Facing Wall Displacements of Soft Clay Backfill Wall Surcharge Influence

Observation

The horizontal displacement of the wall facing unit was increased as the surcharge pressures were increased. While the vertical displacement of the wall subjected to maximum surcharge pressure exhibit minimum displacement at the top of wall face and relatively maximum displacement at the bottom of the wall.

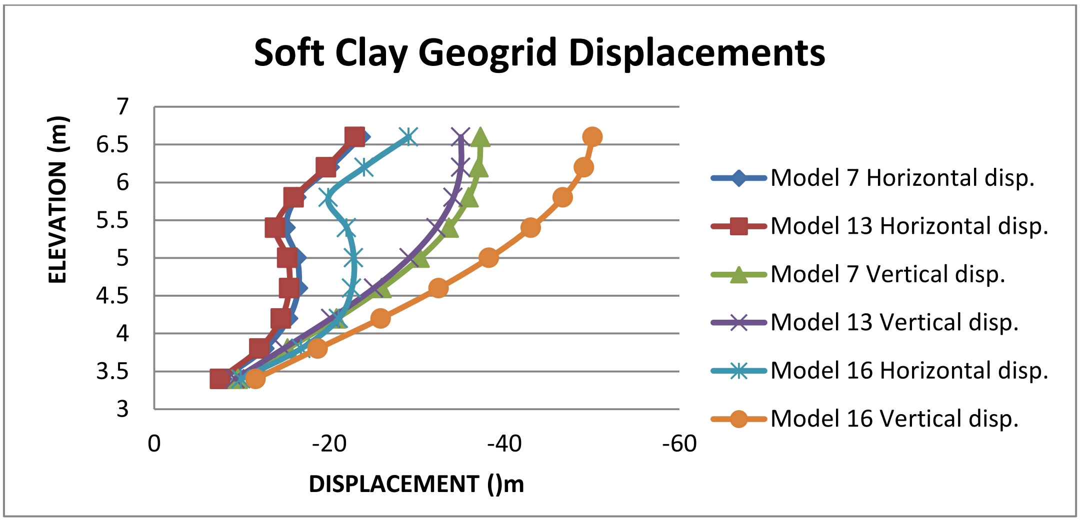

Figure 4. 68 Maximum Geogrid Displacements of Soft Clay Backfill Surcharge Influence

Observation

Geogrid displacements as observed in Figure 4.68 maximum in the vertical direction than horizontal displacements and these maximum displacements were observed at the top portion of the wall.

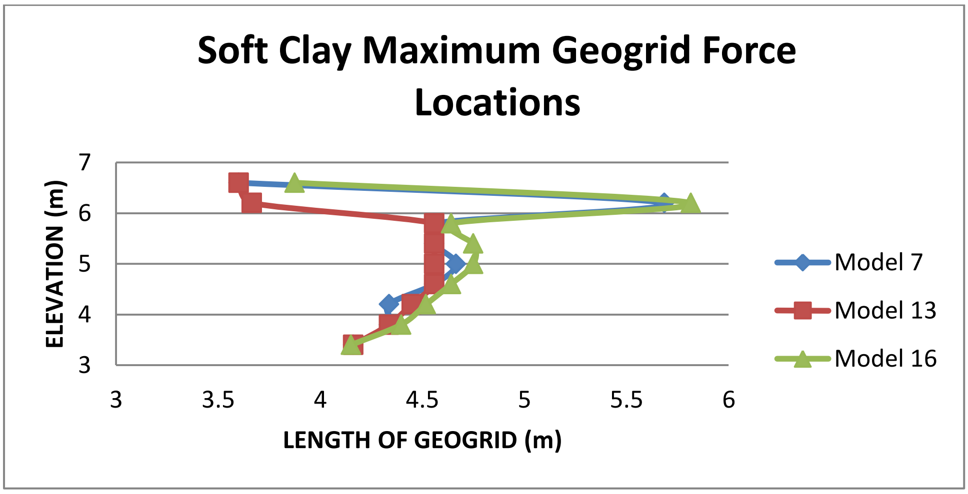

Figure 4. 69 Location of Maximum Force on the Geogrid Surcharge Influence

4.6.2 MEDIUM SAND

All the material properties of the soil, reinforcement length and stiffness were not changed only the application of surcharge pressure after the end of construction was the difference between the three models model 8, model 14 and model 17.

- GRS wall at the end of construction (**model 8**)
- GRS wall after 20 kPa surcharge pressure applied (**model 14**)
- GRS wall after 40 kPa surcharge pressure applied (**model 17**)

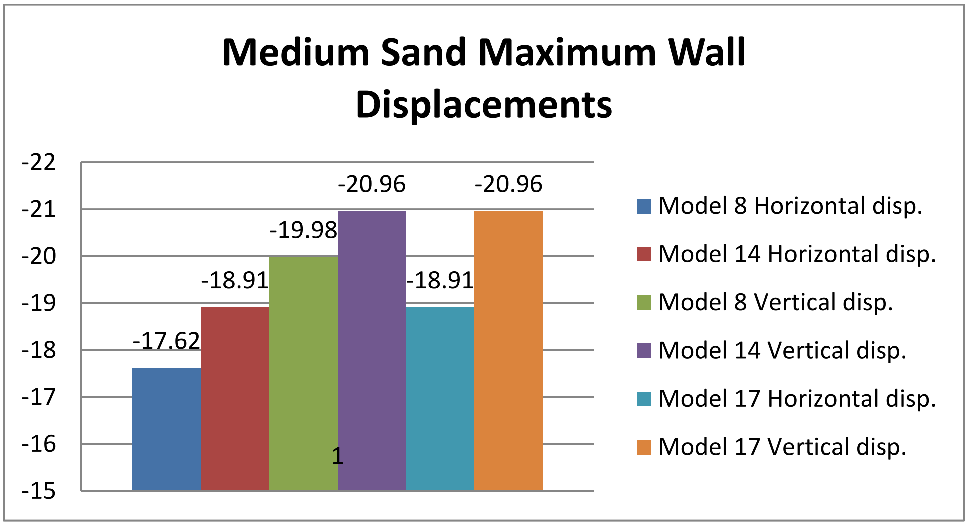

Figure 4. 70 Maximum Wall Displacements of Medium Sand Surcharge Influence

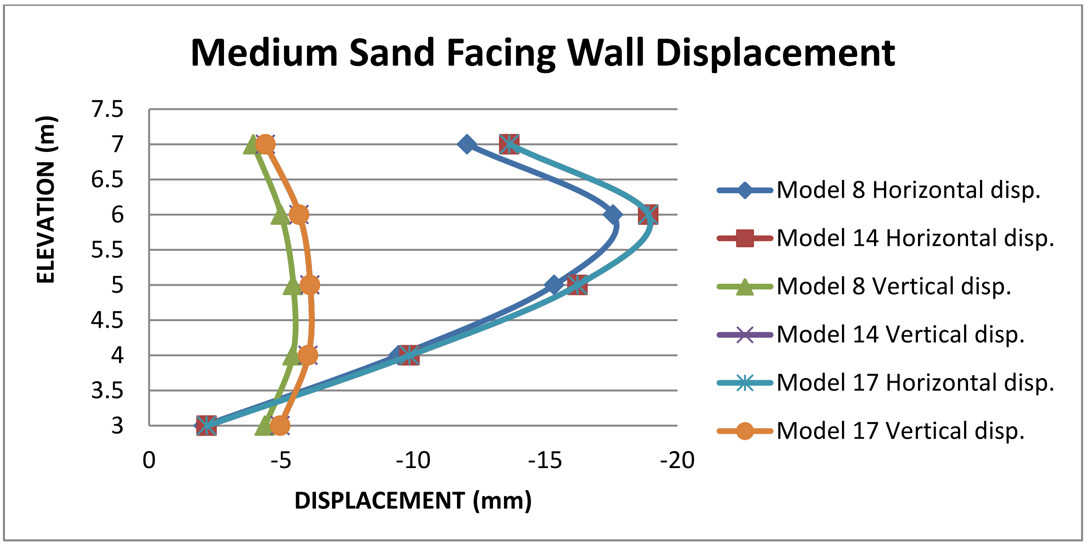

Figure 4. 71 Facing Wall Displacements of Medium Sand Backfill Surcharge Influence

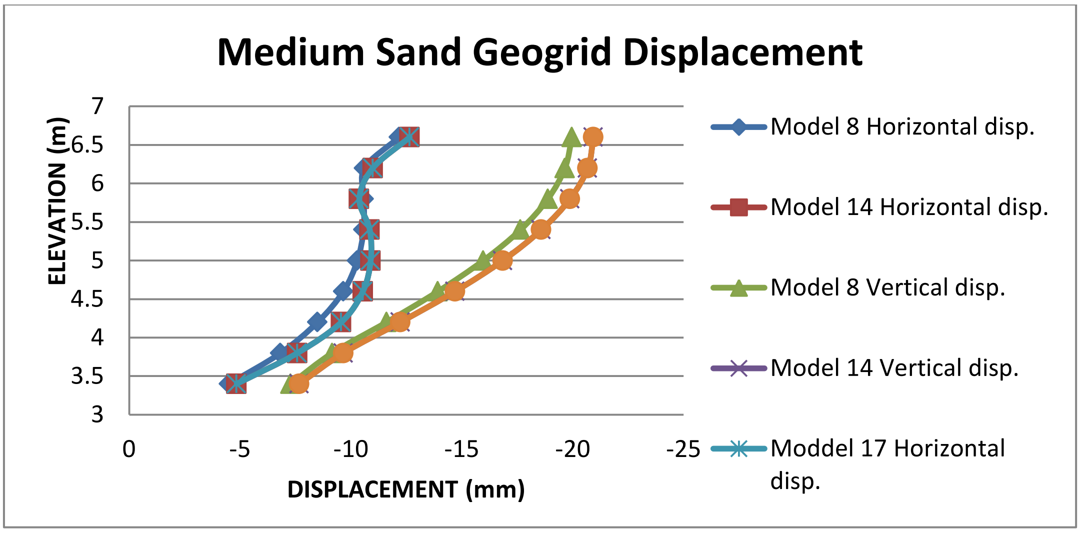

Figure 4. 72 Maximum Geogrid Displacements of Medium Sand Surcharge Influence

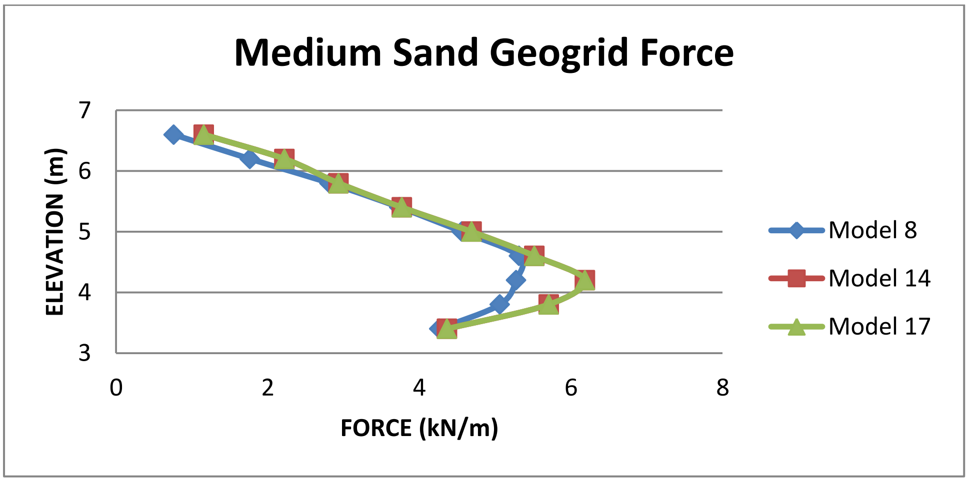

Figure 4. 73 Maximum Geogrid Forces Surcharge Influence

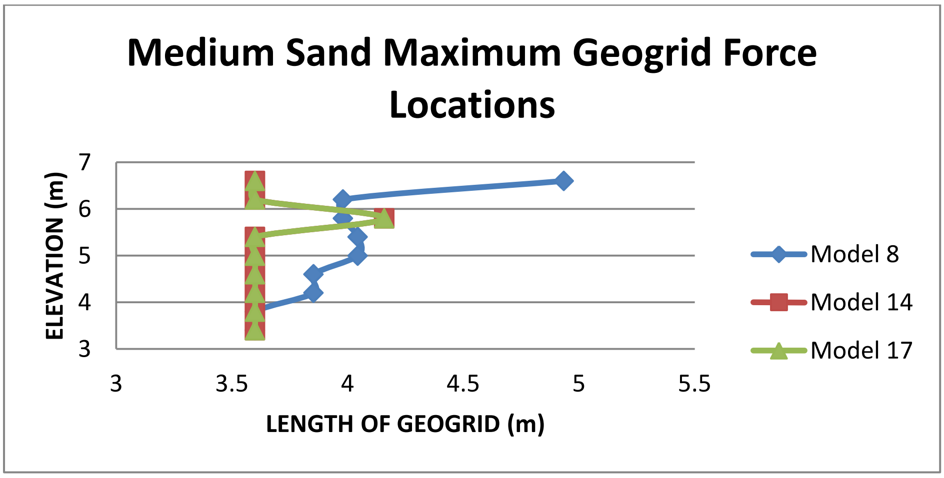

Figure 4. 74 Location of Maximum Loads on the Geogrid Surcharge Influence

4.6.3 STIFF CLAY

All the material properties of the soil, reinforcement length and stiffness were not changed only the application of surcharge pressure after the end of construction was the difference between the three models model 9, model 15 and model 18.

- GRS wall at the end of construction (**model 9**)
- GRS wall after 20 kPa surcharge pressure applied (**model 15**)
- GRS wall after 40 kPa surcharge pressure applied (**model 18**)

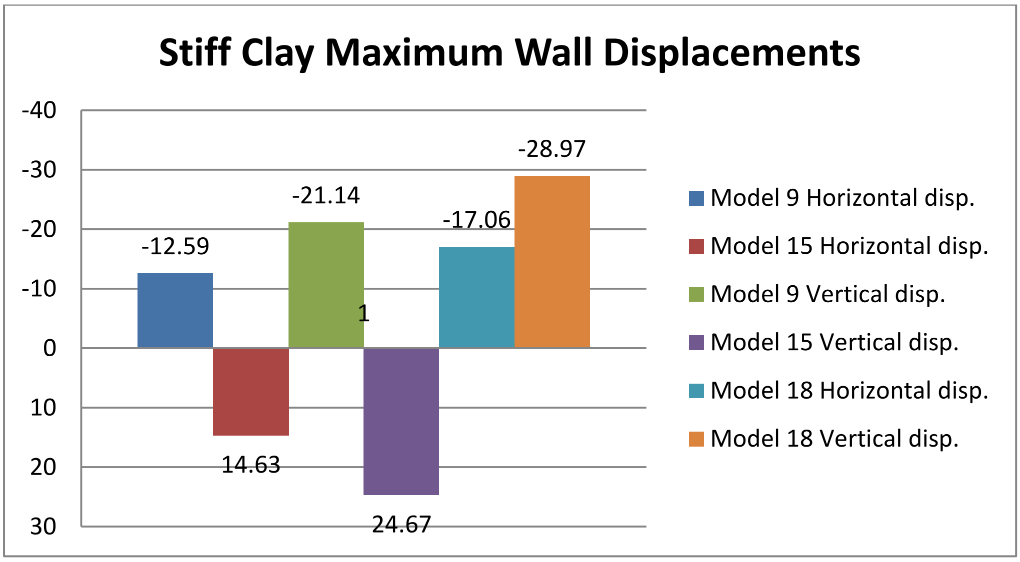

Figure 4. 75 Maximum Wall Displacements of Stiff Clay Backfill Surcharge Influence

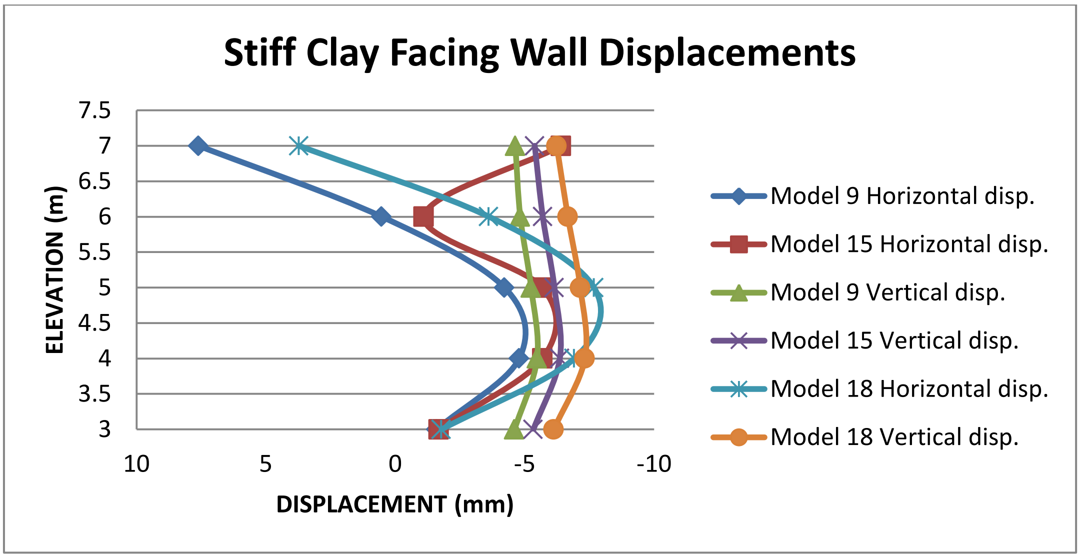

Figure 4. 76 Facing Wall Displacements Surcharge Influence

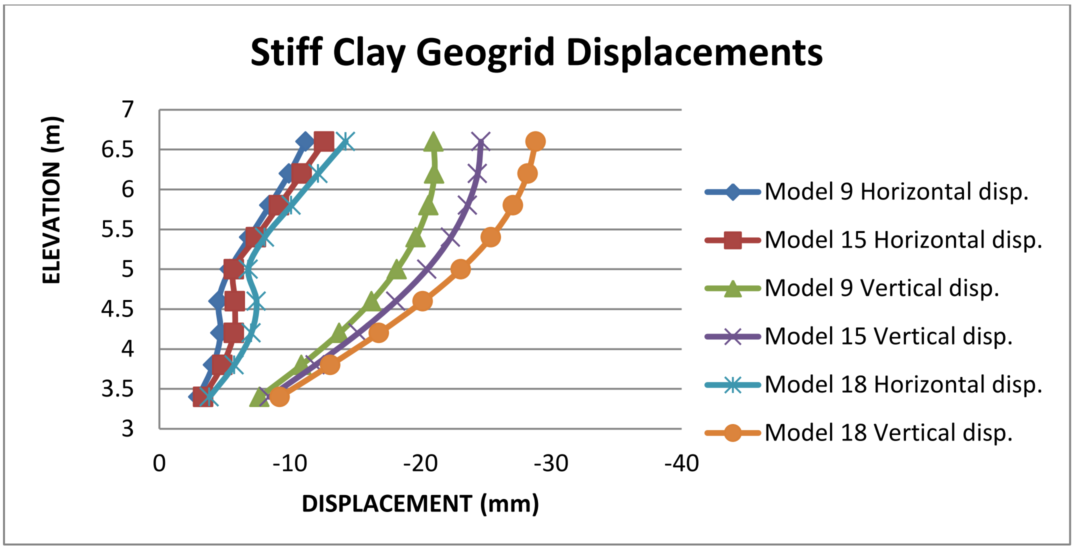

Figure 4. 77 Maximum Geogrid Displacements Surcharge Influence

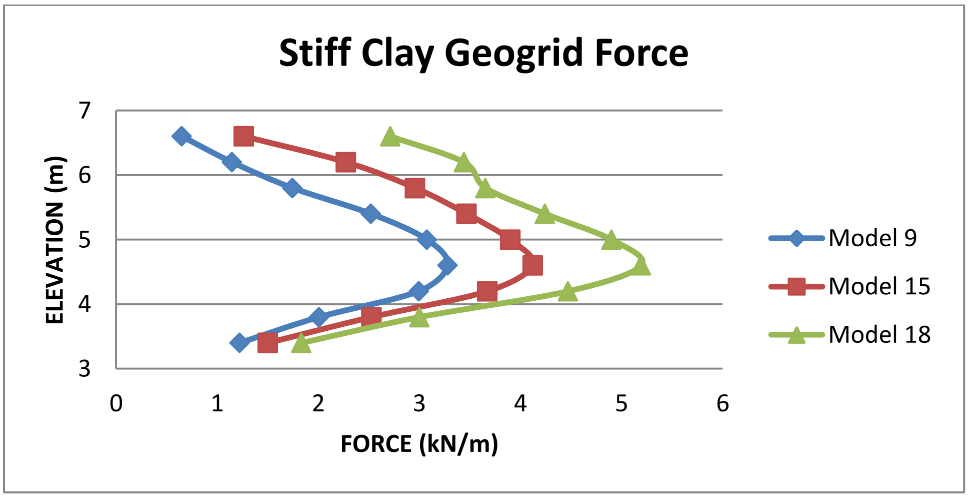

Figure 4. 78 Maximum geogrid Forces

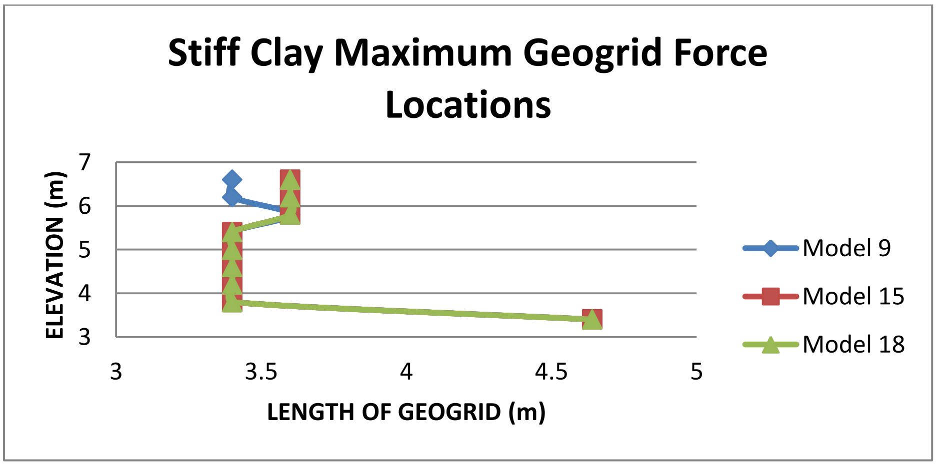

Figure 4. 79 Location of Maximum Geogrid Forces

Generally, the effect of surcharge pressure on the performance of GRS retaining walls was tabulated in table below.

Table 4. 31 Wall displacement for surcharge effects with different backfill soil

Surcharge kN/m^2	**soft clay**		**medium sand**		**stiff clay**	
	Horizontal displ. (mm)	Vertical displ. (mm)	Horizontal displ. (mm)	Vertical displ. (mm)	Horizontal displ. (mm)	Vertical displ. (mm)
EOC	-27.09	-37.33	-17.62	-19.98	-12.59	-21.14
20	-28.94	-35.15	-18.91	-20.96	14.63	24.67
40	-17.06	-28.97	-18.91	-20.96	-17.06	-28.96

CHAPTER 5

CONCLUSION AND RECOMMENDATION

5.1 Conclusion

Following the results obtained from previous section carried out on the different cases presented in this research work, the following concluding remarks can be made:

- The behavior of reinforced soil retaining wall is depends on some factors which can have influence in the general performance of the wall. These factors include the type of backfill material, stiffness of the geogrid, spacing of the Geogrid, length of geogrid and surcharge pressures among others.
- The stiffness of geogrid plays a vital role in the stability of reinforced soil retaining wall. The maximum tensile force line or the failure plane is just behind the facing wall in case of stiff clay backfill wall relative to others.
- Half the reduction or increment of geogrid stiffness results significant wall displacement change for medium sand soft clay backfill materials.
- GRS wall with stiff clay backfill material shows a little bit influence in its performance for geogrid spacing and stiffness variations.
- Relatively cohesive materials exhibit reduced displacements of the wall than less cohesive materials among other property factors.
- Generally the variation of geogrid vertical spacing has much effect than geogrid stiffness variation for such backfill materials in GRS wall displacements.

5.2 Recommendations

Despite of the difficulties to obtained appropriate input data parameters, capturing real simulation of wall construction and model validations, there is high potential for continued research using finite element numerical models, here are some of the ways of improving this research work:

- By studying the effect of changes in the wall geometry for performance of the wall.
- By studying the wall performances against dynamic loadings
- By thoroughly Validate models with different full scale laboratory and field tests
- Plaxis 2D software have its own limitations one may use PLAXIS 3D
- The results were limited for the study parameters only

REFERENCES

1. Admas, Ketchart,Ruckman. "reinforced soil for bridge support application on low volume road." 1999.

2. Ambauen, Spancer J. "numerical simulation of mechanically stabilized earth walls for parametric evaluation of behavior under surcharge loading." 2014.

3. Bathrust, R.J., Walters, D.L.,Hatami, K., and Allen, J.M. "full scale performance testing and numerical modelling of reinforced soil retaining walls." 2001.

4. Bathurst, Hatami and. "development and verification of numerical model for the analysis of GRS walls under working stress condition." 2005.

5. Bowles, Joseph E. *foundation analysis and design.* new york, 1997.

6. Brinkgreve, R.B.J. *plaxis v 8. tutorial manual.* netherlands, 2002.

7. Budha, Muni. "foundation and earh retaining structure." 2008.

8. FHWA. "reinforced soil structure design and construction guide lines." 1990.

9. Fourie, K.J. Fabian and A.B. "clay geotextile interaction in large retaining wall model." 1988.

10. Gourc, JP. "geosynthetices embankments, review of theory and practice." *piscal francis.* 1993.

11. Guru Nanak, dev engineering,. "reinforced soil and geosynthetic engineering." punjaba india, 2012. 2-4.

12. Helwany. "GRS bridge abutments-an effective means to alleivate bridge approach settlement." 2003.

13. J.Huang, A.Bhandari and X.Yang. "Numerical Modeling of Geosynthetic - Reinforced earth structures and geosynthetic soil interactions." *geotechnical engineering journal of the SEAGS and AGSSEA*, 2011: 1-3.

14. KANIRAJ, SHENBAGA R. *Design aids in soil mechanices and foundation engineering.* new delhi, 2008.

15. Khalid Farrag, phD, P.E. & Mrk morvant, P.E. "evaluation of interaction properties of geosynthetices in cohesive soils ." *LTRC reinforced soil test wall*, 2004.

16. M.R. Abdil, S.A. Sadrnejad, M.A. Arjomand. "clay reinforcment using geogrid embedded in thin layers of sand." september 2009.

17. Mirmoradi, S.H and Ehrlich M. "numerical evaluation of the behavior of reinforced soil retaining walls ." *18th international conference on soil mechanices and geotechnical engineering*, 2013.

18. Oyegible, Brain Oluwatobi. "parametric studies on the behavior of reinforced soil retaining walls under static and dynamic loading." 2011.

19. Patias, Bueno. "evaluation of mechanical behavior of brazilian marginal soil for reinforcment." 2006.

20. Ramulu, Mr. Srinivasa Reddy Ayuluril and Mr. D. Sidhu. "bebhavior of reinforced soil retaining walls under static loads by using plaxis." 2017.

21. Tatsuoka. "a new type of integral bridge comprising geosynthetic reinforced soil wall." 2009.

APPENDICES

Appendix 1

Wall displacements

Node	X	Y	Ux	Uy	DUx	DUy
	[m]	[m]	[m]	[m]	[m]	[m]
1	0	1.375	0	-0.00025	0	-2.7E-07
2	0	1.25	0	-0.00025	0	-2.8E-07
3	0	1.125	0	-0.00025	0	-2.8E-07
4	0.091992	1.246509	-4.9E-05	-0.00025	-7.1E-08	-2.8E-07
5	0.091992	1.121509	-4.6E-05	-0.00025	-6.9E-08	-2.8E-07
6	0.183985	1.118019	-9.2E-05	-0.00025	-1.4E-07	-2.9E-07
7	0	0.875	0	-0.00023	0	-2.7E-07
8	0	0.75	0	-0.00021	0	-2.5E-07
9	0	0.625	0	-0.00019	0	-2.3E-07
10	0.091992	0.871509	-3.9E-05	-0.00023	-6.1E-08	-2.7E-07
11	0.091992	0.746509	-3.5E-05	-0.00021	-5.5E-08	-2.5E-07
12	0.183985	0.868019	-7.8E-05	-0.00023	-1.2E-07	-2.7E-07
13	0	1	0	-0.00024	0	-2.8E-07
14	0.091992	0.996509	-4.3E-05	-0.00024	-6.5E-08	-2.8E-07
15	0.183985	0.993019	-8.6E-05	-0.00024	-1.3E-07	-2.8E-07
16	0.275977	0.989528	-0.00013	-0.00025	-2E-07	-2.9E-07
17	0.091992	0.621509	-3.1E-05	-0.00019	-4.9E-08	-2.3E-07
18	0.183985	0.743019	-7E-05	-0.00021	-1.1E-07	-2.6E-07
19	0.275977	0.864528	-0.00012	-0.00023	-1.8E-07	-2.8E-07
20	0.375314	0.645207	-0.00013	-0.0002	-2E-07	-2.5E-07
21	0.325646	0.754867	-0.00013	-0.00022	-2E-07	-2.7E-07
22	0.233653	0.633358	-7.9E-05	-0.00019	-1.3E-07	-2.4E-07
23	0.141661	0.511849	-4E-05	-0.00016	-6.5E-08	-2.1E-07
24	0.283322	0.523697	-8.2E-05	-0.00017	-1.3E-07	-2.2E-07
25	0.424982	0.535546	-0.00012	-0.00018	-2E-07	-2.3E-07
26	0.389937	0.261849	-6.1E-05	-0.0001	-1E-07	-1.3E-07
27	0.40746	0.398697	-9.3E-05	-0.00014	-1.5E-07	-1.9E-07
28	0.265799	0.386849	-5.9E-05	-0.00014	-9.6E-08	-1.8E-07
29	0	0.5	0	-0.00016	0	-2E-07
30	0	0	0	0	0	0
31	0.124138	0	0	0	0	0
32	0.248276	0	0	0	0	0
33	0.372414	0	0	0	0	0
34	0.372414	0.125	-2.9E-05	-5.1E-05	-4.8E-08	-6.9E-08
35	0.248276	0.25	-3.7E-05	-9.4E-05	-6.1E-08	-1.2E-07
36	0.124138	0.375	-2.7E-05	-0.00013	-4.4E-08	-1.7E-07

Appendix 2

Geogrid displacements

Geogrid	Element	Node	X	Y	Ux	Uy
			[m]	[m]	[m]	[m]
1	1	1201	3.4	3.4	-0.0078	-0.00122
	geogrid	1202	3.45	3.4	-0.00766	-0.00428
		1203	3.5	3.4	-0.00752	-0.00585
		1204	3.55	3.4	-0.00738	-0.00649
		1393	3.6	3.4	-0.00724	-0.00689
	2	1393	3.6	3.4	-0.00724	-0.00689
	geogrid	1394	3.664511	3.4	-0.00706	-0.00729
		1395	3.729021	3.4	-0.00689	-0.00767
		1396	3.793532	3.4	-0.00672	-0.00803
		1513	3.858042	3.4	-0.00654	-0.0084
	3	1513	3.858042	3.4	-0.00654	-0.0084
	geogrid	1514	3.919437	3.4	-0.00636	-0.00881
		1515	3.980831	3.4	-0.00615	-0.00915
		1516	4.042226	3.4	-0.00591	-0.00938
		1659	4.10362	3.4	-0.00566	-0.00949
	4	1659	4.10362	3.4	-0.00566	-0.00949
	geogrid	1662	4.162049	3.4	-0.00541	-0.00951
		1661	4.220478	3.4	-0.00516	-0.00948
		1660	4.278907	3.4	-0.00492	-0.00943
		1993	4.337335	3.4	-0.00468	-0.00942
	5	1993	4.337335	3.4	-0.00468	-0.00942
	geogrid	1994	4.392942	3.4	-0.00447	-0.00946
		1995	4.448548	3.4	-0.00427	-0.00951
		1996	4.504155	3.4	-0.00409	-0.00954
		2141	4.559761	3.4	-0.00391	-0.00955
	6	2141	4.559761	3.4	-0.00391	-0.00955
	geogrid	2144	4.612681	3.4	-0.00374	-0.00956
		2143	4.665602	3.4	-0.00359	-0.00955
		2142	4.718522	3.4	-0.00344	-0.00955
		2629	4.771442	3.4	-0.00329	-0.00957
	7	2629	4.771442	3.4	-0.00329	-0.00957
	geogrid	2632	4.821806	3.4	-0.00316	-0.00957
		2631	4.87217	3.4	-0.00303	-0.00956

Appendix 3

Geogrid load

Geogrid	Element	Node	X	Y	N_x
			[m]	[m]	[kN/m]
1	1	1201	3.4	3.4	3.269155
	geogrid	1202	3.45	3.4	3.266284
		1203	3.5	3.4	3.272065
		1204	3.55	3.4	3.265693
		1393	3.6	3.4	3.267976
	2	1393	3.6	3.4	3.30301
	geogrid	1394	3.664511	3.4	3.174403
		1395	3.729021	3.4	3.152796
		1396	3.793532	3.4	3.245708
		1513	3.858042	3.4	3.493056
	3	1513	3.858042	3.4	3.494087
	geogrid	1514	3.919437	3.4	4.103947
		1515	3.980831	3.4	4.707979
		1516	4.042226	3.4	5.267794
		1659	4.10362	3.4	5.740843
	4	1659	4.10362	3.4	5.696587
	geogrid	1662	4.162049	3.4	5.860705
		1661	4.220478	3.4	5.854205
		1660	4.278907	3.4	5.681819
		1993	4.337335	3.4	5.348281
	5	1993	4.337335	3.4	5.356897
	geogrid	1994	4.392942	3.4	5.021033
		1995	4.448548	3.4	4.732805
		1996	4.504155	3.4	4.493545
		2141	4.559761	3.4	4.304587
	6	2141	4.559761	3.4	4.301443
	geogrid	2144	4.612681	3.4	4.140458
		2143	4.665602	3.4	3.992193
		2142	4.718522	3.4	3.856647
		2629	4.771442	3.4	3.733567
	7	2629	4.771442	3.4	3.728452
	geogrid	2632	4.821806	3.4	3.616623
		2631	4.87217	3.4	3.535775